UNIVERSITY OF BIRMINGHAM

Synthesis, Characterisation and Nanoecotoxicological Assessment of a Graphene Oxide – Gold Nanohybrid

by

Taiwo Hassan Akere

A thesis submitted to the University of Birmingham for the degree of

DOCTOR OF PHILOSOPHY

School of Geography, Earth and Environmental Science

College of Life and Environmental Sciences

University of Birmingham

December 2022

Abstract

Contemporary research in nanomaterials is focusing on the unique characteristics of multicomponent nanohybrids and their potential use in various applications. The synergistic properties of graphene oxide-gold nanohybrid (GO-Au) are already being used in applications such as biosensing and cancer detection. However, there is currently no standardised protocol for the synthesis of such nanohybrids. Also, an understanding of the fate and toxicity potential of a GO-Au nanohybrid has become pertinent due to their rapid use and resulting inevitable exposure to organisms and the environment. In addition, the possibility of using a metal-doped nanohybrid as chemical tracers for graphene oxide (GO) in environmental and biological systems is interesting for ecotoxicological studies.

In this research, GO and GO-Au nanohybrid were synthesised and characterised using several techniques including UV-Vis, TGA, TEM, FTIR, AFM, XPS and Raman. The production of the nanohybrid was repeated a number of times to verify reproducibility of the synthesis protocol. Dispersion stability of the nanohybrid in different environmental media as well as the influence of ageing on its quality were also investigated. A series of assays were performed to assess the toxicity of the nanohybrid on water flea (*Daphnia magna*) and cells [zebrafish embryonic cells (ZF4) and human cancer cells (A549)].

The study successfully generated batches of GO-Au nanohybrid that exhibited reproducible characteristics. The nanohybrid also showed good stability in different environmental media and its physicochemical characteristics did not deteriorate over a period of months. The amount of Au in each of the GO-Au nanohybrid samples was highly comparable, suggesting a potential for use as chemical label. Although the nanohybrid did not induce significant acute immobilization or mortality to neonates of daphnia, signs of stress and bioaccumulation were evident from the morphological images of the exposed organisms. Exposure of the nanohybrid induced dose and time dependent cytotoxicity, apoptosis and necrosis to both ZF4 and A549 cells.

The outcome of this research represents a crucial step forward in the development of a standard protocol for the synthesis of GO-Au nanohybrids. It also paves the way towards a better understanding of the nanotoxicity of GO-Au nanohybrid in biological and environmental systems.

Acknowledgement

All praises and thanks are due to Allah by Whose grace this PhD was completed. Indeed, nothing would have been achieved without His favour and mercy. I sincerely thank my lead supervisor, Prof. Eugenia (Éva) Valsami-Jones for her guidance and support throughout my PhD, and for providing funding support at the end of my scholarship. I also thank my co-supervisor, Dr. Hanene Ali-Boucetta for her supervision and advice. I am very grateful to Dr. Diego Martinez and Dr. Aline De Medeiros for their collaboration and technical support for my research.

The assistance of Nicholas Davidson for extensive laboratory support, Christopher Stark for ICP-MS analysis, Theresa Morris for TEM analysis and Caroline Sewell for daphnia laboratory training were invaluable and highly appreciated. I thank all my wonderful colleagues and staff in GEES, School of Pharmacy and the University of Birmingham at large especially Bashiru Ibrahim for their incredible support and friendship.

I am very grateful to the Nigerian government through Petroleum Technology Development Fund (PTDF) for funding this research. I also appreciate the moral and emotional support of my family and friends. And finally, I sincerely thank my wife and kids for their patience and perseverance during my PhD. In the end, I give thanks to Allah the Lord of the worlds.

List of Publications

This thesis has three research chapters that have been published or in preparation for publication in peer-reviewed journals.

- **Akere, T. H.**, De Medeiros, A. M. Z., Stéfani, D., Martinez, T., Ibrahim, B., Ali-Boucetta, H., & Valsami-Jones, E. (2022). Synthesis and Characterisation of a Graphene Oxide-Gold Nanohybrid for Use as Test Material. *Nanomaterials 2023, Vol. 13, page 33*, *13*(1), 33. https://doi.org/10.3390/nano13010033

- **Akere, T. H.**, Ali-Boucetta, H., & Valsami-Jones, E. (2023). Nanotoxicity of Graphene Oxide – Gold Nanohybrid to Daphnia Magna. *Aquatic Toxicology 2023, Vol. 260 (April), page 1-12*. https://doi.org/10.1016/j.aquatox.2023.106552

- **Akere, T. H.**, Ali-Boucetta, H., & Valsami-Jones, E. (2022). Biodistribution and Biocompatibility of Graphene Oxide-Gold Nanohybrid in Zebrafish embryos (*Danio rerio*) and cells (ZF4). Manuscript in preparation

- **Akere, T. H.**, Ali-Boucetta, H., & Valsami-Jones, E. (2022). Cytotoxicity Assessment of Graphene Oxide-Gold Nanohybrid to Human Lung Cancer Cells (A549). Manuscript in preparation

Table of Contents

List of Figures

List of Tables

List of Abbreviations

%	-	percentage
°C	-	degree Celsius
°C/min	-	degree Celsius per minute
µg/L	-	microgram per litre
µg/ml	-	microgram per millilitre
µL	-	microliter
µM	-	micromolar
2D	-	two dimensional
A549	-	human lung cancer cells
AFM	-	atomic force microscopy
ATCC	-	American type culture collection
ATR	-	attenuated total reflection
Au	-	gold
AuNP	-	gold nanoparticles
B12	-	cyanocobalamin
BHW	-	borehole water
C═C	-	alkene functional group
C═O	-	carbonyl functional group
$C_{76}H_{52}O_{46}$	-	tannic acid
Ca	-	calcium
$CaCl_2 \cdot 2H_2O$	-	calcium chloride dihydrate
CCM	-	cell culture media
Cd	-	cadmium
cm^{-1}	-	inverse centimetre
$cm^2V^{-1}s^{-1}$	-	centimetre square per volt per seconds
CO_2	-	carbon dioxide
Cond	-	conductivity

CRM	-	certified reference material
Cu	-	copper
Cu	-	copper
CuO	-	copper (II) oxide
DLS	-	dynamic light scattering
DMEM	-	Dulbecco’s modified eagle medium
DMSO	-	dimethyl sulfoxide
DNA	-	deoxyribonucleic acid
DO	-	dissolved oxygen
EC_{50}	-	half maximal effective concentration
EDTA	-	ethylenediaminetetraacetic acid
ENM	-	engineered nanomaterial
eV	-	electronvolt
FBS	-	fetal bovine serum
Fe	-	iron
FLG	-	few layer graphene
FTIR	-	Fourier-transform infrared microscopy
g	-	gram
g/L	-	grams per litre
GaD	-	graphene and its derivatives
GO	-	graphene oxide
GO-Ag	-	graphene oxide – silver nanohybrid
GO-Au	-	graphene oxide – gold nanohybrid
H_20_2	-	hydrogen peroxide
H_2O	-	water
H_2SO_4	-	sulphuric acid
H_3BO_3	-	boric acid
$HAuCl_4$	-	chloroauric acid
HCL	-	hydrochloric acid

Hg	-	mercury
HH	-	high hardness
HHC	-	high hardness combo
hr	-	hours
ICP-MS	-	inductively coupled plasma – mass spectroscopy
ICP-OES	-	inductively coupled plasma – optical emission spectroscopy
I_D/I_G	-	intensity ratio of D and G bands
ISO	-	international organisation for standardisation
K	-	potassium
K_2HPO_4	-	potassium phosphate dibasic
KCl	-	potassium chloride
kDa	-	kilodalton
KI	-	potassium iodide
$KMnO_4$	-	potassium permanganate
kV	-	kilovolt
L	-	lysosome
LDH	-	Lactate dehydrogenase
LiCl	-	Lithium chloride
M	-	mitochondria
M	-	molar
mg L^{-1}	-	milligram per litre
Mg	-	magnesium
mg	-	milligram
mg/mL	-	milligram per millilitre
Mg^{2+}	-	magnesium ion
$MgSO_4 \cdot 7H_2O$	-	magnesium sulphate heptahydrate
min	-	minute
mL	-	millilitre

mL/min	-	millilitre per minute
MLG	-	multi-layer graphene
mM	-	millimolar
Mn	-	manganese
MTT	-	3-(4,5-dimethylthiazol-2-yl)-2,5-diphenyltetrazolium bromide
mV	-	millivolts
N	-	nucleus
$n \rightarrow \pi^*$	-	n to pi star interaction
Na^+	-	sodium ion
Na_2SeO_3	-	sodium selenite
$Na_2SiO_3 \cdot 9H_2O$	-	sodium metasilicate nonahydrate
$Na_3C_6H_5O_7$	-	trisodium citrate
NaBr	-	sodium bromide
$NaHCO_3$	-	sodium bicarbonate
$NaNO_3$	-	sodium nitrate
Ni	-	nickel
NM(s)	-	nanomaterial(s)
nm	-	nanometre
NOM	-	natural organic matter
NP(s)	-	nanoparticle(s)
OECD	-	organisation for economic cooperation and development
OH	-	hydroxyl functional group
P	-	potassium
p	-	probability value
Pb	-	lead
PBS	-	phosphate-buffered saline
pH	-	potential of hydrogen

PI	-	propidium iodide
ppb	-	parts per billion
ppm	-	parts per million
PSPD	-	position sensitive photo detector
PTM	-	peritrophic membrane
RbCl	-	rubidium chloride
rGO	-	reduced graphene oxide
rGO-Au	-	reduced Graphene oxide – gold nanohybrid
ROS	-	reactive oxygen species
rpm	-	revolutions per minute
s	-	seconds
SCENIHR	-	Scientific Committee on Emerging and Newly Identified Health Risks
SD	-	standard deviation
$SrCl_2 \cdot 6H_2O$	-	strontium chloride hexahydrate
TEM	-	transmission electron microscopy
temp	-	temperature
TGA	-	thermogravimetric analysis
Ti	-	titanium
TiO_2	-	titanium dioxide -
TN	-	total nitrogen
TOC	-	total organic carbon
UPW	-	ultrapure water
USEPA	-	united state environmental protection agency
UV-Vis	-	ultraviolet-visible spectroscopy
$Wm^{-1}K^{-1}$	-	watt per metre per kelvin
XPS	-	X-ray photoelectron spectroscopy
ZF4	-	zebrafish embryo cells
Zn	-	zinc

ZnO	-	zinc oxide
ζ	-	zeta potential
μm	-	micrometre
π→π*	-	pi to pi star interaction

Chapter 1:

Introduction

1.1. Background

Since the advent of nanotechnology in the 1980s, our society has been transforming remarkably, and will likely continue to do so to meet our growing and evolving needs. Faster and powerful computers, more accurate medical devices, sunscreens, cost and quality efficient water filters are some of the remarkable applications involving nanotechnology. From environmental pollution, to increasing energy demand, scarcity of potable water and biomedical constraints, the quest for solutions to some of the world's problems has driven intense research into nanomaterials [1]. On the forefront of these applications are carbon-based nanomaterials such as graphene and its derivatives [graphene oxide (GO), reduced graphene oxide (rGO)], carbon nanotubes [single and multi-walled nanotubes] and carbon dots [2].

Research into graphite and other carbon materials dates as far back as 1800s [3], [4]. However, none of these efforts describe the unique properties of graphene [5]. The discovery of these properties by researchers from the University of Manchester [6] propelled huge interest in the material. Graphene-based materials represent a recent addition to the nanomaterials family and yet have already found many applications for example in electronics, medicine, agriculture and energy and have been incorporated in many consumer products: drug nanocarriers, high-capacity batteries, lightweight and strong materials for automotive and aerospace, biosensors, biomedical devices, water desalination, anti-corrosion coatings etc [5]–[8].

More recently, research work has focused on exploring multicomponent nanohybrids, which offer the advantage of combining multiple functionalities into

a single advanced material [9]–[11]. A popular combination of such hybrid materials are those involving metal or metal oxide nanoparticles (like TiO_2, ZnO, Au, CuO) and carbon nanomaterials (such as graphene oxide, carbon nanotubes, fullerenes). For instance, both GO and silver nanoparticles are known to exhibit antibacterial properties [12], [13]. However, graphene oxide-silver nanocomposites (GO-Ag) have been reported to have a superior antimicrobial capability compared to their individual components [14], [15].

Similarly, graphene oxide – gold nanohybrid (GO-Au) have been reported to demonstrate synergistic features beyond their individual capabilities such as increased electrical conductivity, catalytic activity, higher surface area, optical and medical properties [16], [17]. These features have rapidly increased the use of such nanohybrids in various applications for example cancer detection, bioimaging and biosensing [18]–[20].

The expanding use of GO-Au nanohybrid in various applications will ultimately lead to their release into the environment, deliberately or unintentionally, from manufacturing facilities as well as throughout the lifecycle of the products. Released nanomaterials from atmospheric emissions, solid waste and waste water effluents will eventually deposit on land or leach to ground and surface waters [21].

Unlike natural nanomaterials that plants and animals have adapted to, engineered materials (especially emerging ones such as nanohybrids) pose novel threats that require critical evaluation of their potential harm to humans and

ecosystems. As with any new discovery, there are concerns about the potential of novel nanohybrids to cause toxicity over and above that of their individual components [22], [23]. Their safety to the ecosystem and human health is yet to be fully demonstrated since the very features that make them so advanced may also be the source of concern to ecotoxicologists, specifically in terms of their ability to bypass biological barriers.

1.2. Research Gap

Currently, literature search did not identify any toxicity studies of a GO-Au nanohybrid. The nearest toxicity study are two research works on the toxicity of reduced graphene oxide-gold nanocomposite (rGO-Au) – one on daphnia [24] and the other on algae [25]. However, reduced graphene oxide is markedly different from GO in terms of mechanical strength, electrical conductivity, dispersion stability and hydrophilic behaviour [26]–[28]. In addition, these studies used nanocomposites – mixture of nanomaterial with other matrices – which are very different from nanohybrids that are formed by the combination of nanomaterials via chemical bonding [29].

Also, there is no standardized protocol for the synthesis of GO-Au nanohybrids. It is therefore unclear how in different formulations the two components are conjugated, quantitatively and qualitatively, and whether performance, but also potential ecotoxicity, may be affected. Most of the available research work on GO-Au has focused on the applications of the nanohybrid [18], [19], [30]. For ecotoxicological studies however, it is important that critical physicochemical

parameters of the GO-Au nanohybrid are evaluated and correlated to its toxicity. This is to ensure reproducibility and compatibility of the results.

1.3. Aims and Objectives of Research

The general aim of this PhD research is to understand the behaviour, fate and toxicity of a GO-Au nanohybrid in the environment. Specifically, the research aims to develop a standardised protocol for the synthesis of a GO-Au nanohybrid and evaluate the nanotoxicity of this nanohybrid in different biological models. This overall aim has been divided into three distinct sub-aims and are described below.

1.3.1. Aim One

The first aim is to synthesise and characterise graphene oxide (GO) and a graphene oxide-gold nanohybrid (GO-Au). GO was synthesised using a modified Hummer's method as described by Becerril et al. (2008). The GO-Au nanohybrid was synthesised using the synthesised GO and chloroauric acid as a gold precursor using a modification of the protocol developed by Song et al. (2014). The GO and GO-Au nanohybrid were characterised by ultraviolet-visible spectroscopy (UV-Vis), dynamic light scattering (DLS), Raman spectroscopy, transmission electron microscopy (TEM), atomic force microscopy (AFM), thermogravimetric analysis (TGA), Fourier-transform infrared microscopy (FTIR), X-ray photoelectron spectroscopy (XPS) and inductively coupled plasma – optical emission spectroscopy (ICP-OES).

1.3.2. Aim Two

The second research aim was to assess the nanotoxicity of GO and GO-Au nanohybrid on neonates (less than 24hr old) of *Daphnia magna*. A 48hr acute immobilisation test was carried out to investigate mortality and immobilisation of daphnids exposed to GO and GO-Au nanohybrid. The toxicity test carried out was an acute immobilisation assessment carried out on daphnia and a bioaccumulation study. Sequel to the toxicity tests, TEM imaging of daphnia tissue and ICP-MS quantification of the Au in the exposed organisms were performed. The dispersion stability of the nanomaterials in daphnia culture media (borehole and HH combo) and a chemical analysis of both culture media were also evaluated.

1.3.3. Aim Three

The third research aim was to investigate the cytotoxic effect of GO and GO-Au on two cell lines: zebrafish embryonic cell (ZF4) and human lung cancer cells (A549). The cell assays undertaken were MTT, LDH, cellRox and apoptosis/necrosis. In addition, dispersion stability of GO and GO-Au nanohybrid in the cell culture media were performed.

1.4. Thesis Structure

The first chapter of this thesis is an introduction to the research area and justification for the work. The aims and objectives of the research are enumerated and broadly described. The chapter also covers a review of the literature relating

to the main areas of this research. This includes foundational knowledge about nanomaterials, nanotechnology, graphene oxide and graphene oxide-gold nanohybrids. It also explores ecotoxicology and factors influencing their assessment. Daphnia as a model aquatic toxicity organism as well as cells and cytotoxicity mechanisms are described.

The second chapter covers the analytical and experimental methodologies used in the research. Synthesis process of the nanomaterials, characterization techniques and protocols for the daphnia toxicity experiments and cellular toxicity are described. The third chapter presents the results of the synthesis and characterization of GO and GO-Au nanohybrid. In the fourth and fifth chapter, results and discussion on the nanotoxicity assessment of GO and GO-Au nanohybrid on daphnia and cells are presented respectively. The last chapter (sixth) concludes the thesis with recommendations for future work.

1.5. Nanotechnology and Nanoparticles

Nanotechnology (also known as nanotech) is the term used to describe the industrial development, design and use of matter that has at least one-dimension in the nanoscale: 1 to 100nm (**Figure 1**). The origin of nanotechnology as a concept is credited to a speech given by Richard Feynman at a meeting of the American Physics Society in 1959 [33] while the term nanotechnology was first used by Norio Taniguchi [34]. Nanotechnology has inspired the manufacturing of numerous novel devices and materials for a diverse range of applications in energy, agriculture, medicine, aerospace, consumer goods, military, transportation etc [35].

According to the European Commission's Scientific Committee on Emerging and Newly Identified Health Risks (SCENIHR), particles that possess one or more of their dimension in the size range between 1 and 100 nm are referred to as nanoparticles [36]. Nanomaterials (NMs) is defined by the same organisation as "material with one or more external dimensions in the nanoscale, or an internal structure, which could exhibit novel characteristics compared to the same material without nanoscale features". The development and use of nanomaterials is of great interest to scientists due to their relatively large surface to volume ratio which is a crucial factor in enhancing other mechanical and physical features [37].

1.5.1. Natural and Engineered Nanomaterials

The presence of natural nanoparticles can be traced back to millions of years ago during the formation of the Earth over billions of years ago [38]. They have been ever-present and occur across all the spheres in the earth. Despite their widespread presence around humans, natural nanoparticles have only been discovered and studied few decades ago as a result of advancement in analytic methods which enabled their observation along with a better understanding of their unique attributes.

Unlike natural nanoparticles, their engineered counterparts, described as engineered nanomaterials (ENMs), are manufactured by humans through manipulation of their properties to suit specific applications. ENMs are fabricated to enhance consumer goods and solve problems in many technical frontiers [39]. In terms of quantity, ENMs can provide the same functionality in much smaller

volumes compared to natural nanomaterials. ENMs can be synthesised to have defined shapes and sizes for specific applications. They are required to undergo extensive characterization which is necessary to minimise unintended effects [40].

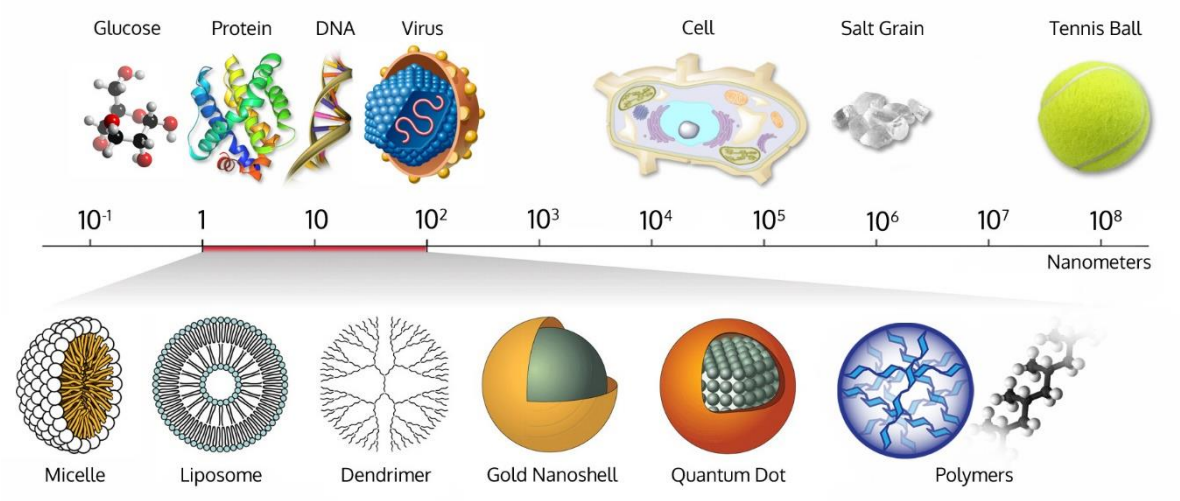

Figure 1: Size comparison of bio-nanoparticles on a nanometre scale [41]

1.5.2. Nanohybrids and Nanocomposites

Technical developments have now reached beyond the use of individual nanomaterials and are looking for bringing additional functionalities by combining or merging different types of nanomaterials e.g. metals and carbon-based materials. The quest to find solutions to human and environmental challenges have driven research into exploring the combination of organic and inorganic substances (**Figure 2)**. The products of this merger are new superior materials that combine multiple features [42]. The surface of carbon-based materials such

as graphene oxide that is rich in electron and oxygen enables functionalisation with inorganic molecules for various applications.

A nanocomposite is a physical mixture of materials that have at least one of their components in the nanoscale range (1-100 nm). Nanohybrids, on the other hand, are materials formed when the inorganic component is synthesised *in situ* or when the materials are bound via chemical bonding [43].

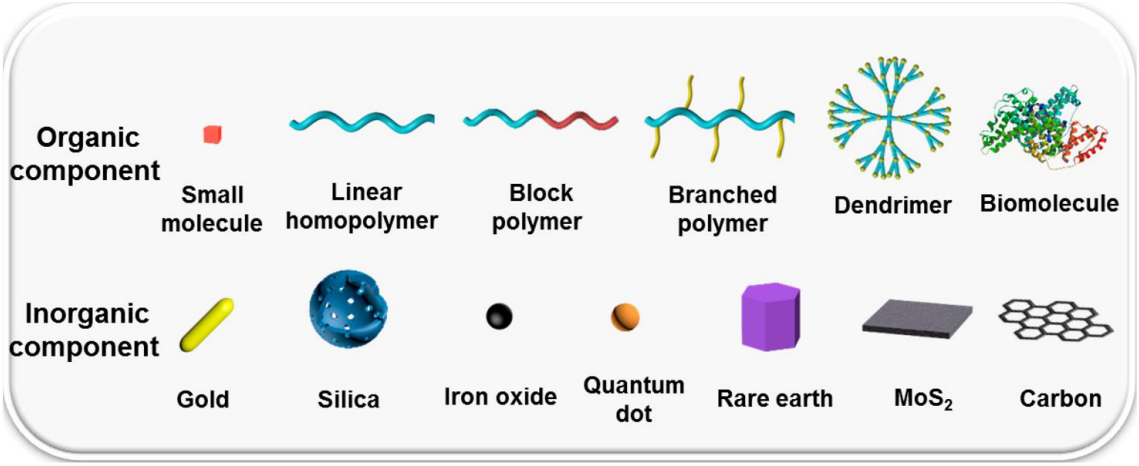

Figure 2: Common inorganic and organic components used in making nanohybrids [11]

1.6. Graphene and its derivatives (GaD)

Graphene is a form of carbon with an atom thick layer of carbon atoms arranged in hexagonal lattice. Graphene, a two-dimensional (2D) structure, is the basic structure of many other forms of carbon such as graphite fullerenes and carbon nanotubes [44]. Carbon nanotubes and fullerenes are essentially graphene sheet 'rolled up' to tube and ball shape respectively, while graphite is made up of several stacked sheets of graphene held together by Van der Waals forces [45] (**Figure 3**).

Graphene is derived from graphite which is a stack of graphene layers held together by van der Waal force. Having a thickness of just one atom and density of 0.77 mg/m^2 makes graphene the thinnest and the lightest known material respectively [46]. Graphene is nearly transparent (takes in only 2.3% of light) and many times stronger than steel. It is a great conductor of heat and electricity, better than copper [47].

Graphene oxide (GO), reduced graphene oxide (rGO), few layer graphene (FLG), multi-layer graphene (MLG) and graphene nanosheets are considered as the graphene derivatives or family. The surface chemistry of the GaDs varies significantly, and this determines their chemical properties such as dispersibility, stability and hydrophilicity or hydrophobicity [48].

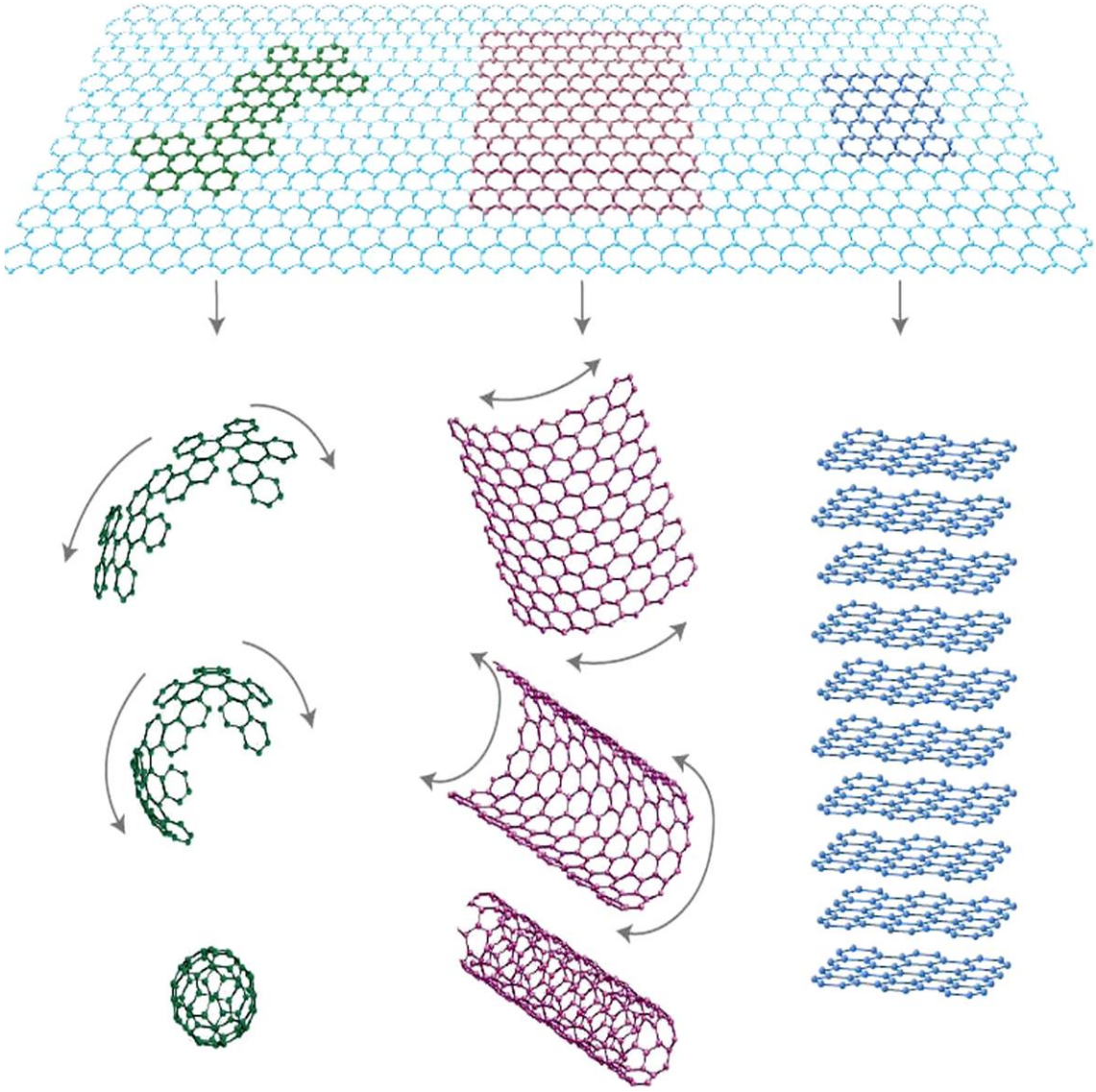

Figure 3: Graphene (top) and other forms of carbon. Bottom L-R: fullerene, carbon nanotubes and graphite [1]

1.6.1. Properties

The key properties of graphene are briefly described here and summarised in **Figure 4**.

(a) Reactivity

Graphene has high chemical reactivity because all its atoms are available for reaction from two sides (the only form of carbon to be able to do so). The more the defects in a graphene structure, the higher the reactivity. Stanford researchers also found single layer graphene to be far more reactive than any multilayer variant [49].

(b) Thermal Conductivity

Graphene has high thermal conductivity. Early studies reported a very high thermal conductivity for suspended single layer graphene of 5300 $Wm^{-1}K^{-1}$ [50]. However, lower values in the range of 1500 – 2500 $Wm^{-1}K^{-1}$ [51], [52] were measured by later studies. The large disparity could be as a result of graphene quality and measurement techniques.

(c) Electron Mobility

This is the measure of how fast an electron can move through conductors and semiconductors. Graphene is known to have remarkable charge carrier mobility of more than 200,000 $cm^2V^{-1}s^{-1}$ [5].

(d) Mechanical Strength

The breaking strength of graphene was observed by Changgu et al [53] to be 1.0 tera pascals (Young's modulus) and the intrinsic tensile stress was 130 gigapascals. This is more than 100 times stronger than copper, establishing graphene as the strongest substance ever measured.

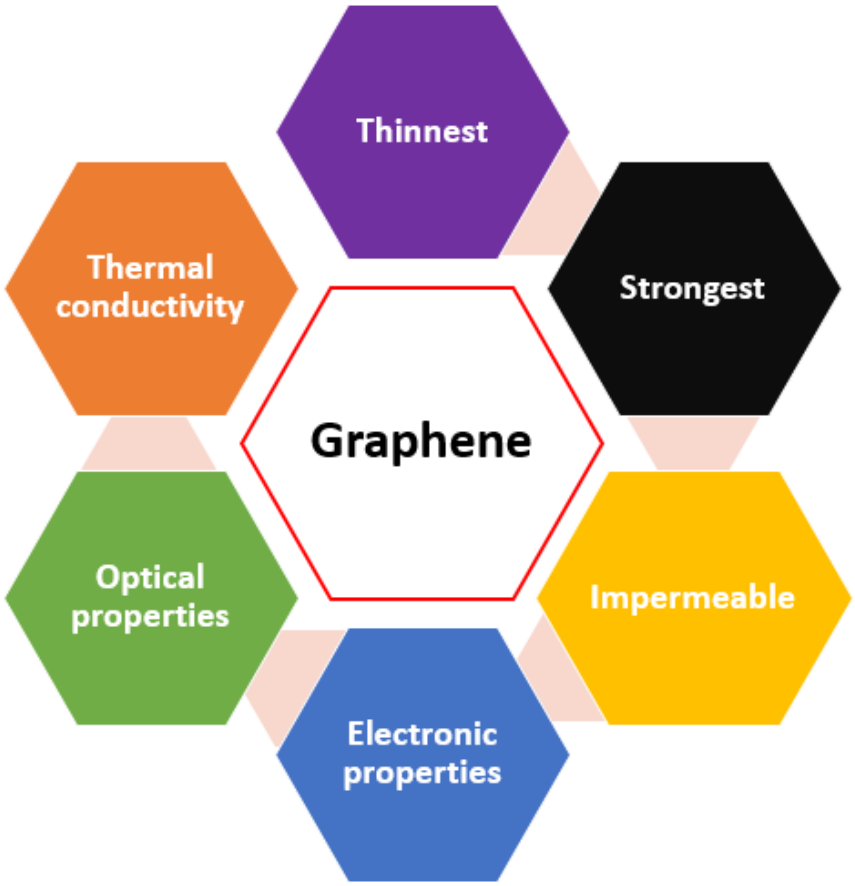

Figure 4: Highlight of some of the key features of graphene

1.7. Graphene Oxide (GO)

GO is a single-layered variant of graphene with many oxygenated functional groups produced through the oxidation of graphite with powerful oxidants (**Figure 5**). GO is composed of oxygen, hydrogen and carbon molecules. Unlike graphene, GO is hydrophilic making it soluble in many aqueous and organic solvents [54]. However, GO is an electrical insulator and has low electrical conductivity. GO has many unique properties that have made it useful for many applications.

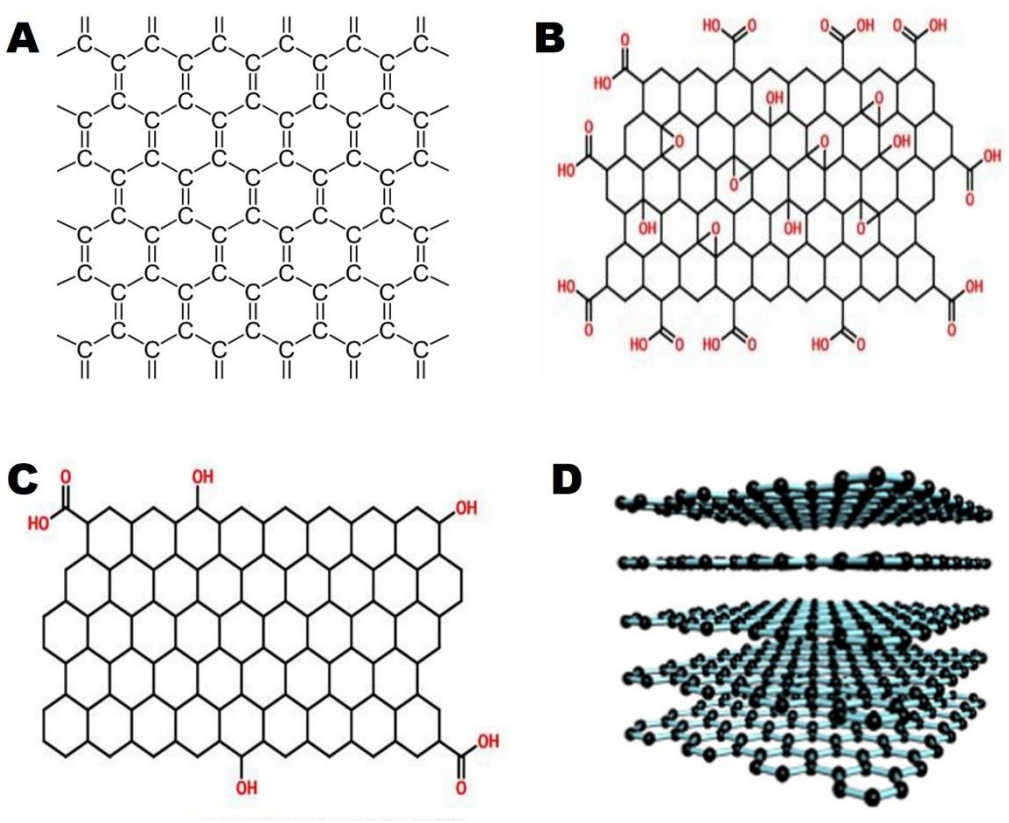

Figure 5: Molecular structure of graphene (A), graphene oxide (B), reduced graphene oxide (C) and few layer graphene (D)

1.7.1. Applications of GO

The main applications of GO are briefly described here and summarised in **Figure 6**.

(a) Electronics

The electrical conductivity properties of GO has been exploited in electronic processes and devices such as screen and inkjet printing [55], field effect transistors [56] and light emitting diodes [57].

(b) Energy Storage

Highly efficient solar cells that are durable and have high quantum efficiency are now being made from materials based on GO sheets [58], [59]. GO is also being used as components in making solar cell electrodes.

(c) Membranes

GO-based membranes have been developed that are totally impermeable to all substances except water or allows selective movement of liquid, vapor and gaseous substances [60], [61]. This application is useful for water filtration and gas separation.

(d) Biomedical Applications

Fast and sensitive biosensors for detecting biomolecules are being made with GO, thanks to their affinity for some proteins and DNA [62]. Also, functionalised GO have been applied in gene and drug delivery for cancer treatment [63], [64].

(e) Environmental Application

The ability of GO to form both covalent and noncovalent bonds with many molecules makes it useful in making composites for removing toxic gases released by industrial process from the atmosphere [65]–[67]. GO has also been used in converting one of the major greenhouse gases into less harmful substances [68], [69].

(f) Water Purification

GO has high adsorption ability which has been harnessed in water purification. Scientists have been able to demonstrate the removal of water pollutants such heavy metals and organic dyes from aqueous solutions [70]–[72].

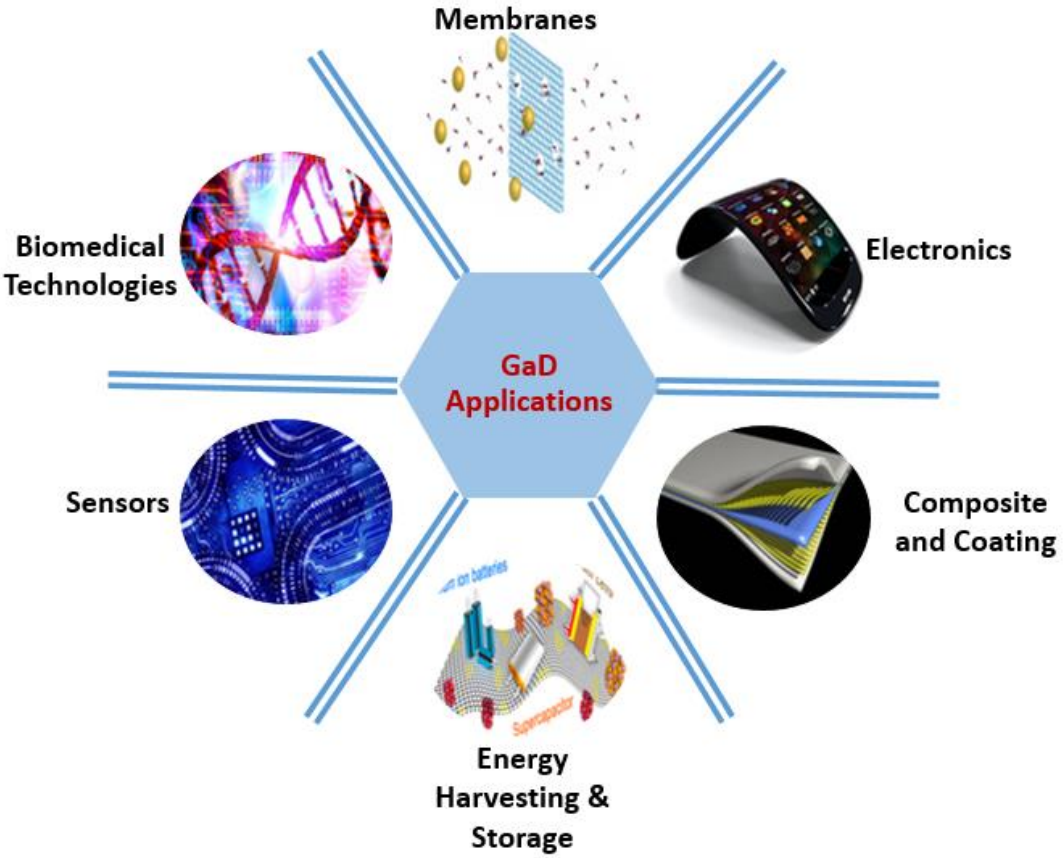

Figure 6: Schematic highlighting some of the applications of GO

1.7.2. Synthesis of GO

Few methods exist for the synthesis of GO. They mostly involve oxidising graphite with strong agents in an acidic medium. The pioneering attempt at synthesising GO was made by Benjamin Brodie in 1859 [4]. In his work, graphite was treated with two strong oxidising agents: fuming nitric acid and potassium chlorate. He named the product “graphic acid” due to its weak acidity. Another researcher, L Staudenmaier, modified the Brodie’s method by adding a new reagent and altering some steps [4]. He introduced sulfuric acid and added minute quantities of potassium chlorate in a sequence to reduce the risk of explosion.

Hummer's method, developed by Hummers and Offeman in 1957 [73], is the most widespread synthesis method for GO due to its relative ease and effectiveness. However, the method is considered not to be eco-friendly due to the release of toxic NOx during the synthesis [74]. Hence, several modifications of the Hummers methods were developed [75]–[78]. The modified Hummers method (**Figure 7**) involves stirring high quality graphite in concentrated sulphuric acid and strong oxidizing agents (potassium permanganate and sodium nitrate). Hydrogen peroxide is used at the end of the reaction to neutralise excess potassium permanganate. The mixture is finally washed with hydrochloric acid and water.

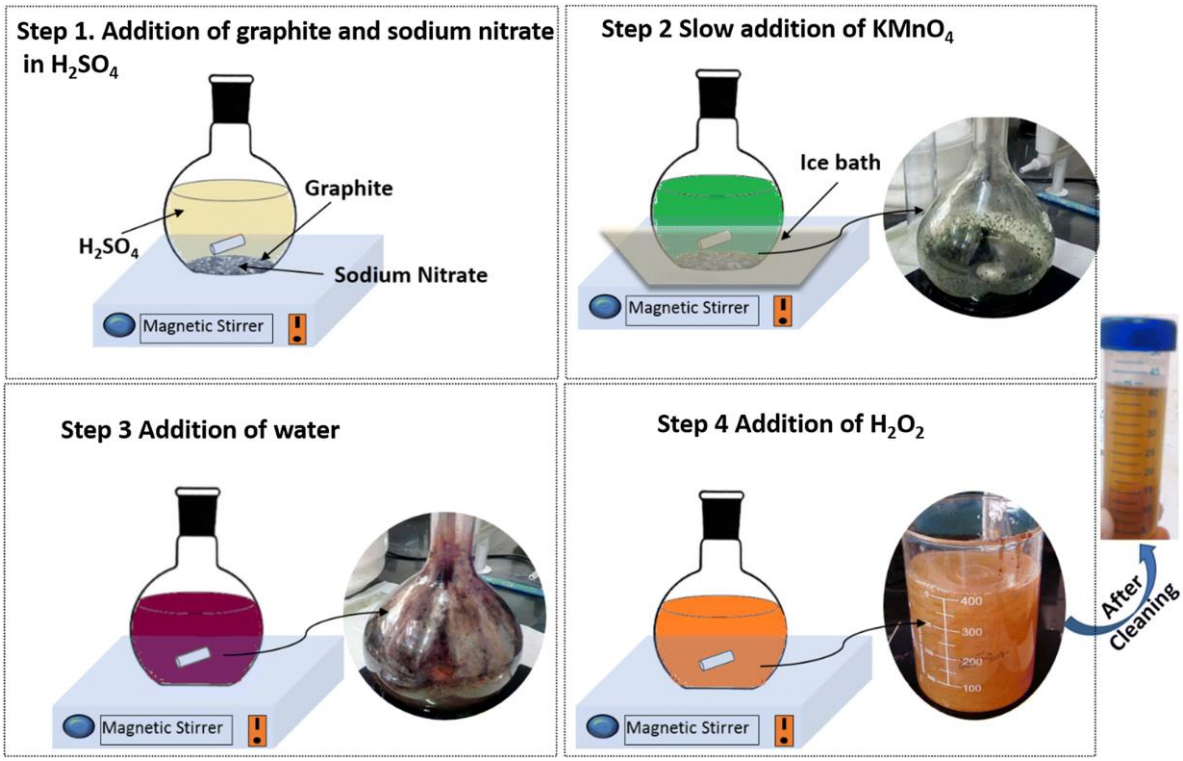

Figure 7: A step-by-step description of the modified Hummer's method for GO synthesis [79]

1.7.3. Toxicity of GO

The large surface area and small size of GO gives it the potential to cause harm. The toxicity of GO is determined by a range of factors including concentration, functional group, surface charge, shape and size [48]. For instance, GO tends to be stable in the presence of high organic matter, and vice versa [80]. Consequently, the stability of GO in dispersion media influences its bioavailability and uptake by aquatic organisms. The toxicity of GO is due largely to the induction of reactive oxygen species (ROS) production which causes oxidative stress [81].

Many studies have been carried out to understand the ecotoxicity of GO to mono- and multicellular organisms across the food chain including bacteria [82], microalgae [83], human cells [84], worm [85], fish larvae [86], daphnia [87]–[89], zebrafish [90], mice [91]. Many of these studies have reported that GO induces oxidative stress, loss of cell viability and damage to internal structures. However, there are mixed results on other endpoints such concentration/dose- and time-dependent effects. As such, a clear-cut conclusion on the ecotoxicological effects of GO is difficult to reach. This is due to differences in the characterization of the GO used and the experimental setup [92].

1.8. Graphene Oxide – Gold Nanohybrid

Research into the functional modification of GO is rapidly progressing due to the relative ease of processing and mass production. Interestingly, functionalisation not only prevents agglomeration of GO in aqueous media but it also preserves the inherent properties of GO and gives rise to new characteristics [9]. A hybrid of GO and AuNPs has been found to exhibit interesting characteristics such as increased electrical conductivity, catalytic activity, higher surface area, optical and medical properties etc [93], [94]. These synergistic features make the GO-Au nanohybrid suitable for application as nanosensors and catalyst for industrial processes [30].

1.8.1. Applications of GO-Au Nanohybrid

1.8.2. Biosensors

An aptasensor based on GO, Au and DNA nanohybrid was developed for copper ions detection [95]. The novel large-scale substrate is reported to have wide application in biosensing.

1.8.3. Chemical Synthesis

Owing to AuNPs affinity for some metal oxides and substances like silica [96], a GO-Au nanohybrid has shown promising application as catalyst for oxidation and hydrogenation reactions [16].

1.8.4. Biomedical Application

A nanomotor technique made of GO and Au nanoparticles was developed for screening cancer cells. The fast and accurate method enables detection of miRNA at single-cell level [97].

1.8.5. Electrochemical

A GO-Au nanohybrid was used to fabricate high-performing electrodes that were able to sensitively and selectively detect ascorbic acids in pharmaceutical products and human serum [32].

1.9. Fate, Behaviour and Toxicity of GO and GO-Au

Similarly to other nanomaterials, the expanding use of GO and GO-Au nanohybrid in numerous applications predisposes the environment and humans to the uncertainties around their ecotoxicological effects. As the nanomaterials enter environmental and biological systems, many changes that can influence their fate, movement and toxicity could occur such as aggregation, dissolution, degradation, oxidation and reduction reactions with bio- micro and macromolecules [98]. These changes may alter the chemical composition and physical properties of GO and GO-Au nanohybrid [99]. An understanding of these changes is therefore necessary in evaluating their risk to human health and the environment.

Under relevant environmental conditions, GO can become highly reactive and undergo reduction reactions. GO can be reduced by sunlight exposure and reducing agents typically present in the aquatic environment. Another important factor is adsorption to organic (such as proteins and natural organic matter) and inorganic (such as heavy metals) matter in aquatic media [100]. This can trigger chemical reactions, modify the surface of GO and influence transport of adsorbed species [101]. The interaction of GO with humic acid, for instance, is known to improve GO stability [102]–[104].

The ability of GO to form moderately stable dispersions can be attributed to the hydroxyl, carboxyl and epoxy functional groups on its surface which makes GO hydrophilic in nature [105]. However, GO stability is also affected by the chemical nature of solution. One of the key factors influencing the stability of GO in solution is electrostatic repulsion between each of the GO sheets [106]. The degree of repulsion can be altered by GO sheet size and pH, resulting in aggregation or dispersion of the GO.

The degradation of GO can occur in many forms (**Figure 8**). Photodegradation of GO can happen as a result of exposure to UV radiation [100]. GO can also undergo degradation during industrial application as catalyst. Interaction of GO with mono- and multicellular organisms often ends in depuration and biodegradation in the digestive tract, resulting in a more defective GO than the original GO [107]–[109].

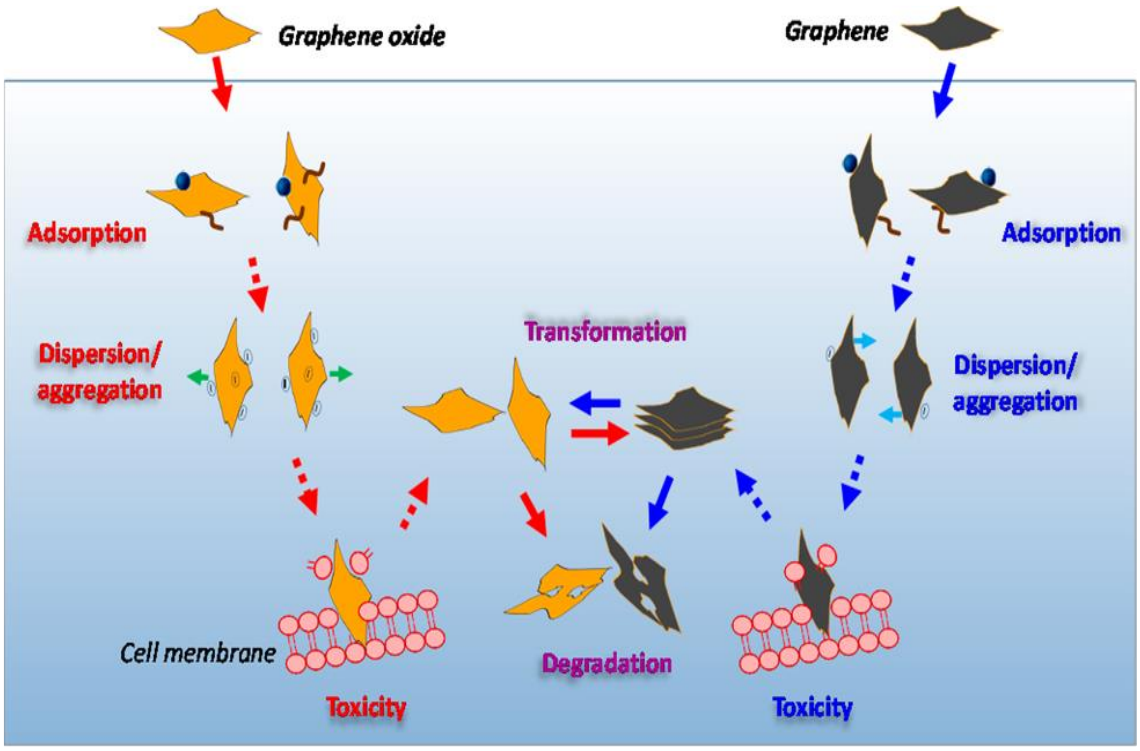

Figure 8: Environmental behaviour of graphene and GO [100]

1.10. Daphnia: A model organism

The use of daphnia for research in natural science and ecotoxicological studies dates back many centuries [110]. Daphnia play an important role in the food web as primary consumers. These freshwater organisms have become a model species for ecotoxicological research for many reasons: (1) they are sensitive to chemical and biological changes in their environment; (2) they are relatively easy and inexpensive to culture and manage; (3) the transparent nature of their body makes direct observation suitable for some experiments; (4) daphnia can be found in many aquatic environments; (5) they produce clones through asexual reproduction that are useful for experimental comparison and reproducibility.

These characteristics have led to the development of several test standards for using daphnia in ecotoxicology [111]–[115]. Daphnia are commonly used as fish feed in aquaculture and as test organisms in ecology and ecotoxicology [116].

1.10.1. Biology and Ecology of Daphnia

Daphnia are small freshwater crustaceans that are found in the northern hemisphere and southern Africa. They belong to the Phyllopoda subclass due to their possession of gills and appendages (**Figure 9**) [117]. As filter feeders, daphnia feed on loose organic matters, bacteria and unicellular algae, and are usually found in shallow lakes and ponds. There are up to 50 species of genus Daphnia, with *Daphnia magna* being one of the most common [118]. Daphnia reproduces by cyclic parthenogenesis, an alteration of sexual and asexual reproduction cycles [119].

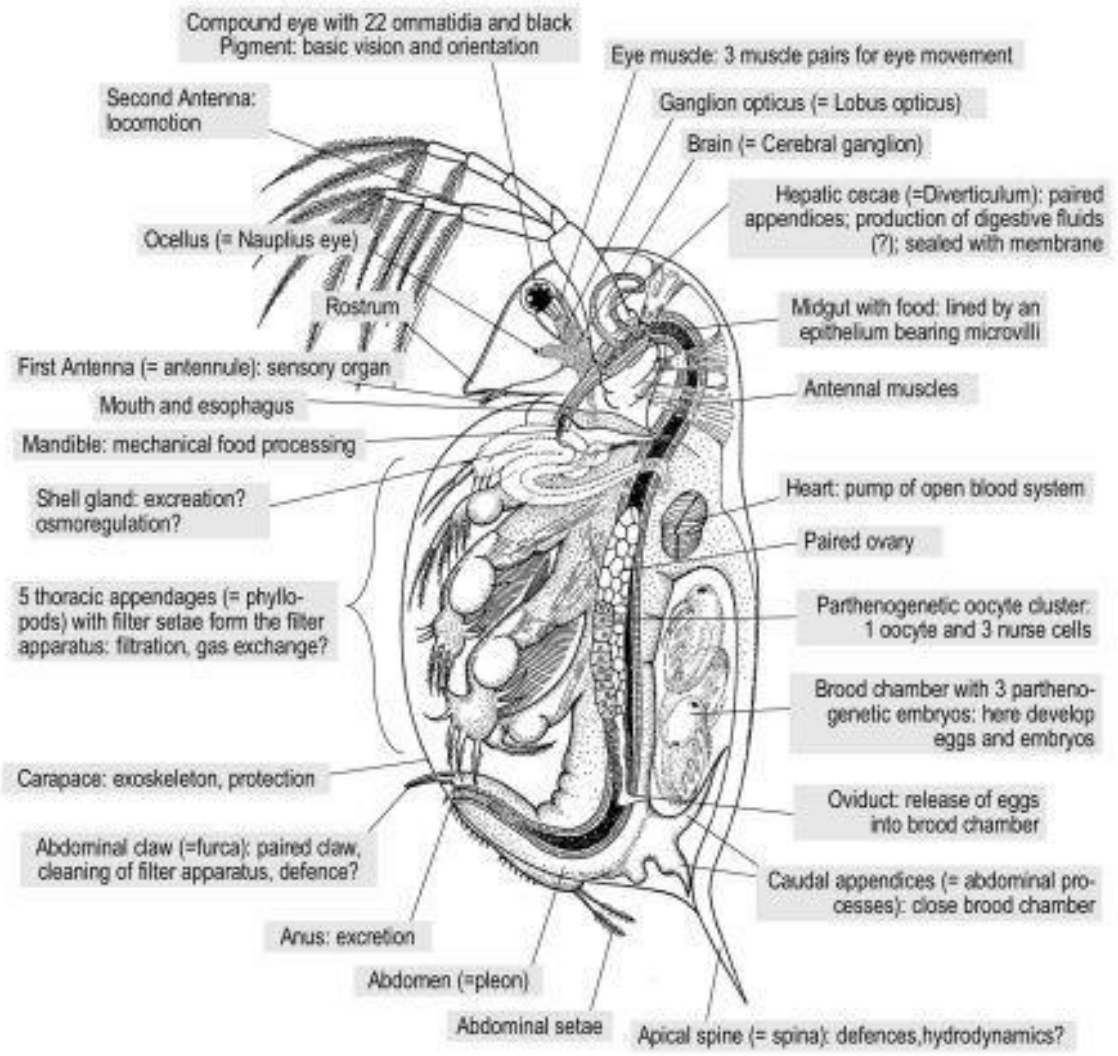

Figure 9: Schematic of the functional annotation of the anatomy of daphnia [118]

1.10.2. Use in ecotoxicology

Daphnia have been extensively used for ecotoxicological studies [120]–[123]. Both lethal (mortality, immobilisation) and sublethal effects (growth, feeding habit, swimming pattern) are commonly used as endpoints in many daphnia experiments (**Figure 10**). Lethal effects are determined by EC_{50} - concentration of the toxicant that causes effect on 50% of the exposed organism. A daphnia is considered dead if no heartbeat is produced while they are considered immobile if they are unable to swim at least 15 seconds after mild agitation. A daphnia acute toxicity test usually last for 48 – 72 hrs while chronic studies run for 7-21 days.

The toxicity of a wide range of substances has been tested on daphnia including nanoparticles [124]–[126], fullerenes [127], [128], GO [129], polymers [130], heavy metals [131], organic pollutants [132], pharmaceutical products [89] and nanoplastics [133]. The studies revealed that the mechanism of lethal toxicity in daphnia is induction of oxidative stress and damage to internal. Other sublethal effects reported are loss of body parts, growth distortion and irregular swimming patterns.Toxicity of chemical substances to daphnia is concentration and time dependent. Exposure within 24hrs does not often induce severe harm to daphnia, whereas severe damage can be inflicted when the exposure time is extended to 48 - 72 hrs [87], [132]. Daphnia have also shown the ability to bioaccumulate a variety of organic and inorganic substances [134]–[136]. The substances are then released from the organism’s gut (depuration) within a short time after the end of exposure period.

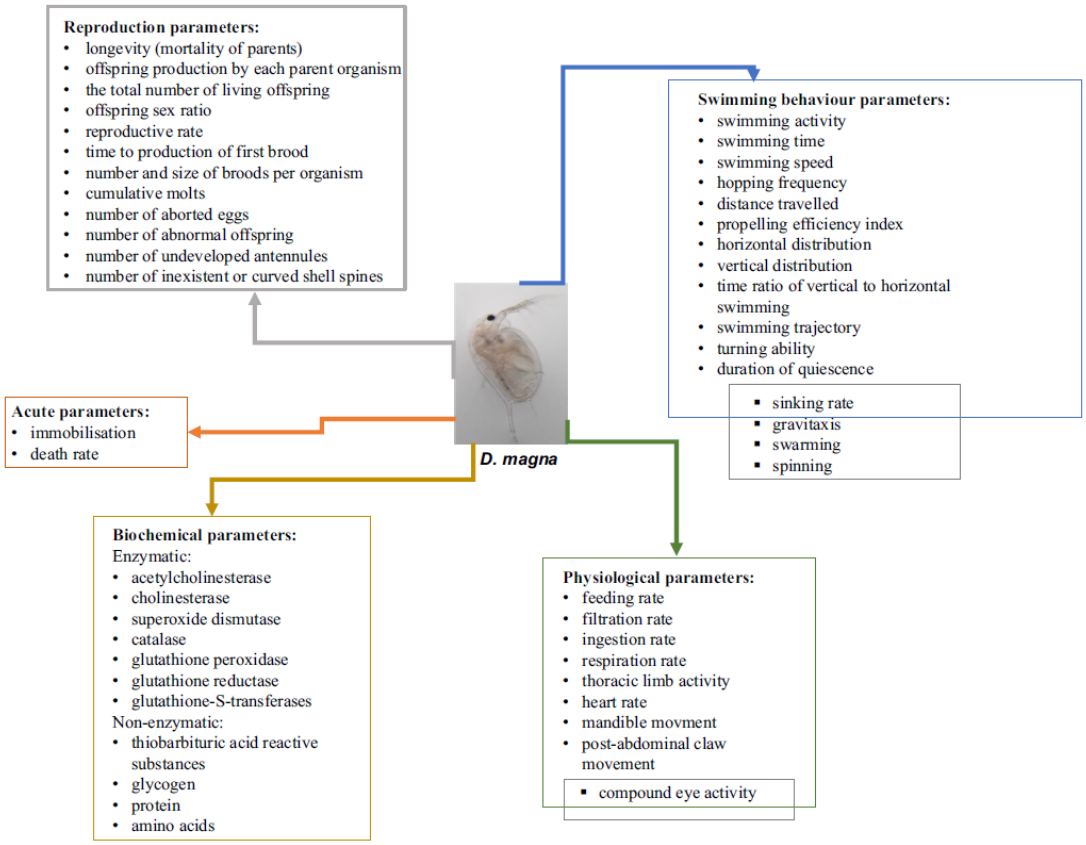

Figure 10: Parameters commonly used in assessing toxicity in daphnia [89]

1.11. Cytotoxicity Mechanism

Organic and inorganic nanomaterials have remarkably been used for numerous medical applications such as pharmaceutical products, targeted drug delivery, medical implants, detection of macromolecules [137]–[139]. The efficiency of these applications is directly related to the successful interaction of the NMs with cell's intra and extracellular components [140]. However, this interaction can also trigger biological responses from the cell after internalisation. Many nanotoxicological studies have demonstrated the adverse effects that NMs can cause in various cells [141]–[143], chiefly due to the inhibition of cell growth, generation of ROS that causes oxidative stress, DNA damage and cell death.

The inherent morphological features of NMs such as size, shape and surface charge can be an additional source of toxic effects on cells. In addition, coatings and functional groups present on the surface of NMs have influence on the response from biological system [144]. Even the number of particles arriving at the membrane interface is an important factor in the internalisation process and subsequent response [140].

The safe manufacturing and application of nanotechnology especially in healthcare and biomedical applications necessitates that crucial cellular toxicity assessments of NMs be undertaken before commercial use. It is therefore important to understand the mechanisms underlying the complex NMs-cell relationship.

1.11.1. Interaction of NMs with cells

The application of nanomaterials in biomedicine can only be achieved if they successfully interact in succession with extracellular environment, cell membrane, cytoplasm and internal organelles such as nucleus and mitochondria [140]. Upon interaction with cells, NMs can be internalised and subsequently produce biological responses (**Figure 11**). The extent and kind of response is influenced by many factors, mainly as a result of the physical and chemical attributes of the NMs, the type of cell or tissue involved and the intracellular interaction of NPs with cell organelles [145]. A suitable level of interaction is necessary for biomedical applications, as weak interaction of NMs can lead to feeble collision with cell membrane resulting in adhesion.

The most important agent of influence on the interaction of cells and NMs is the chemical makeup of the NMs such as surface charge, shape, size, functional groups, hydrophilic or hydrophobic nature. These factors determine the uptake by the cells and subsequent interaction of the cell structures with the NPs [146].

The process of ingestion of substances by cells, known as endocytosis, can be divided into two depending on the type of substances taken in [147]–[149]. Phagocytosis (cell eating) is the cellular ingestion of large particulate matter (greater than 0.5 μm) such as cell debris and bacteria. This only occurs in certain types of cells that are specialised in consuming large entities such as dead cells and pathogens [150]. On the other hand, most eukaryotic cells undergo pinocytosis (cell drinking) – the process of ingestion of dissolved molecules in extracellular fluid. Pinocytosis is further split into divisions based on the fate of the molecule being internalised and the molecular mechanisms [151], [152].

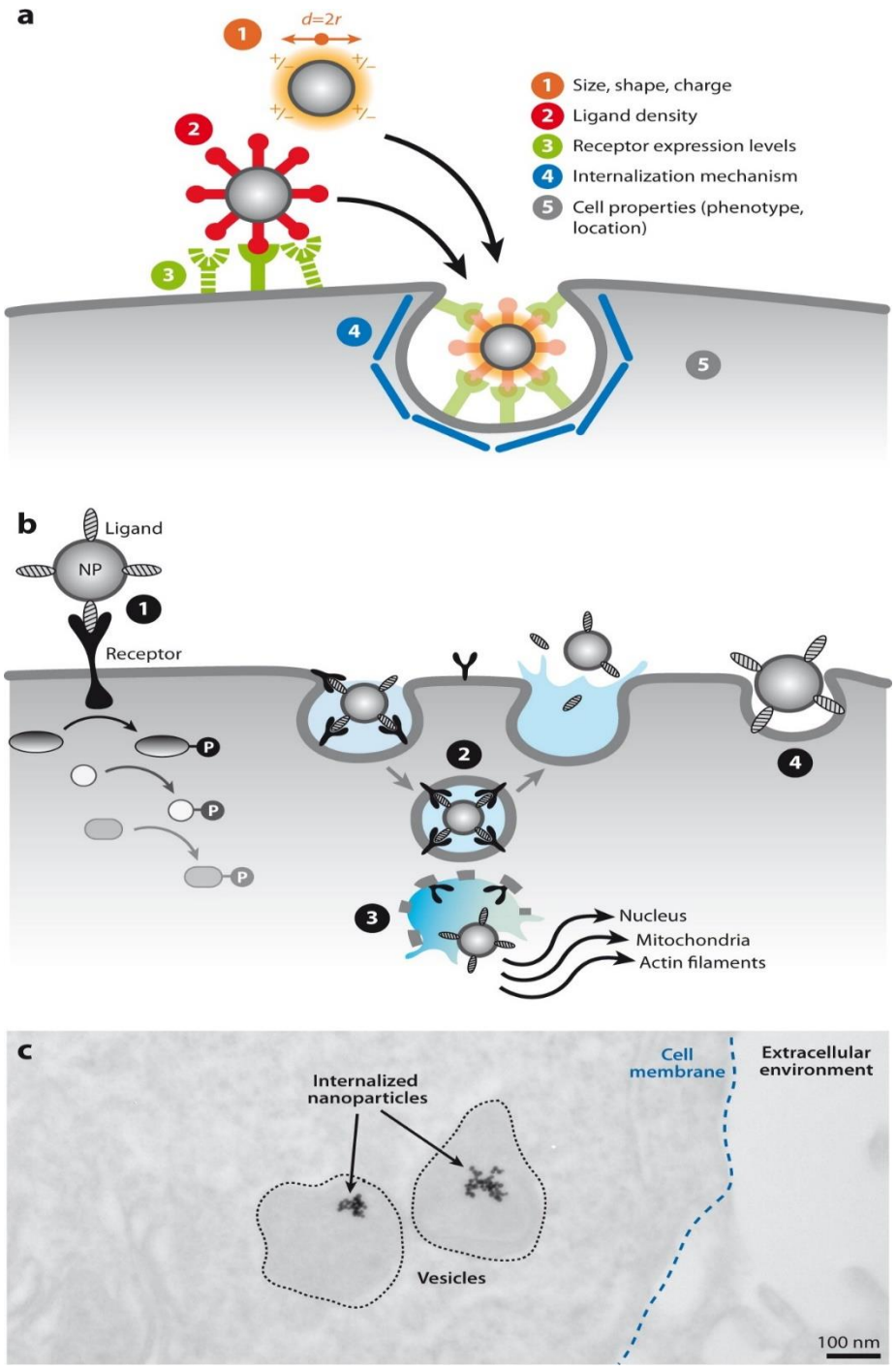

Figure 11: Description of the interaction of cells and nanomaterials (NMs). (a) Some of the factors that affect the cell-NMs interaction (b) cells interacting with NMs coated with ligands, NPs-L. ❶ NPs-L attaches to receptors on the cell membrane, triggering a signalling cascade outside the cell. ❷ Internalisation or exocytosis of the NPs-L can also occur in a vesicle. After attaching to membrane receptors, NPs-L enters the cell before exiting ❸ Internalised NPs can leave the vesicle and interrelate with cell organelles ❹ The cell membrane and NPs can also interact in a nonspecific manner. (c) 15nm gold NPs coated with transferrin are internalised by HeLa cells [144]

1.12. Models for cytotoxicity assessment

The growing public concern against the use of animals for scientific research has promoted the search for alternatives that totally avoid the use of animals or minimise the suffering or number of animals used [153]. The principles of 3Rs developed many decades ago advocate for the replacement of animals in scientific research or reduction in the number and pain that live animals are exposed to [154]. *In vitro* assays (use of cells) are considered a suitable replacement to animal testing due to minimal ethical concerns, cheap cost and quicker process [155]. In addition, assessment of toxicity using *in vitro assays* has the advantage of avoiding the use of whole animal or altering the animal's physiology [156].

1.12.1. Zebrafish embryo cells (ZF4)

The use of zebrafish (*Danio rerio*) and its cell lines as models for biomedical and ecotoxicological research has increased in recent times [157]. This is mainly due to the vast genetic study and conservation of the biochemical pathway between mammals and zebrafish [158]. The ZF4 cell line, derived from a day-old zebrafish embryo, has shown huge potential as a model cell for ecotoxicological studies and biomedical research [159] (**Figure 12**). The ZF4 cells are particularly attractive for research due to their ability to grow at room temperature, remaining viable for extended periods and their potential for high throughput testing [160]. ZF4 has been used for a wide range of research such as toxicity of nanoparticles [161] and rare-earth metals [162], mineral deficiency in fish [142], assessment of

oxidative stress [163], ROS generation [164] and development of antiviral vaccine [163].

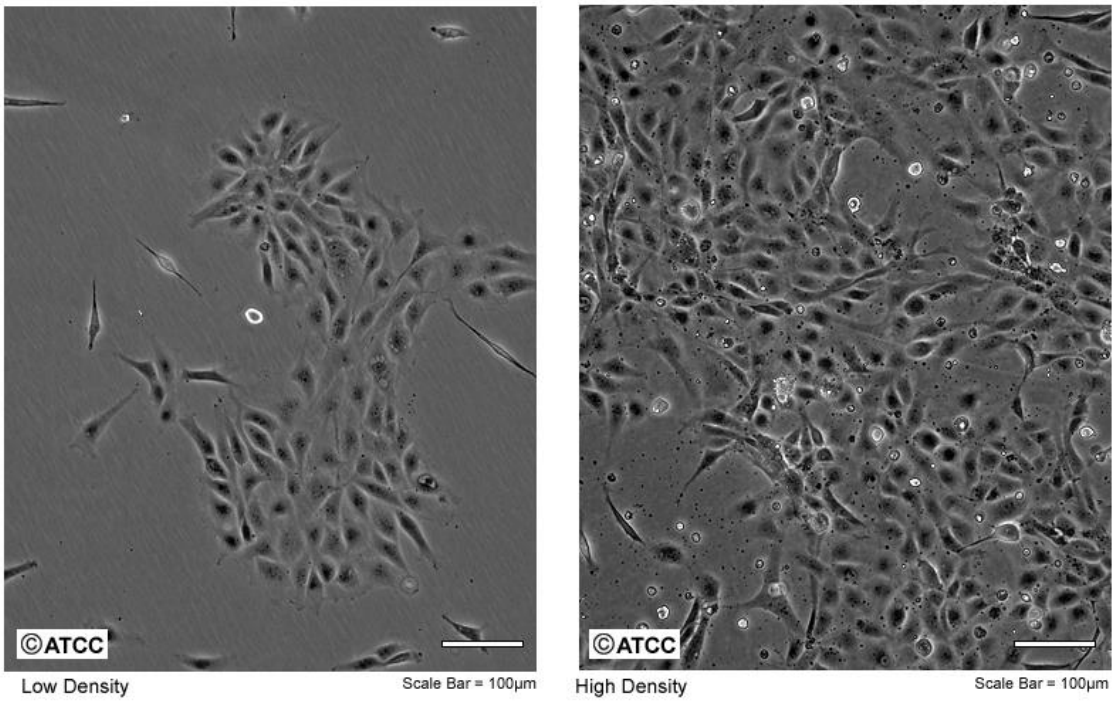

Figure 12: Cultured ZF4 cells in low (left) and high (right) density by American Type Culture collection, ATCC (2022)

1.12.2. Human carcinoma cells (A549)

Isolated in 1972, A549 is a human cancer cell line cultured from the adenocarcinoma tissue in the lungs of a middle-aged Caucasian male [166]. Naturally, A549 cells are thin and grow on the surfaces of tissues and organs [167] (**Figure 13**). The A549 cell line is easy to grow and have been used extensively in toxicological [141], immune-oncology, drug development [168] and

cancer research [169]. A549 cells have also been used in studies on nanoparticles uptake [143] and toxicity [170].

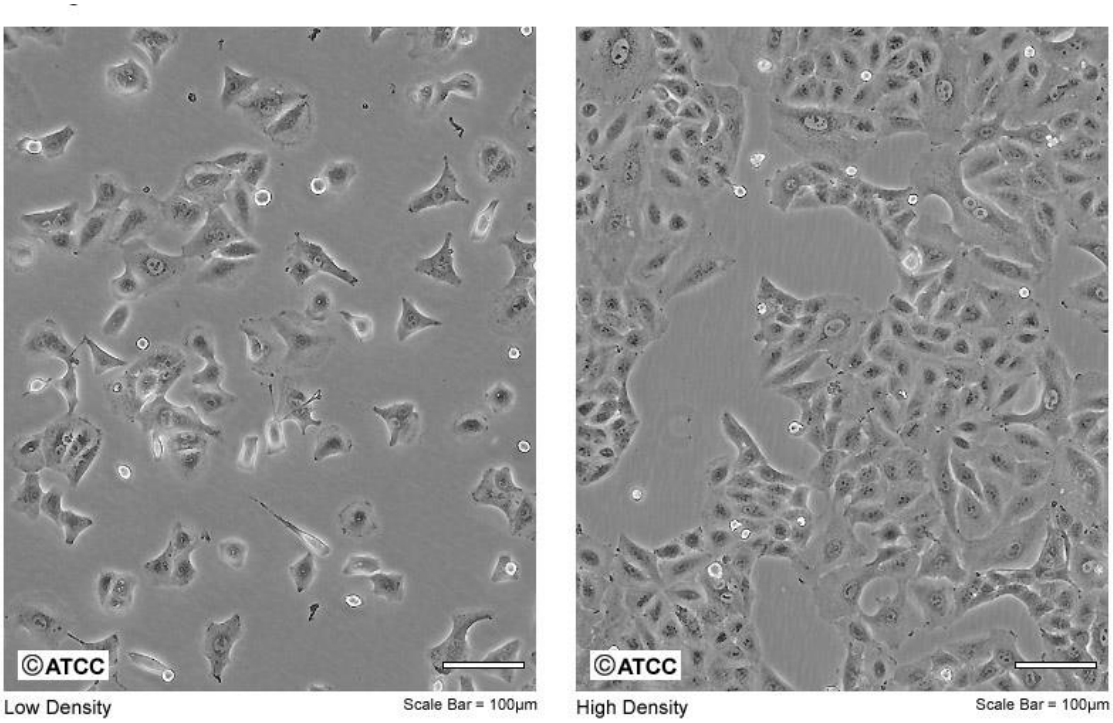

Figure 13: Cultured A549 cells in low (left) and high (right) density by American Type Culture collection, [171]

Chapter 2:

Methodology

2.1. Synthesis of Nanomaterials

2.1.1. Materials

Graphite flakes, sodium nitrate ($NaNO_3$), sulphuric acid (H_2SO_4, 98% w/w), potassium permanganate ($KMNO_4$), hydrogen peroxide (H_2O_2, 30% w/w), chloroauric acid ($HAuCl_4$), tannic acid ($C_{76}H_{52}O_{46}$) and trisodium citrate ($Na_3C_6H_5O_7$) were all purchased from Sigma Aldrich (Dorset, UK). Each of the chemicals were utilised as purchased without additional purification. Deionised water was used in all the experiments.

2.1.2. Synthesis of Graphene oxide (GO)

GO was synthesised using a modification of the Hummer's method [31]. In brief, 5.0g of graphite flakes, 3.75mg of sodium nitrate ($NaNO_3$) and 370mL sulphuric acid were mixed in a 1L twin neck round bottom flask under magnetic stirring at room temperature. After 10 mins, the mixture was cooled in an ice bath for another 10mins. 22.5g of potassium permanganate was slowly added to the mixture while stirring until it turned into a dark green paste. The stirring continued for 72 hours in a fume hood at room temperature. The mixture was then diluted with 500mL of ultrapure water and stirred continuously for 1 hour at 95°C. A rapid temperature increase and violent effervescence were observed. The temperature was then reduced to ~60°C and 15mL of hydrogen peroxide (3%) was added to the mixture drop wise to reduce the potassium permanganate. The mixture was continuously stirred overnight at ambient temperature. A yellow tint coloration could be seen.

The suspension was then transferred into two 50mL tubes for ease of handling and vigorously mixed with a vortex. The suspension was centrifuged twice at 6,000 rpm for 15mins at 25°C. The mixture was then treated with 30mL sulphuric acid, 5mL hydrogen peroxide and 965mL ultrapure water to remove organic impurities and oxidant ions. The resultant mixture was stirred with a glass rod and centrifuged again. The black residue was re-suspended with ultrapure water and dialyzed (cut-off: 14,000 kDa) in ultrapure water for 72 hours. The purified GO (45mL) was freeze dried (Berta 1-8 LSCplus, Christ, Herlev, Denmark), stored in a sealed bottle and kept in a desiccator until further experiment were performed (**Figure 14**).

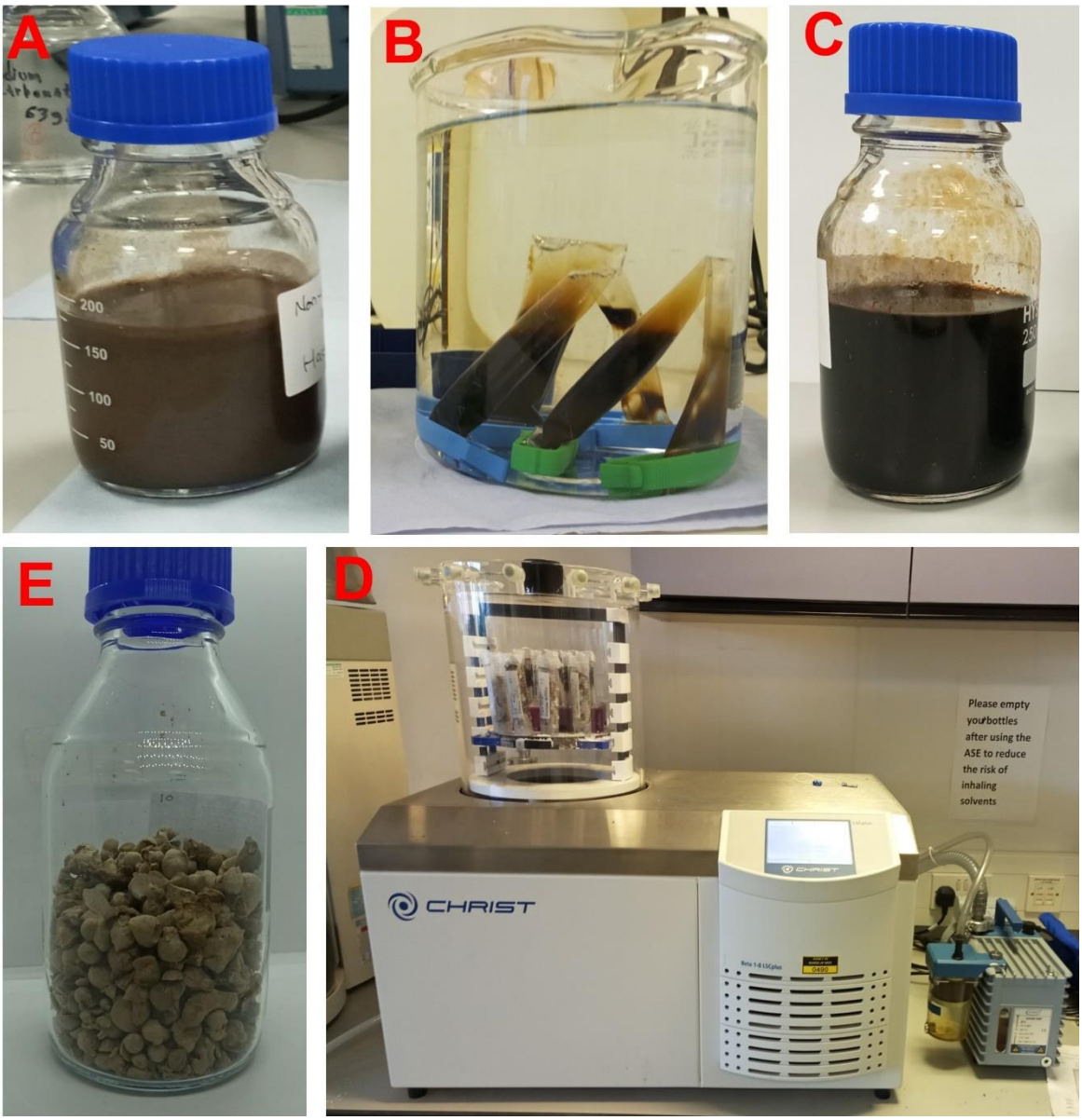

Figure 14: Post synthesis process: A - impure GO; B – purification using dialysis tubing; C – purified GO; D – freeze drying process; E – freeze dried GO

2.1.3. Synthesis of Graphene Oxide-Gold Nanohybrid (GO-Au)

The GO-Au nanohybrid was synthesised using a modification of the method developed by Song et al. (2014). In brief, 60mg of the synthesized GO was dispersed in 750mL of ultrapure water at room temperature under magnetic stirring for 1 hour. Then, chloroauric acid (150mg) was added to the GO

dispersion. The mixture was then stirred continuously for 1 hour, after which a solution of sodium citrate (75 mL) was added and stirred for a further 30 min. The mixture was then heated to 80°C for 1 hour. The final dispersion was then diluted with ultrapure water and centrifuged 3 times (at 7,000 rpm for 15min each time). The supernatant was discarded and the final GO-Au nanohybrid was collected. The nanohybrid was purified using dialysis tubing (cut-off: 14,000 kDa) for 48 hours. Purified GO-Au (82mL) was stored in a refrigerator at 4°C.

2.2. Characterization Methods

2.2.1. Ultraviolet-Visible Spectroscopy (UV-vis)

UV-vis spectroscopy is non-costly, simple and fast technique for measuring light transmittance or absorbance [172]. It is suitable for a broad range of organic substances and some inorganic compounds. When light passes through a medium, UV-vis spectrometer measures the transmittance or absorbance as a function of the wavelength which ranges from 200 - 800nm (**Figure 15**).

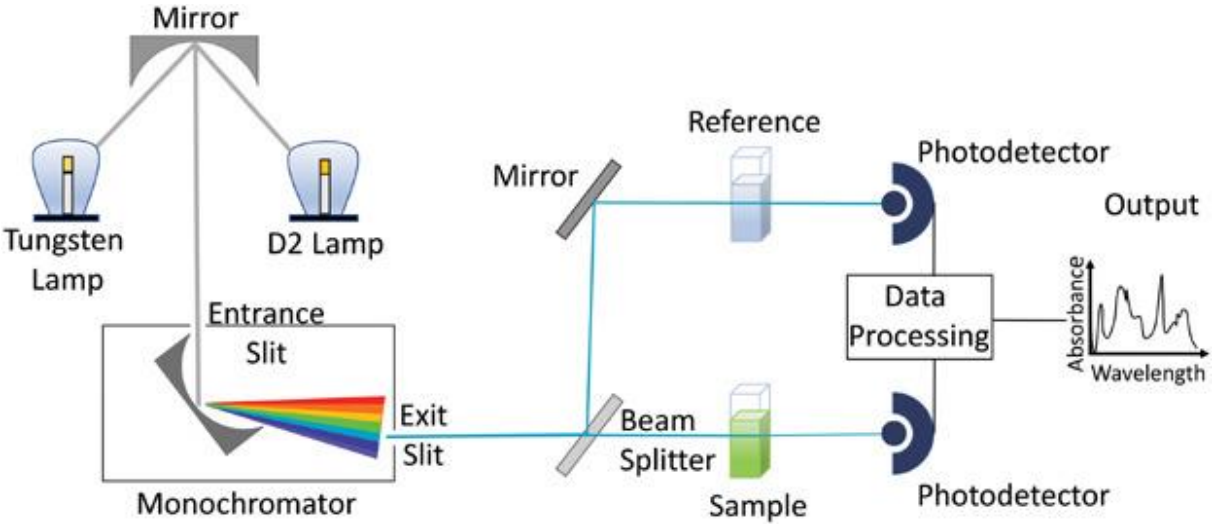

Figure 15: Schematic of the main parts of a UV-vis spectrophotometer [172]

UV-vis spectroscopy is performed to examine the extent of oxidation of the graphene oxide sheets [173]. The absorption spectra obtained can be used as mechanism of identification of GO sheets. The UV-vis spectra of GO sample typically show a sharp maximum peak around 230nm which indicates π→π* transitions of C═C bonds, and a weaker peak (shoulder) at around 300nm which indicates n→π* transitions of C═O bonds.

The UV-vis absorbance and spectra of GO and GO-Au nanohybrid were measured by UV-2600 Shimadzu spectrophotometer using quartz cells. The spectra for the samples were measured from 800 – 200 nm.

2.2.2. Dynamic Light Scattering (DLS)

The DLS is an instrument suitable for estimating hydrodynamic diameter and surface charge (zeta potential). Zeta potential gives an indication of suspension

stability and can also be used to measure the size distribution of small particles in solution. The functioning of the DLS system is based on the principle that particles dispersed in a solvent collide continually and move in a random manner (Brownian motion) [174]; their movement is a function of their size and hence tracking them allows measurement of their size. In the primary design of a DLS instrument (**Figure 16**), laser beam is passed through a cuvette containing the sample to be measured. The particles scatter the incident light which is then detected at various angles allowing positioning of the particles and thus their movement to be detected.

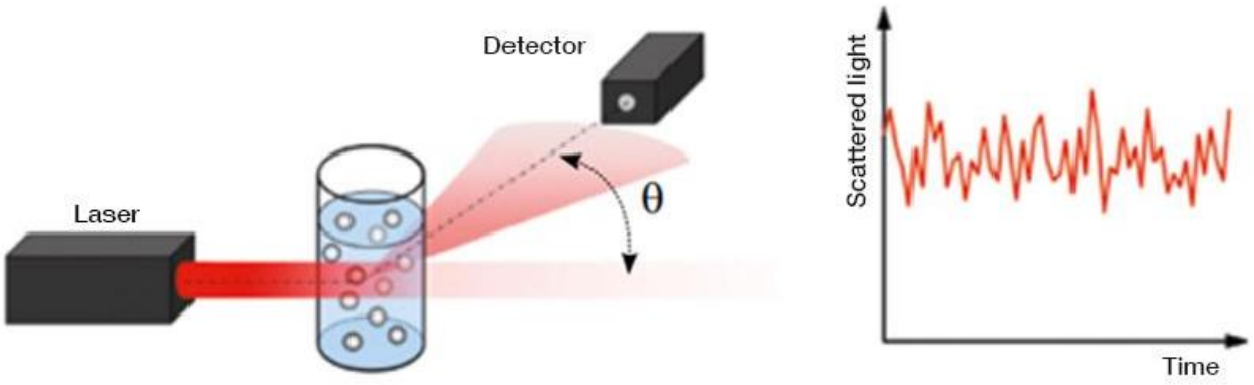

Figure 16: The primary layout of a DLS system [175]

The DLS instrument used in this thesis is a Malvern Zetasizer Nano ZS (Malvern, UK). Freeze dried GO were dispersed in ultrapure water to a final concentration of 1 mg L^{-1}. The dispersion was sonicated for 80 mins to obtain uniform dispersion. 1mL of the dispersion was placed in a zeta cell and measured at room temperature. Mean Z value was obtained for three replicate measurements.

2.2.3. Raman Spectroscopy

This non-destructive technique is commonly used to obtain structural information of carbon-based materials. Raman spectra are obtained when the scattering light from a sample excited by high-powered laser beam is sent through a spectrophotometer (**Figure 17**). The difference in energy between the scattered and incident light is the Raman shift.

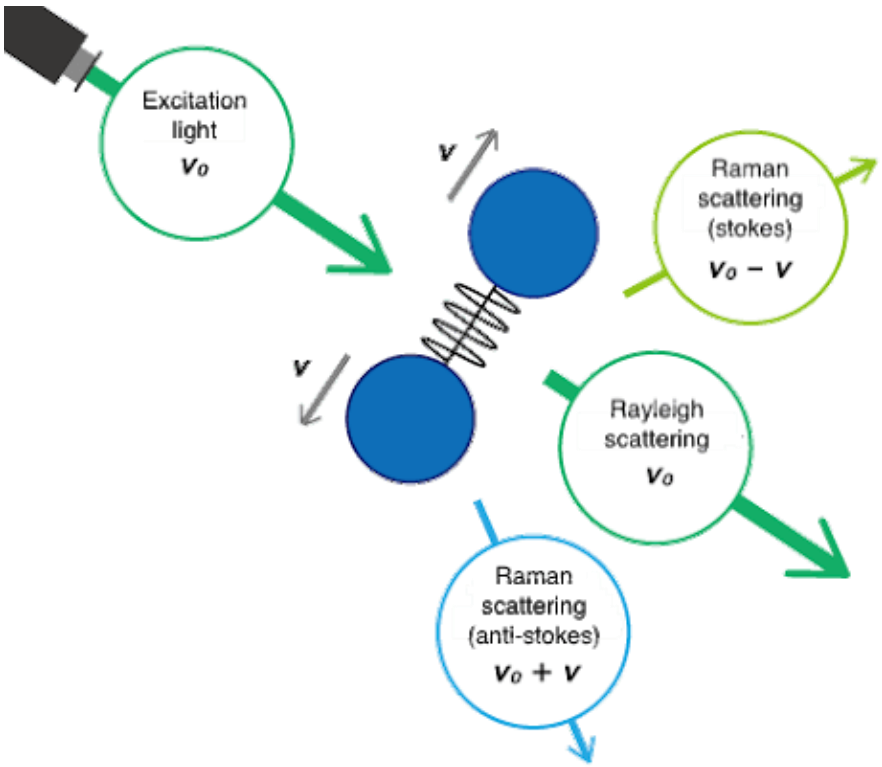

Figure 17: Scatterings that occur as a result of interaction of light on a substance [176].

Raman can be used to determine the stacking order, defects and number of layers of graphene [177]. A high-resolution Raman image can distinctively identify

the number of layers of graphene sheets [178], [179]. The Raman spectrum of GO normally have two peaks: the D peak falls within ~ 1300 - 1400 cm^{-1} range while the G peak at ~ 1500 - 1600 cm^{-1}. The D band indicates the defect region, and the G bands indicates graphitic region [180].

The Raman spectra of the nanomaterials used in this research were obtained using Renishaw InVia. The samples were prepared by sandwiching small quantity of sample flakes between two microscopic glass slides to reduce the particle size. The Raman spectra were taken at random points with 20 acquisitions. The green laser of 532nm wavelength was used. The spectrum range was 400 – 4000 cm^{-1}.

2.2.4. Transmission Electron Microscopy (TEM)

TEM is high-intensity electron microscope used for producing elaborate images of high magnification by focusing beam of electrons of a specimen. In principle, the TEM functions similarly to the light microscope but unlike light microscope that uses rays of light to generate image, TEM uses a beam of electrons (**Figure 18**) [181].

TEM is employed to determine the thickness of graphene sheets. As the name suggests, TEM beams stream of electron on a sample that generates a contrast due to electron density differences [180].

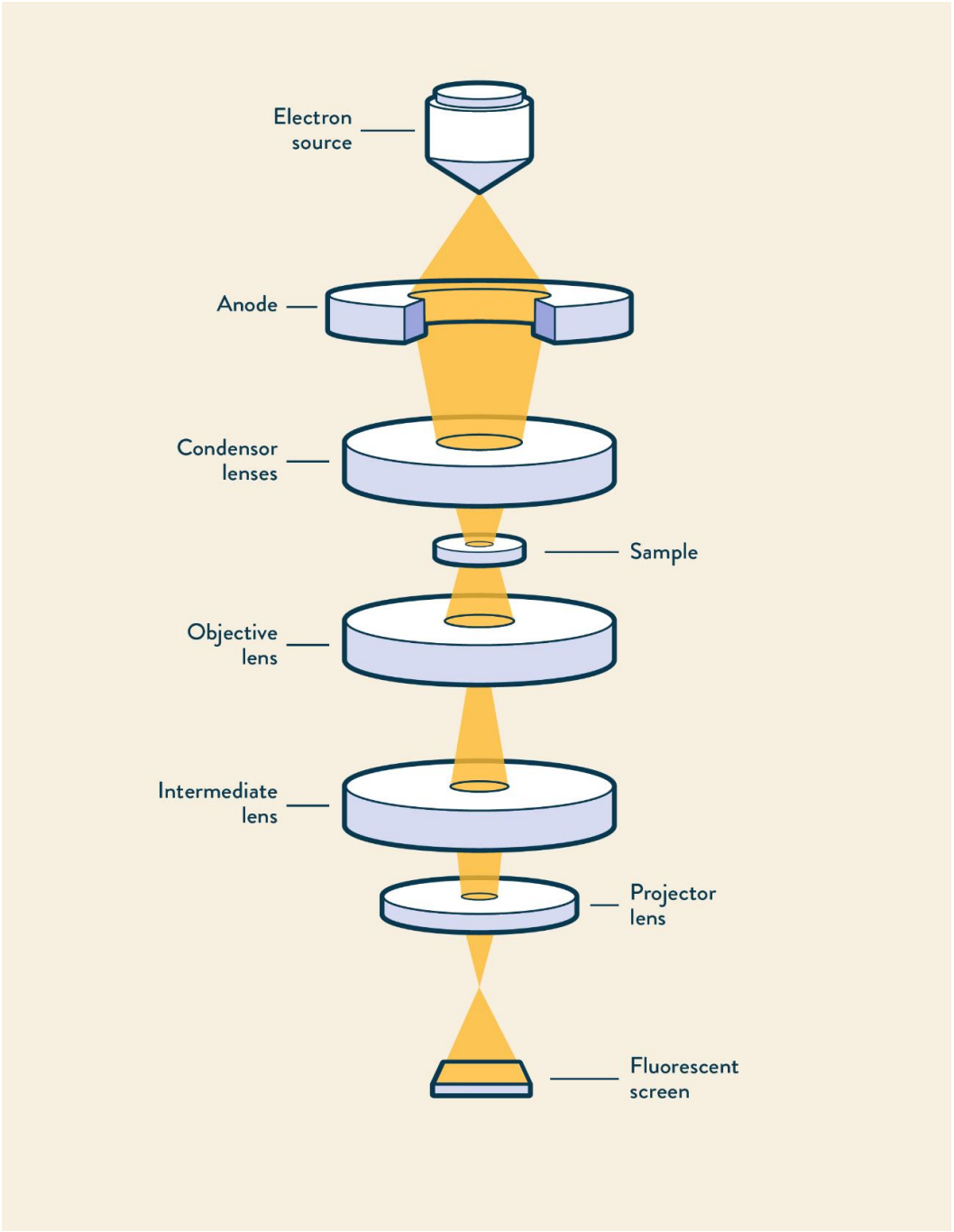

Figure 18: Schematic of the key components of a TEM [182]

2.2.4.1. Imaging of GO and GO-Au nanohybrid

TEM was used to obtain high quality images of GO and GO-Au nanohybrid. A single drop of the homogenised sample was deposited on a Formvar/carbon grid. The deposit was left to dry off and then examined under a Joel 1400 Bio TEM using an 80 kV electron beam current.

2.2.4.2. Imaging of exposed daphnia

Daphnids exposed to GO and GO-Au nanohybrid were imaged using TEM. Euthanized whole daphnia were fixed immediately with 1 - 2ml of 2.5% glutaraldehyde in a 0.1 M phosphate buffer suspension. The fixed daphnids were dehydrated in ethanol and embed in epoxy resin. 0.1 µm section of the embedded samples was cut using a ultramicrotome a diamond knife. The images were then visualised using JEOL 1400EX microscope.

2.2.5. Atomic Force Microscopy (AFM)

AFM is high resolution scanning probe microscope that produces sample images by scanning the surface. It is commonly employed to evaluate the shape, thickness and surface morphology of graphene sheet [183], [184]. The height profile and surface image of GO obtained from AFM can be used to access the presence of irregularities in the sheet morphology [185]. A typical AFM works by scanning the surface of sample with the tip on the cantilever (**Figure 19**). The motion produced by the side to side and up-down movement of the AFM tip is

reflected off the cantilever by a laser beam and captured by a position sensitive photo detector (PSPD).

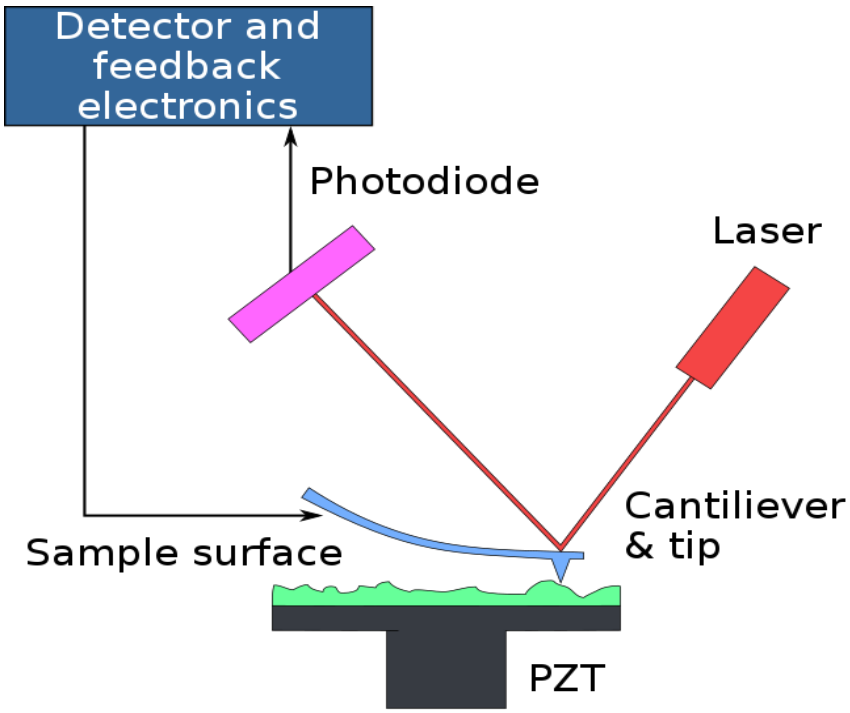

Figure 19: A schematic of how a typical AFM works

An AFM scanning was done by depositing drops of samples on a glass slide and left to dry off. The slide was then mounted on the microscope. Imaging of the samples was done in peak force tapping using multimode 8 microscope with Nanoscope 5 controller (Brucker, Durham, UK). The images were then analysed on Gwyddion (2.59) software. For GO size distribution, ImageJ software (1.53a) was used.

2.2.6. Thermogravimetric Analysis (TGA)

TGA is an analytical technique used for determining the thermal stability of a material. While a material is subjected to a regulated temperature increase, the change in mass of the material is quantified as a function of temperature. For graphene and its derivatives, TGA can be used to estimate the non-graphene constituents and residues. TGA analysis in this work was carried out on a Perkin Elmers' TGA 8000 machine using the following parameters: synthetic air flow rate at 50 mL/min; 10°C/min (**Figure 20**).

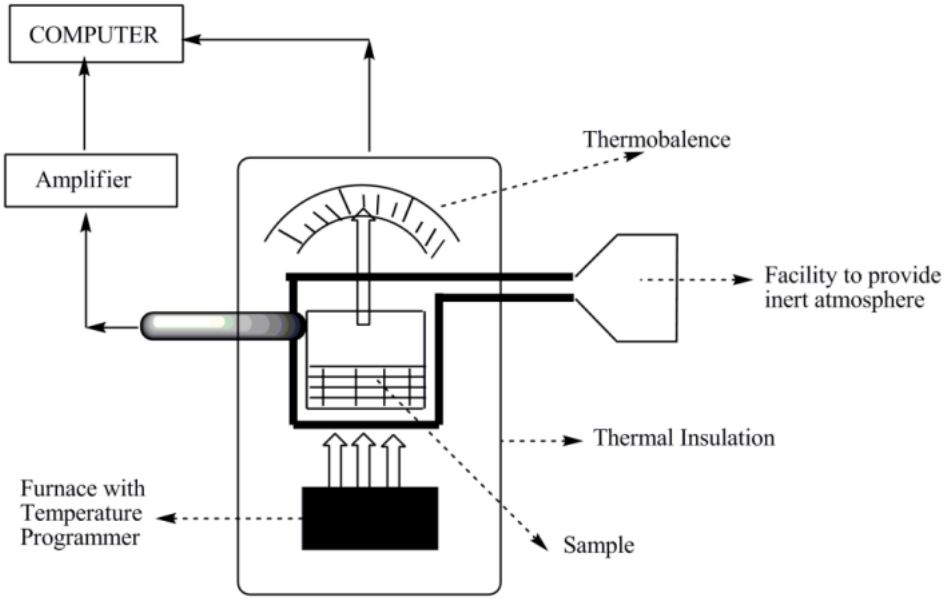

Figure 20: Illustration of the major components of TGA [186]

2.2.7. Fourier Transform Infrared Spectroscopy (FTIR)

FTIR is an analytical technique that is used to identify the chemical bonds present in a substance. This is achieved by the production of a distinctive absorption spectra of a material when infrared radiation is passed through it [187]. For 2D materials such as graphene and its derivatives, FTIR is useful in measuring the functional groups associated with the GO content and residual materials. Although FTIR is quite easy and simple to use, the spectrum for different bonds can overlap. Hence, there is a need for a proper check of the broad spectrum.

Figure 21: The FTIR Spectrophotometer used for this research

The FTIR spectra analysis of the GO sample was measured using Frontier MIR spectrophotometer (PerkinElmer, Beaconsfield, UK) (**Figure 21**). Small quantity of GO flakes was placed on the crystal and was measured in attenuated total reflection (ATR) mode.

2.2.8. Inductively Coupled Plasma Mass Spectrometry (ICP-MS)

ICP-MS, introduced in 1980, is an analytical technique used for quantifying elements in ionic form [188]. Unlike other forms of mass spectrometry, ICP-MS utilises inductively coupled plasma (ICP) to measure the mass to charge ratio of ions by ionising the sample followed by measurement by a mass spectrometer [189]. ICP-MS is able to detect metals, many non-metals and even isotopes at very low concentrations. The main components of an ICP-MS instrument are ICP (source of ion), a mass spectrometer and a detector (**Figure 22**).

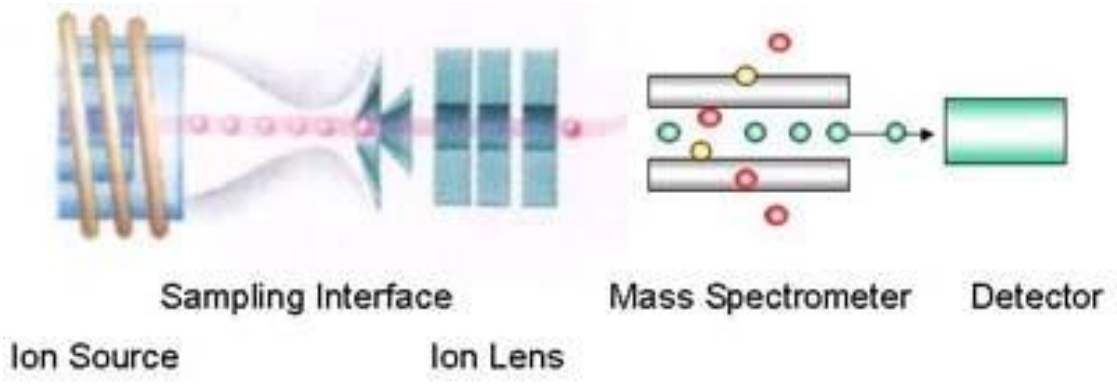

Figure 22: The basic structure of ICP-MS [190]

2.2.8.1. Quantification of Au in GO-Au Nanohybrid

ICP-MS (Perkin Elmer NexION 300x) was used to quantify the concentration of Au in the synthesized nanohybrid. 100µl of the GO-Au nanohybrid was digested in 900µl of HCl (15M) overnight. An aliquot of the digested sample was further diluted using 2% HCl to ppb levels. Afterwards, the sample was centrifuged at 7500 rpm for 15mins. The supernatant was characterized by a UV-vis spectrophotometer for the detection GO. In the absence of GO, the supernatant was analysed for Au on ICP-MS. Five replications of this measurement were performed.

2.2.8.2. Quantification of Au in Daphnia

ICP-MS was also used for the quantification of Au in daphnids exposed to GO-Au nanohybrid. Whole daphnia were euthanized using liquid nitrogen. They were then mechanically homogenized in 2% nitric acid (HNO_3) using a Precellys 24 instrument (2 cycles of a 30s pulse at 6000 pulse speed). The homogenised samples were then digested in Aqua Regia. 100µL of homogenate was deposited in 900µL of Aqua Regia overnight. 100µL of the digested sample was mixed with 9900µL of 2% Nitric acid. The final mixture was centrifuged, and the supernatant was analysed by ICP-MS.

2.3. Daphnia Toxicity Experiments

2.3.1. Daphnia Culture and Maintenance

The daphnia used for this study were third brood of Bham2 strain acquired from the Daphnia Facility of the University of Birmingham, UK. The organisms were maintained in borehole water at 20°C (**Figure 23**). A photoperiod ratio of 16hr to 8hr light and darkness respectively was maintained. The daphnids were fed daily *with Chlorella vulgaris* (green algae) at the rate of 100µL per 10 daphnids. Maintenance media were renewed every other day.

Figure 23: Daphnia during culturing at the Daphnia facility of University of Birmingham

2.3.2. Acute Toxicity Test

Acute toxicity test was conducted according to the OECD 2004 Acute Immobilization Test protocol. Daphnia neonates (<24 hr) were exposed to a range of concentrations (0, 5, 10, 20, 50 and 100 mg/L) of GO and GO-Au nanohybrid for 48hr. NOM was used to stabilise the nanomaterials in the media. Protocols for the preparation of the test solutions are presented in appendix I (Table S6 and S7). Record of mortality and immobilization was taken at 24 and 48hrs. The organisms were maintained in borehole water and HH combo media at 20°C. A photoperiod ratio of 16hr to 8hr light and darkness respectively was observed.

2.3.3. Bioaccumulation

Daphnids (<24 hr old) were exposed to 5ml of toxicants (GO and GO-Au nanohybrid) of different concentrations (1, 50 and 100 mg/L) for 7 days. The culture media was changed on day 3 and 5. On day 7, daphnia samples were collected and rinsed with ultrapure water. The organisms were split into 3 groups: the first group were processed for quantification of Au using ICPMS, the second group were processed for TEM imaging, and the last group were imaged (whole organism) using light microscope.

2.3.4. Light Microscope Observation

Light microscope is a laboratory equipment that makes small objects visible by magnifying them with the use of lenses and visible light [191]. Light microscopes

are versatile as they can be adapted for use on broad range of samples with little preparation. A microscope is essentially made up of a light source (bulb or LED) and an imaging system (glass lenses) [192] (**Figure 24**).

Daphnids exposed to GO and GO-Au nanohybrid were examined live under a light microscope. After bioaccumulation exposure, 3 daphnids were randomly sampled from each concentration of GO and GO-Au nanohybrid. The organisms were washed with ultrapure water and transferred to a new media. One at a time, the daphnids were carefully placed on a thin glass slide and imaged using a Nikon stereomicroscope (SMZ800, Japan) with NIS Elements software.

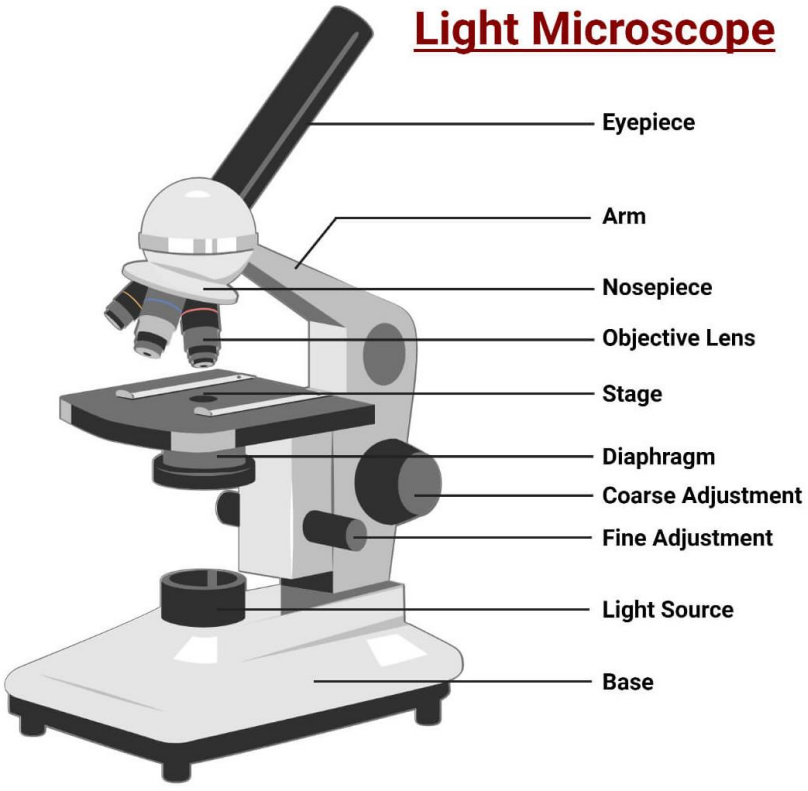

Figure 24: The basic components of a light microscope

2.3.5. Daphnia Media Characterisation

2.3.5.1. Borehole

Borehole water as a natural medium was used for several experiments in this research including daphnia culture and maintenance, toxicity tests and dispersion stability study. Natural waters are acceptable as standard for toxicity experiments and culturing of model organisms [114], [193]

Borehole water samples were collected in triplicate at the EcoLab of the University of Birmingham, Edgbaston, UK. The sample collection was done with few days' interval between each sampling. The results presented here are averages of each day, represented with letters A to E. The pH, conductivity and dissolved oxygen were analysed with Thermo Scientific Orion, Star A Series while the total organic carbon and total nitrogen were measured with Shimadzu TOC-L CPH + TNM-L analyser. The heavy metals were quantified using ICP-MS from PerkinElmer.

2.3.5.2. High Hardness (HH) Combo Media

HH combo media is an artificial water that supports the growth and survival of aquatic organisms [194]. The media is composed of all the nutrients necessary for the growth and reproduction of algae and daphnia [195].

To prepare HH Combo media, 4 ml of compounds #1-7 (**Table 1**), 8 ml of compound #8 (**sodium bicarbonate)** and 200 µl of Sodium Selenite (Na_2SeO_3

40 µg/ml) to 3.5L of dH_2O. The final volume is adjusted t0 4 litres and the mixture is aerated for 24hr. Then the pH was adjusted to 7.6 – 7.8. After the pH adjustment, 4 ml of animate and 2ml of vitamin (VIM) were added.

Table 1: Chemical composition of HH Combo media

#	**Compounds**	**Stock (g/L)**
1	Calcium chloride dihydrate ($CaCl_2 \cdot 2H_2O$)	110.28
2	Magnesium sulphate heptahydrate ($MgSO_4 \cdot 7H_2O$)	113.5
3	Potassium phosphate dibasic (K_2HPO_4)	1.742
4	Sodium nitrate ($NaNO_3$)	17
5	Sodium metasilicate nonahydrate ($Na_2SiO_3 \cdot 9H_2O$)	28.42
6	Boric acid (H_3BO_3)	24
7	Potassium chloride (KCl)	5.96
8	Sodium bicarbonate ($NaHCO_3$)	63
9	Sodium Selenite (Na_2SeO_3)	0.04

#	**Animate Solution**	**Stock (g/100 ml)**
10	Lithium chloride (LiCl)	31
11	Rubidium chloride (RbCl)	7

12	Strontium chloride hexahydrate ($SrCl_2 \cdot 6H_2O$)	15
13	Sodium bromide (NaBr)	1.6
14	Potassium iodide (KI)	0.33

#	**Vitamin Stock Solution (VIM)**	**Concentration**
15	Biotin (*d*-biotin)	10 mg into 96 ml dH_2O
16	B12 (cyanocobalamin)	10 g into 89 ml dH_2O

2.4. Cellular Toxicity Assessment

This section gives a detailed description of the materials and methods used for the assessment of cell toxicity. Following the synthesis and characterization of GO and GO-Au nanohybrid, cellular toxicity experiments were carried out using two cell lines. The stability of the nanomaterials in the cell culture media were also monitored.

2.4.1. Materials

Two cell lines were used for all the cell experiments: Zebrafish embryonic cells (ZF4) and human lung adenocarcinoma cells (A549). ZF4 (ATCC® CRL-2050™) and A549 cells (ATCC CRM-CRL-185) were both acquired from American type culture collection (ATCC). F12 Nutrient Mixture, Dulbecco's modified eagle medium (DMEM), penicillin/streptomycin (15070), 0.25% trypsin-EDTA (15090),

fetal bovine serum (FBS) and phosphate-buffered saline (PBS) were bought from Gibco. Alexa fluor 488® Annexin V/PI cell death and CellRox deep read reagent kit from Invitrogen (Paisley, UK) and CytoTox 96 ® non-radioactive cytotoxicity assay from Promega (Southampton, UK) were used in this experiment.

2.4.2. Cell Culturing and Maintenance

The A549 cells were cultured in a complete cell culture media (CCM) and incubated in a humidified atmosphere of 5% CO_2 at 37 ºC. The CCM was prepared using F-12 nutrient mixture media, supplemented with 10% FBS, 1% penicillin (100 µg/mL) and streptomycin (100 mg/mL). The ZF4 cells were also purchased from ATCC and cultured in CCM according to the manufacturer's instructions. In summary, the cell vial was thawed, resuspended in CCM in ratio 1:9 mL and incubated in a humidified atmosphere of 5% CO_2 at 28 ºC. The CCM ZF4 was prepared using DMEM media supplemented with 10% FBS, 1% penicillin and streptomycin. The cells were passaged after they attained 80% confluence (day 4) by removing media, washing with PBS, detaching with 1.5 mL of 0.25% trypsin for 2 mins and diluting with CCM to a total volume of 10mL. 2mL of the diluted cell suspension was seeded on T75 flasks with 6mL CCM. This process was done once every week for proper maintenance of the cell line.

2.4.3. MTT Assay

MTT assay is a colour-based scientific technique used to assess cytotoxicity and cell viability by quantify the metabolic activity of cells [196] (**Figure 25**). The

technique works on the reduction of tetrazolium salt (MTT, yellow in colour) by cellular enzymes to form insoluble formazan crystals (purple) [197]. The crystals are solubilised and analysed using a spectrophotometer at an absorbance of 500 – 600 nm.

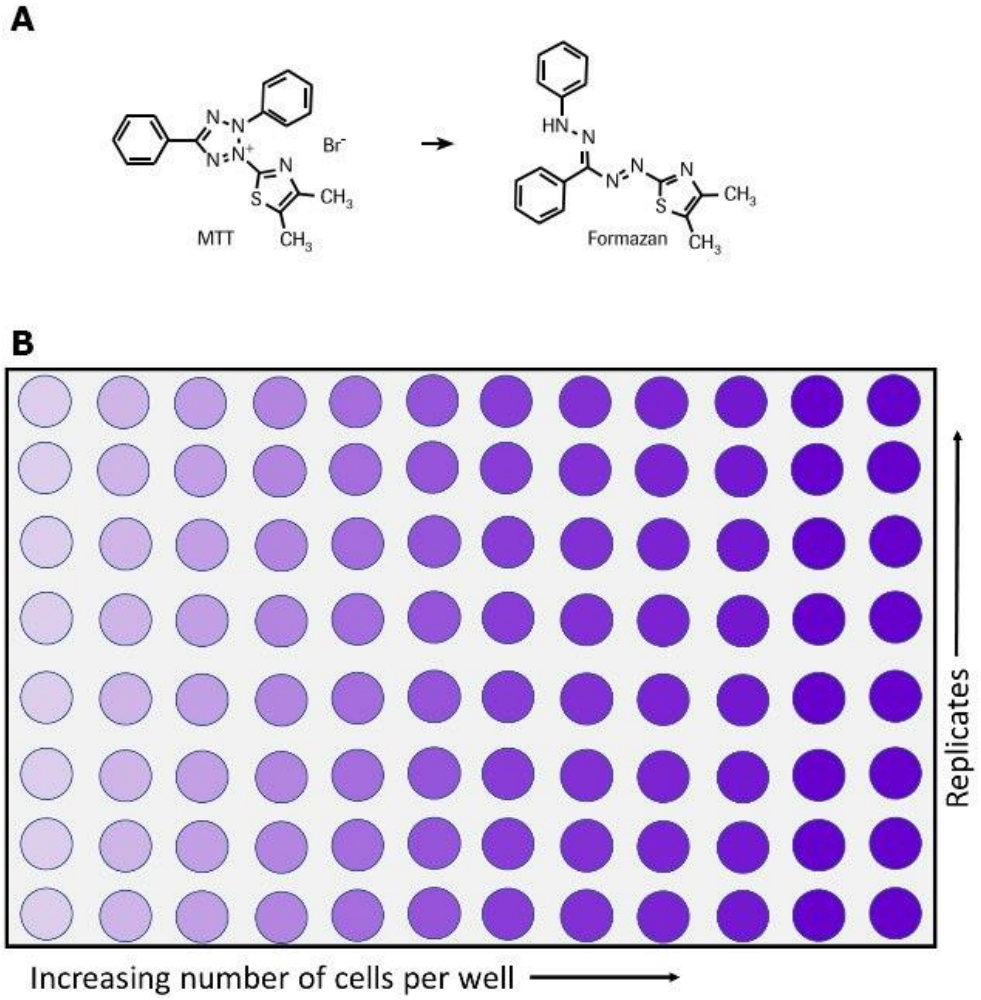

Figure 25: (A) Chemical reduction of MTT to form Formazan (B) A 96-well plate showing increasing quantity of viable cells. The light wells contain the least cells while darkest well contain the most viable cells [198]

The metabolic activity of ZF4 and A549 cells exposed to GO and GO-Au was assessed using MTT assay. The cells were seeded in transparent 96 well plates (flat bottom) at a density of 7,000 cells per well in 100 µL of CCM. The cells were

incubated overnight for attachment at 37 °C under 5% CO_2. After 24hrs, the cells were treated with a range of concentrations of the nanomaterials (2.5 – 150 mg/L) for 48hr. The positive and negative control cells were treated with 20 % dimethyl sulfoxide (DMSO) and CCM respectively. The stock solution of the MTT (5 mg/ml) was prepared in sterile phosphate buffered saline (PBS) and filtered with 0.2 μm Acrodisc syringe filter. The media was removed post treatment and 120 μL of the MTT solution, diluted in CCM at 1:6 ratio, was added. After 4 hours, the MTT solution was replaced with 200 μL of DMSO for 15 mins to solubilize the formazan crystals in darkness with a gentle agitation. The absorbance was measured at 570nm using microplate reader. The percentage MTT was calculated as follows:

$$\%\ Metabolic\ activity = \frac{A570\ nm\ of\ treated\ and\ untreated\ samples - A570\ nm\ of\ media\ only}{A570\ nm\ of\ maximum\ of\ untreated\ cells - A570\ nm\ of\ media\ alone} \times 100\%$$

2.4.4. LDH Assay

This non-radioactive colorimetric assay uses the quantification of lactate dehydrogenase (LDH) release, an enzyme found in most living cells, as an indication of cytotoxicity [199]. LDH is released into the CCM when there is a damage to the cell membrane. The assay measures the amount of LDH released in a plate reader by measuring visible wavelength in a 96-well plate.

The percentage plasma membrane damage in the ZF4 and A549 cells caused by exposure to GO and GO-Au was measured using LDH assay. Cytotox 96 non-

radioactive cytotoxicity assay kit (Promega, UK) was used for the assessment according to the manufacturer's instructions. After cell seeding and incubation with same concentrations used in MTT, 50 μL of supernatant was transferred to a new 96 well plates (flat bottom). An aliquot (50 μL) of the reconstituted substrate was added to each well and incubated for 15 mins in darkness. The reaction was terminated by the addition of 50 μL of stop solution. The absorbance, which indicates the amount of LDH released into the media, was then measured at 490 nm using a microplate reader. The percentage LDH released was calculated as follows:

$$\%\ LDH\ released$$

$$= \frac{A490\ nm\ of\ treated\ and\ untreated\ samples - A490\ nm\ of\ media\ only}{A490\ nm\ of\ maximum\ of\ untreated\ cells - A490\ nm\ of\ media\ alone} \times 100\%$$

2.4.5. Detection of ROS Generation

Reactive oxygen species (ROS) are very reactive radicals that are produced as by-products from the breakdown of oxygen and are normally present at low, regulated level in living cells. However, upon exposure to unfavourable environmental conditions, cells generate elevated amount of ROS that oxidise and modify cell components. Cytometric assays have been developed to measure ROS as an indication of oxidative stress [200].

For the detection of ROS in this research, CellRox deep red reagent kit from Thermofisher (UK) was used. The ZF4 and A549 cells were seeded on a 12 well plate (density = 5 x 10^4 cells per well) and incubated overnight for adhesion. The

cells were then treated with GO and GO-Au at concentrations 1, 50 and 100 µg/mL for 24 hrs while the positive control was treated with menadione (50 µM) for 1 hr. After incubation, the cells were detached with trypsin and centrifuge at 1,500 rpm for 5 mins. Then the cells were stained with 5 µM CellRox deep red reagent diluted in phenol free RPMI 1640 media for 1hr at 37 °C in darkness. The quantity of ROS produced was analysed using BD LSRFortessa X20 cell analyser. by acquiring 10,000 events.

2.4.6. Cell Death Assay

The induction of apoptosis after exposure of the ZF4 and A549 cells to GO and GO-Au was assessed using Annexin V-FITC/PI assay kit using the manufacturer's protocol. The cells were seeded on 6 well plates for 24 hrs (density = 2 x 10^5 cells per well) and treated with GO and GO-Au at concentrations 1, 50 and 100 µg/mL for 24 hrs. The positive control was incubated for 24hrs with 10% DMSO and 6 hrs with 1 µM Staurosporine as necrosis and apoptosis inducers. The cells were then detached with trypsin and centrifuge at 1,500 rpm for 5 mins at 4°C. Thereafter, the pellet was resuspended with 100 µL of Annexin binding buffer and incubated with 1µL of PI and 5 µL of Annexin V-FIC for 15 mins in darkness at room temperature. Post incubation, the cell suspension was diluted with 400 µL of Annexin binding buffer and analysed using the BD LSRFortessa X20 cell analyser with 10,000 events acquisitions. Spectral overlap was compensated for electronically between fluorophores. The maximum excitation and emission spectra for Alexa Fluor 488 Annexin V stain and PI stain were 488/499 nm and 535/617 nm respectively.

2.5. Dispersion Stability

2.5.1. Daphnia Media

The dispersion stability of the GO and GO-Au (both at 100 mg L^{-1}) in ultrapure water (control), borehole water and high hardness combo media (see **Table T3** for quality parameters), with and without natural organic matter (NOM) (Suwannee River NOM; International Humic Substances Society; final concentration: 20 mg L^{-1}) was monitored using a modification of the OECD (Organisation for Economic Co-operation and Development) 318 guideline. The samples were kept static, and an aliquot (100 µL) was taken from the surface of the dispersion at 0, 24 and 48 hrs. Care was taken during aliquot sampling to avoid agitating the whole sample. The stabilities of the nanomaterials were compared in triplicates using the detection of GO at the absorbance of 230 nm measured using spectrophotometer analysis (microplate spectrophotometer, TECAN, Spark). The chemical constituents of the NOM are [% w/w of dry, ash-free sample]: water (5.69), ash (4.01), carbon (50.7), hydrogen (3.97), oxygen (41.48), nitrogen (1.27), sulphur (1.78).

2.5.2. Cell Media

The dispersion stability of the nanomaterials (GO and GO-Au) was evaluated for both ZF4 and A549 cells following the OECD guideline 318 [201]. The stability was monitored using a modification of the OECD 318 guideline. The nanomaterials were dispersed in CCM for respective cells (final concentration = 100 mg L^{-1}). 1mL of each sample was kept static in an eppendorf tube, and an

aliquot (100 µL) was taken from the surface of the dispersion at 0, 24 and 48 hrs. Care was taken during sampling to avoid agitating the whole sample. The samples were measured in triplicates using spectrophotometric analyses (microplate spectrophotometer, TECAN, Spark).

2.6. Data Analyses

Expermental data were recorded as means with standard deviation. Statistical analyses were performed using GraphPad Prism (9.0). Flow cytometry data were analysed using FlowJo software (v10.8.0, Ashland, US). EC_{50} values – the concentration that causes at least 50% of daphnia to show acute toxicity effect – was measured by Probit analyses using PriProbit software [202]. Test of normality and homogeneity of variance were done using Chi-square goodness of fit and Bartlett's test respectively. Differences between means of GO and GO-Au treatments were evaluated using one-way analysis of variance (ANOVA) while differences between control and the treatments was calculated using two-way ANOVA followed by Dunnet's test. Means were considered statistically different at p-value <0.05.

Chapter 3:
Synthesis and Characterization

This chapter has been published as follows:

Akere, T. H., de Medeiros A. M. Z., Martinez, D. S. T., Ibrahim B., Ali-Boucetta, H., and Valsami-Jones, E. Synthesis and characterisation of a Graphene Oxide-Gold Nanohybrid for Use as Test Material**.** *Nanomaterials***, 2023,** *13* (1), 33; https://doi.org/10.3390/nano13010033

3.1. Introduction

Since the advent of nanotechnology in the 1980s, our society has been transforming remarkably, and will likely continue to do so to meet our growing and evolving needs. Faster and powerful computers, more accurate medical devices, sunscreens, cost and quality efficient water filters are some of the remarkable applications involving nanotechnology. From environmental pollution, increasing energy demand, scarcity of potable water and biomedical constraints, the quest for solutions to some of the world's problems has driven intense research into nanomaterials [1]. On the forefront of these applications are carbon-based nanomaterials such as graphene and its derivatives [graphene, graphene oxide (GO), reduced graphene oxide (rGO)], carbon nanotubes [single and multi-walled nanotubes] and carbon dots [2].

Graphene-based materials represent a recent addition to the nanomaterials family and yet have already found many applications for example in electronics, medicine, agriculture and energy and have been incorporated in many consumer products: drug nanocarriers, high-capacity batteries, lightweight and strong materials for automotive and aerospace, biosensors, ingenious biomedical devices, water desalination, anti-corrosion coatings etc [5]–[8].

More recently, research work has focused on exploring multicomponent nanohybrids, which offer the advantage of combining multiple functionalities into a single advanced material [9]–[11]. A popular combination of such hybrid materials is that involving metal or metal oxide nanoparticles (like TiO_2, ZnO, Au, CuO) and carbon nanomaterials (such as graphene oxide, carbon nanotubes,

fullerenes). For instance, both GO and silver nanoparticles are known to exhibit antibacterial properties [12], [13]. However, graphene oxide-silver nanocomposite (GO-Ag) have been reported to have a superior antimicrobial capability compared to their individual components [14], [15].

Similarly, graphene oxide – gold nanohybrid (GO-Au) have been reported to demonstrate synergistic features beyond their individual capabilities such as increased electrical conductivity, catalytic activity, higher surface area, optical and medical properties etc [16], [17]. These features have rapidly increased the use of this nanohybrid in various applications such as cancer detection, bioimaging and biosensing [18]–[20].

Unlike natural nanomaterials that plants and animals have adapted to, engineered materials (especially emerging ones like nanohybrids) pose novel threats that require critical evaluation of their potential harm to humans and ecosystems. As with any new discovery, there are concerns about the potential of novel nanohybrids to cause toxicity over and above that of their individual components [22], [23]. Their safety to the ecosystem and human health is yet to be fully demonstrated since the very features that make them so advanced may also be the source of concern to ecotoxicologists, specifically in terms of their ability to bypass biological barriers. A number of studies have demonstrated adverse effects to human cells [84], bacteria [203], algae [204], water fleas [87], fish larvae [205], rodents [91] and marine mammals [203].

Currently, there is no standardized protocol for the synthesis of GO-Au nanohybrids. It is therefore unclear how in different formulations the two components are conjugated, quantitatively and qualitatively, and whether performance, but also potential ecotoxicity, may be affected. Most of the available research work on GO-Au has focused on the applications of the nanohybrid [18], [19], [30]. For assessing its safety however, it is important that critical physicochemical parameters of the GO-Au nanohybrid are evaluated and correlated to its toxicity. This is to ensure reproducibility and compatibility of the results.

Herein, the production of a graphene oxide-gold nanohybrid that will be suitable for nano-ecotoxicological studies was carefully designed and evaluated. Specifically, the aspects that were researched include i) synthesis and characterization of GO and GO-Au ii) stability of the nanohybrid in different environmental media iii) quantification of Au in the GO-Au nanohybrid and iv) evaluation of ageing effect on the nanohybrid.

3.2. Results and Discussion

3.2.1. Characterization of Graphene Oxide

As can be seen in **Figure 24A**, the final yield post-synthesis of GO exhibited a dark brown colour which is characteristic of GO. An aliquot of the GO was freeze dried for further characterization and to determine its concentration (1.0 g/L). The surface morphology of the GO was evaluated by transmission electron microscopy (TEM) and atomic force microscopy (AFM) (**Fig. 24B-C**). Using the TEM method described by Kumar et al. [206] for estimating the number of layers, the GO sheets were mostly single layer and exhibited flake-like structure as shown in **Figure 24B**. This is corroborated by the cross-sectional height profile of the GO flakes thickness measured by AFM height scan (appendix, **Fig. S1**). The measurement showed 1 nm thickness for most of the GO flakes. According to recommended classification [2], [8], the GO sheets fall within single to few layers GO. The average lateral size of the GO was 114 nm, with a size range between 5.86 and 269.53 nm.

UV-vis spectroscopy was performed to examine the extent of oxidation of the GO sheets. The absorption spectra can be used as a mechanism of identifying GO sheets. As shown in **Figure 24D**, the UV-vis spectrum of the GO sample shows a sharp maximum peak around 230nm which indicates $\pi \rightarrow \pi^*$ transitions of C═C bonds. The spectrum also showed a weaker peak (shoulder) at around 300nm which indicates $n \rightarrow \pi^*$ transitions of C═O bonds. This result confirms that the prepared sample contains GO, and is consistent with the UV-vis spectra described by others [180], [185], [207].

As expected, the mean zeta potential value of the GO samples was -56.4 ± 2.4 mV (pH = 7.9), suggesting a negative charge and a good stability [208]. The influence of pH on zeta potential (measure of surface charge) can have implications in environmental fate. The weak forces that bind nanoparticles together when they agglomerate can be altered by changes in pH [209]. In toxicity exposures where pH is expected to be maintained within certain range, a moderately stable suspension of particles provides some confidence on a low likelihood of agglomeration occurring in low ionic potential media.

In addition, Raman spectroscopy, a non-destructive method, was used to obtain structural information on the carbon-based nanomaterials as suggested by others [177]. It is used to determine the stacking order, defects and number of layers of graphene [178], [179]. GO normally has two peaks: the D peak falls within 1300 - 1400 cm^{-1} range while the G peak at 1500 - 1600 cm^{-1}. The D band indicates a defect region, and the G band indicates a graphitic region [180]. For the GO described here, as shown in **Figure 24E**, the D peak was seen at 1343 cm^{-1} and the G peak appeared at 1586 cm^{-1}. This further confirms the presence of GO in the synthesised sample. Also, the I_D/I_G ratio of 0.84 was recorded, indicating high level of defects, showing that this GO has undergone an oxidation process and intense exfoliation.

To identify the various surface functionalities on the GO, FTIR technique was employed. The FTIR spectrum for our GO sample is shown in **Figure 24F**. The graphite oxidation resulted in the formation of the following broad bands: 3212

cm^{-1} matching the O-H stretching vibrations that are typical of carboxyl and hydroxyl functional groups [207], [210], [211]; 1719 cm^{-1} corresponding to C=O stretching vibrations implying the presence of carbonyl and carboxyl groups [122]; 1622 cm^{-1} showing the contribution of cyclic aromatic groups; 1050 cm^{-1} matching the C-O stretching vibrations which are the typical absorption bands of ethers [122], [179].

To assess thermal stability and behaviour of the synthesised GO, TGA analysis was performed as shown in **Figure 24G**. The GO exhibited two decomposition stages at approximately 190°C and 550°C respectively. The initial weight loss up till 100°C resulted from evaporation of water content while the loss from 150 - 200°C can be attributed to loss of hydroxyl and acidic functional groups [212]. The final weight loss up to 700°C originated from the breakdown of carbonyl groups formed during the process of GO oxidation [213].

The chemical make-up of the GO surface was evaluated by XPS, and the results are presented in **Figure 24H-I**. The XPS spectra represents the intensity of photoelectrons emitted from the various atoms on the GO surface. The analysis of the XPS survey spectrum showed that the surface chemistry of the GO is composed of 68.15% carbon and 31.85% oxygen. The elevated percentage of oxygen confirms the oxidation of GO. The absence of commonly reported impurities such as sulphur and nitrogen indicate the high level of purity of the GO dispersion. The C1s scan shows the different carbon-oxygen groups present on the GO surface (**Table 2**).

Table 2: Analysis of C1s scan by XPS showing the chemical groups in GO

Functional Groups	Binding energy (eV)	% Atomic
Aromatic carbon (-C=C-)	284.13	9.98
Aliphatic carbon (-C-C-)	284.96	35.98
Hydroxyl/epoxy (C-O)	286.93	45.68
Ester (COO)	288.67	8.35

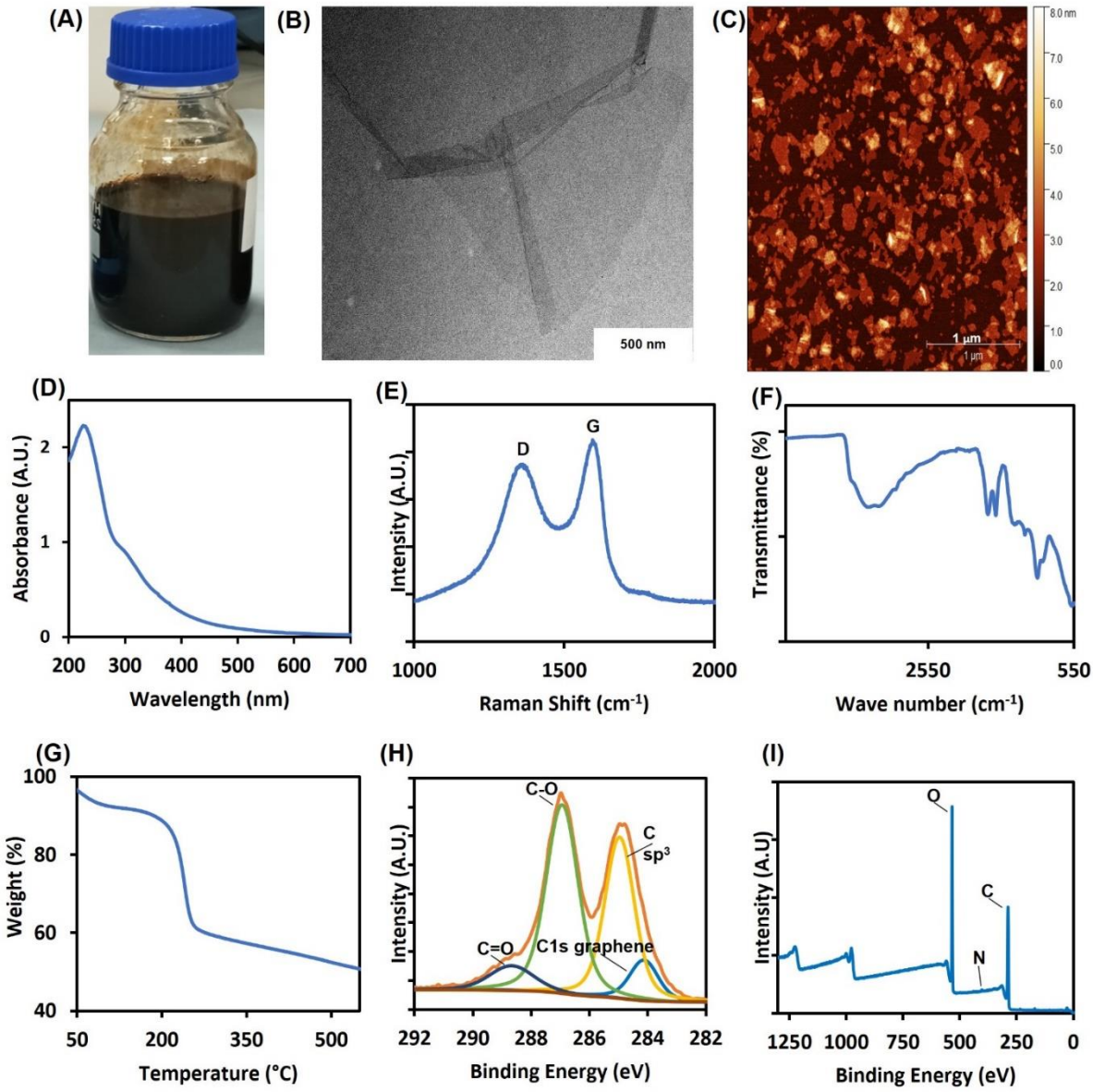

Figure 26: Characterization of graphene oxide (GO) prepared using modified Hummer's method. (A) Purified GO stock dispersion a concentration of 2mg/mL in ultrapure water, (B) TEM image of GO dispersion, (C) AFM topographic image (D) UV-vis absorption spectrum, (E) Raman

spectrum, (F) FTIR pattern, (G) thermogravimetric analysis spectrum (H) high resolution C1s XPS spectrum, (I) survey XPS spectrum

3.2.2. Characterization of Graphene Oxide-Gold Nanohybrid (GO-Au)

Three different batches of the GO-Au nanohybrid (X, Y and Z) were prepared and compared as shown in **Figure 25**. The synthesis method was optimised to produce the highest yield of GO-Au nanohybrid possible, over 80mg (> 2mg/mL). Previous studies have produced GO-Au nanohybrid suspensions within the range of 5 – 20mL [32], [214]–[216]. On characterization, it was found that all the three batches were very similar, suggesting reproducibility of the modified synthesis method of the GO-Au nanohybrid.

It is important to note that there are major differences between this modified synthesis protocol and the original protocol of Song et al (2014). Firstly, the original protocol has been scaled-up significantly. In the work presented here, 60mg of graphene oxide and 150mg of chloroauric acid were used as against the 4mg of graphene oxide and 5-20mg of chloroauric acid of the original protocol. Scaling up or down in the synthesis of nanoparticles can induce significant chemical changes on the final product [217], and it may not result in a product with properties corresponding to those of the original synthesis. Furthermore, modified synthesis conditions may result in a product of variable consistency, particularly in the case of a hybrid material.

Additionally, the optimised protocol presented here produced a significantly larger yield which cannot always be guaranteed when scaling up, but which was essential for a material that would be recommended for toxicological studies, where significant quantities are necessary to allow for testing a range of concentrations and carrying out replicate tests. The final yield of the GO-Au nanohybrid from our work was over 80 mg. Although the yield from the original protocol was not reported, judging by the volume of the reagents used, it is likely to have been less than 4mg. It is generally recognised that scaling-up of nanoparticle synthesis does not automatically translate to high yield of good quality [218]. A good volume of yield is highly required and useful for extensive ecotoxicological assessments, and addressing this limitation was central to our study.

Lastly, a crucial element in the optimised protocol is the introduction of purification at the end of the synthesis to remove impurities such as by-products generated during the synthesis process. These impurities may influence the behaviour, bioavailability and toxicity of a nanomaterial [219]. Since the focus of our synthesis is for ecotoxicological studies, it is important to rid the GO-Au nanohybrid of any impurities. The original protocol, however, was designed for a different application which did not require purification.

The UV-vis spectra of the nanohybrid (Fig. 2A) indicated the presence of AuNP on the GO sheets. Typically, the surface plasmon resonance for AuNP is seen as a peak at around 520 - 570 nm. As shown in **Figure 25B**, the integrity of the graphene sheets was not affected by the AuNPs conjugation as evident by the

presence of D and G peaks in the Raman spectra of the GO-Au nanohybrid. Notably, there was a small increase in the I_D/I_G ratio calculated for the GO-Au nanohybrid from 0.84 to 0.89 following the functionalization of Au NPs onto the GO surface. This suggests that defects were introduced onto the GO surface as a result of the attachment of the AuNPs. This is very similar to what Song et al. (2014) reported when pure GO sheets were conjugated with AuNPs and showed that the I_D/I_G ratio increased from 0.77 to 0.82 after conjugation. The thermal stability analyses of the GO-Au nanohybrid revealed that the three samples behaved similarly, as shown in **Figure 2C**. Approximately 20% of original weight was lost at around 200°C which corresponds to the evaporation of moisture and hydroxyl or acidic moieties while another 10 – 20% of weight was lost around 400°C, which may be attributed to the decomposition of carbonyl functional groups [220]. The thermal stability of the nanohybrids thus reflects the gradual decomposition of its GO component, and correlates well with the TGA results of the pure GO described earlier, with small deviations likely due to the presence of AuNPs.

As shown in the TEM images of the nanohybrids (**Figure 25D-F**), both GO and AuNPs can be visually observed on the images, confirming the functionalization of AuNPs onto the surface of the GO sheets. In addition, the average size of the AuNPs was found to be around 17.09 ± 4.6 nm from the TEM analysis. The even and planar shape of the GO sheets provided a suitable high surface area for the attachment of the AuNPs. Bonding of AuNPs to GO surfaces occurs via noncovalent bonds such as hydrogen bonds and electrostatic interactions [9],[221]. As can be seen in **Figure 25D-F**, AuNPs show limited tendency to

aggregate in all the nanohybrid batches. This is not unexpected as the likelihood of aggregation increases as the quantity of the starting $HAuCl_4$ is increased [32].

XPS was employed to determine the chemical composition of the GO-Au nanohybrid. The C1s scan and survey spectrum results are presented in figure S3 and S4. The GO-Au nanohybrid showed 67.15% of carbon, 29.83% of oxygen and 3.02% of gold. Similar to the GO alone, the high oxygen content in the GO-Au nanohybrid is due to oxidation and the absence of any further features in the spectra confirms purity of the nanohybrid. Deconvolution of the high resolution C1s spectrum as highlighted in **Table 3** revealed the percentage content of the respective functional groups on the GO-Au nanohybrid.

In addition, FTIR analysis of the GO-Au nanohybrid showed to be similar to that of GO alone as shown in **Figure S2**. The observed signals between 3200 – 3700 cm^{-1} match those of hydroxyl groups and carboxyl acids while the absorptions at 1720 cm^{-1} are due to carbonyl groups. The cyclic aromatic groups and the ethers can be identified by the signals at 1622 and 1030 cm^{-1} respectively.

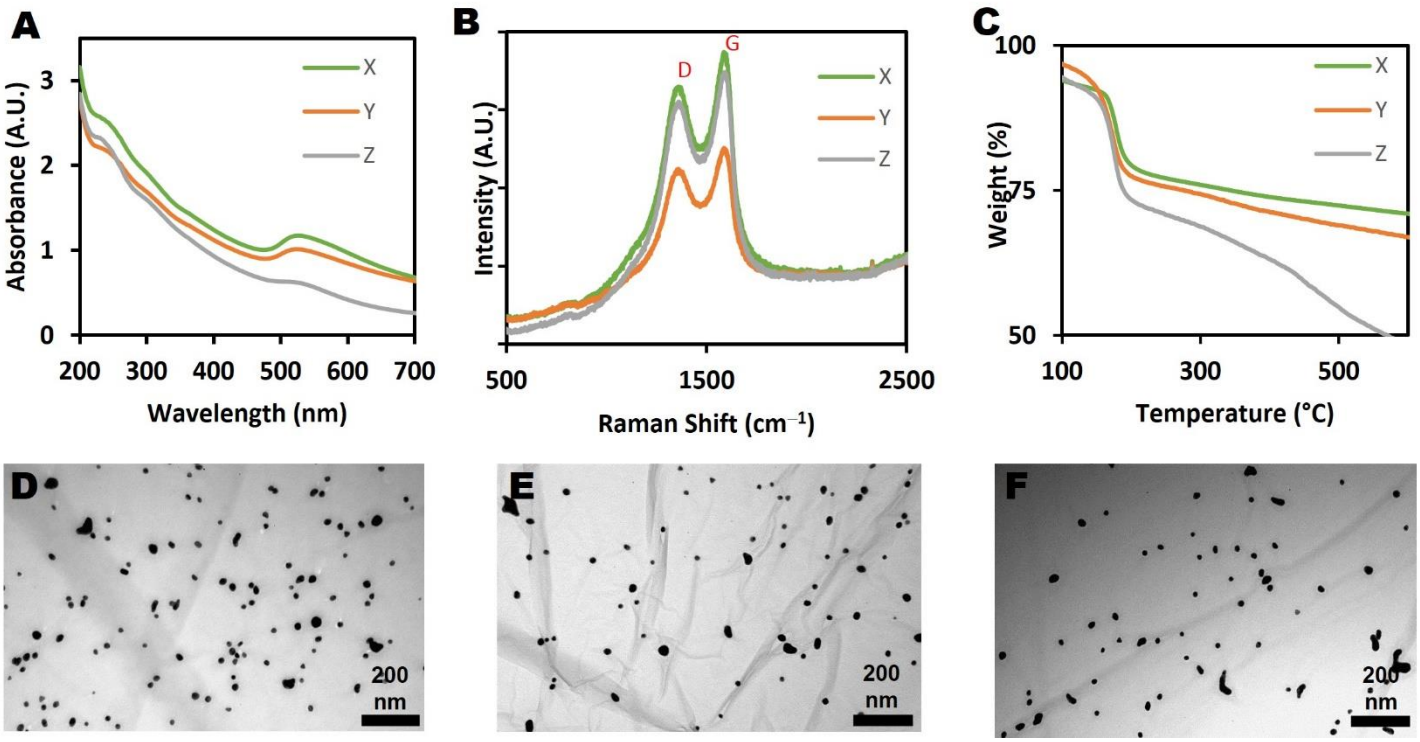

Figure 27: Characterization of three batches of GO-Au nanohybrid (X, Y & Z): (A) UV-vis absorption spectrum, (B) Raman spectrum, (C) TGA spectrum, (D-F) TEM images corresponding to each of the 3 replicate nanohybrids.

Table 3: Analysis of C1s scan by XPS showing the chemical groups in GO-Au

Functional Groups	Binding energy (eV)	% Atomic
Aromatic carbon (-C=C-)	288.93	7.37
Aliphatic carbon (-C-C-)	285.03	35.04
Hydroxyl/epoxy (C-O)	287.09	45.37
Ester (COO)	284.12	9.92
π- π* transition in aromatic	290.67	2.3

3.2.3. Evaluation of Nanohybrid Ageing

The effect of ageing on the quality of the GO-Au nanohybrid was assessed using two nanohybrids produced 4 months apart. Aged GO-Au was produced in July 2021 while pristine GO-Au was produced in November 2021 (**Fig. 26A-B**). Both nanohybrids were stored for a month in darkness at a temperature of 4°C.

Figure 26C presents the UV-Vis of the pristine and aged nanohybrids highlighting that both nanohybrids show a maximum peak at around 230 nm which is characteristic of GO. In addition, both nanohybrids include AuNPs as indicated by the plasmon band seen around 520 nm which is distinctive of AuNPs. Apart from the slight difference in absorbance, which is due to the difference in sample concentration, the two nanohybrids appear identical. This suggests that there has been no significant effect of ageing on the samples.

In order to investigate any visual or morphological changes between the pristine and the aged nanohybrids, samples were examined under TEM. As shown in **Figures 26D-E,** the TEM images confirm that the successful conjugation of the AuNPs was not affected by ageing as well as the presence of single layered GO. In addition, the size distribution of the AuNP is still similar in both aged and pristine nanohybrids.

The stability of the synthesised GO-Au nanohybrid could be due to the mild conditions of the synthesis which involved only moderate temperature (80°C). This indicates that the sp2 hybridization of graphene-based materials is stable at moderate temperatures (≤ 120°C) in agreement with other literature [222], [223].

Graphene oxide, however, becomes generally unstable at high temperatures, above 200°C [224].

The toxicity and reactivity of nanomaterials can be sensitive to ageing and chemical transformations. Depending on the chemical constituent of the media, ageing can influence nanomaterials both structurally and compositionally and, in turn, their interaction with other molecules in the media as well as bio-uptake. The lack of evidence of ageing in the GO-Au nanohybrid adds to the weight of evidence that the proposed synthesis protocol produces a nanohybrid that is suitable for toxicity testing and will remain stable even for longer term exposures, which are not uncommon in ecotoxicity testing.

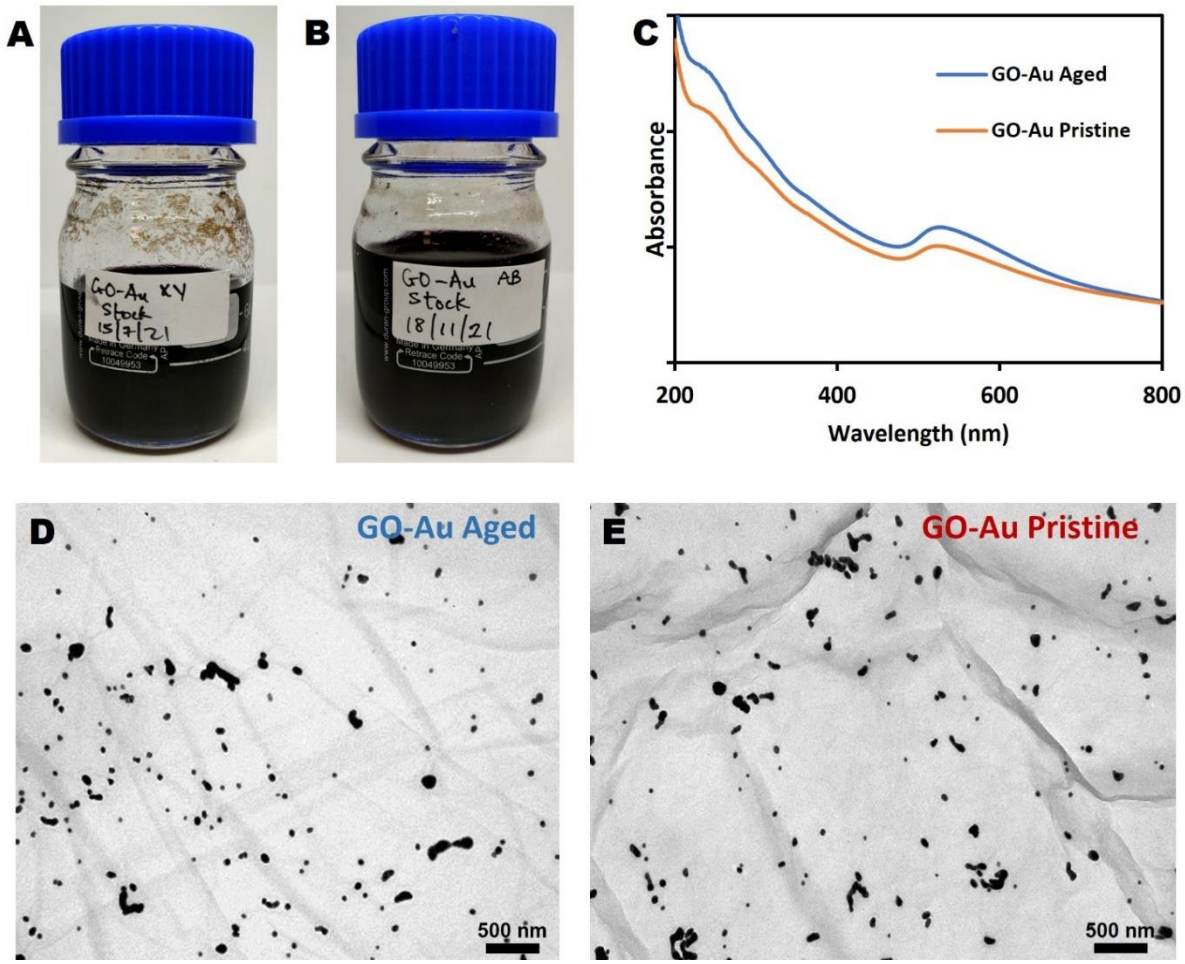

Figure 28: Characterization of pristine and aged (by 4 months) GO-Au nanohybrid. (A) Stock of aged nanohybrid (GO-Au XY), (B) Stock of pristine nanohybrid (GO-Au XY) (C) UV-vis spectra of the two nanohybrids, (D) TEM image of GO-Au Aged (E) TEM image of GO-Au Pristine

3.2.4. Quantification of Au on GO-Au nanohybrid

The use of ICP-MS has benefits beyond just characterization of nanoparticles; it is a convenient method for the quantification and detection of nanoparticles in biological assays [225]. Specifically, the accuracy of using ICP-MS to determine Au has been well established [226]–[228]. Investigating quantitatively the presence of AuNP in a sample is very crucial to understanding their environmental and biological effects [226], [229]. Gold standard solutions were

used to generate a range of gold concentrations (0.01 – 1.0 mg/L) for calibrating the ICP-MS instrument.

The concentration of Au in each of the 3 batches of the GO-Au nanohybrid was measured using the ICP-MS. The average concentration of Au as measured in each of the X, Y and Z replicates was 0.128 ± 0.005, 0.144 ± 0.003 and 0.128 ± 0.01 mg/L respectively which corresponds to an average of 1300 mg/L of Au in the neat suspension of the GO-Au nanohybrid (**Figure 29**).

The similarity in the results demonstrates the reproducibility and reliability of our optimised protocol for the synthesis of the GO-Au nanohybrid. Knowing the concentration of AuNP will allow a better comprehension of the toxicity of GO-Au nanohybrids in environmental media [230]. In addition, AuNPs can be used as chemical labels to determine the fate and transport of GO-Au in biological or environmental systems [231]. This is particularly relevant for GO, as its compositional tracking against the carbon dominated background of environmental matrices is especially challenging. Instead, GO can be traced through this compositionally stable nanohybrid, involving measurement of Au concentration by, for example, ICP-MS, as a proxy for the presence of the GO-Au nanohybrid.

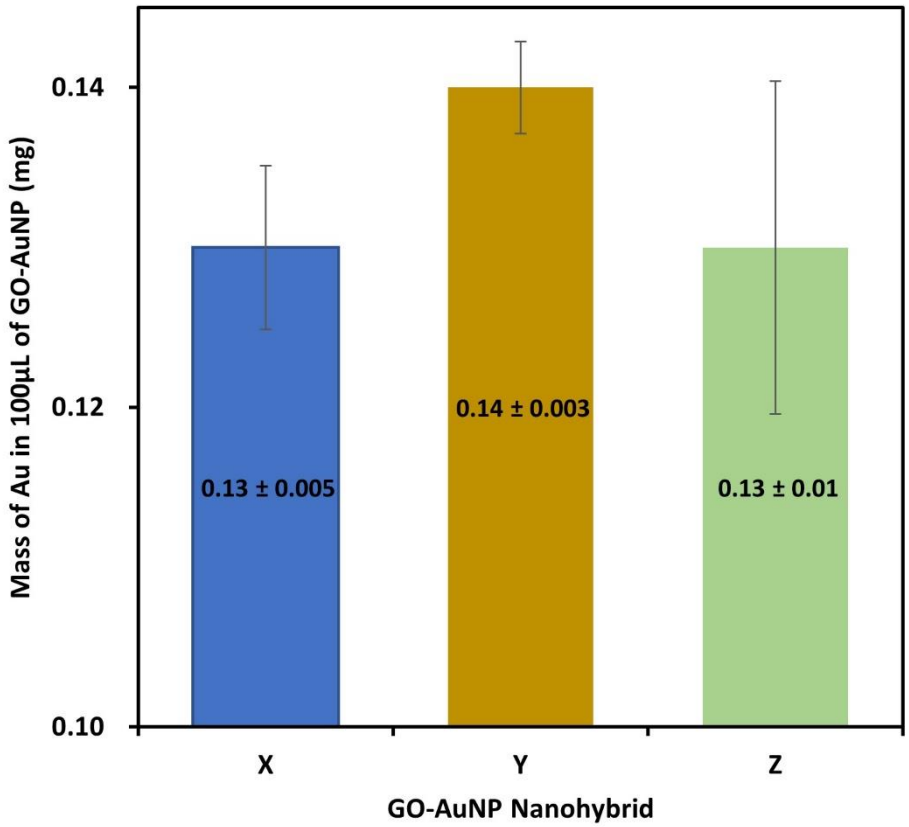

Figure 29: Mass of Au measured in 100 µL of each of the GO-Au nanohybrid samples X, Y and Z. Values shown are average of triplicate samples with standard deviation

3.3. Conclusions

In this study, we have synthesised a GO-Au nanohybrid and optimised the ratio between GO and AuNPs in the nanohybrid produced. The nanohybrid was found to have uniform distribution of AuNPs on the GO sheets and exhibited good stability. This is the first study to show a reproducible standardized protocol for the synthesis of GO-Au nanohybrids. Standardization of practice especially protocols is a major focus in the development of nano- and other advanced materials and their toxicological assessments. A comprehensive evaluation of physical and chemical properties of the material in a realistic media that mimics the natural environment is also an essential requirement.

This output is significant because unlike many other nanomaterials, GO-Au nanohybrid is not yet commercially available and a standardised protocol for a reproducible well-tested hybrid could support commercialisation. The high yield of the synthesis method further enables using the nanohybrid in ecotoxicological research which often requires a good quantity of the same material for consistency and reproducibility testing in toxicological studies.

This research paves the way for critical evaluation of the nanotoxicological assessment of GO-Au nanohybrid in biological and environmental systems especially given that the stability and characteristics of the GO-Au nanohybrid were not impacted by ageing for up to 4 months.

Chapter 4:

Nanotoxicity Assessment of Graphene Oxide-Gold Nanohybrid on *Daphnia magna*

This chapter has been published as follows:

Akere, T. H., Ali-Boucetta, H., & Valsami-Jones, E. (2023). Nanotoxicity of Graphene Oxide – Gold Nanohybrid to Daphnia Magna. *Aquatic Toxicology 2023, Vol. 260 (April), page 1-12*. https://doi.org/10.1016/j.aquatox.2023.106552

4.1. Introduction

As it is with the fate of many nanomaterials, it is unavoidable these GO-Au nanohybirds, once commercialised, will be released to the aquatic ecosystem [203]. Potentially, this could setoff deleterious effects to organisms at each level of the food chain [232]. With the uncertainty around the toxicity of GO-Au nanohybrids, it is vital to understand whether or not they might induce any acute or chronic harmful effect on sensitive organisms such as *Daphnia magna*. In addition, since daphnia are known to bioaccumulate chemicals [87], [124], [128], an evaluation of the bioaccumulation of GO-Au nanohybrid becomes necessary to gain insight into how the nanohybrid may spread through the food web. There is a potential risk to human health through the consumption of contaminated seafoods such as clams and fish.

The nanotoxicity of GO-Au nanohybrid on daphnia has not been broadly investigated. Hence, this research aims to evaluate the toxicity of graphene oxide – gold nanohybrid to neonates (< 24 hrs old) of *Daphnia magna* in different media. Specifically, this work focused on (i) assessing acute immobilization of daphnia neonates (ii) bioaccumulation of the nanohybrid by daphnia (iii) fate and transport of the nanohybrid in daphnia (iv) dispersion stability of the nanohybrid in various daphnia media.

4.2. Results and Discussion

4.2.1. Assessment of the Impact of NOM on dispersion stability of GO-Au Nanohybrid

Evaluation of the stability of nanomaterials dispersion is one of the properties that have been identified as fundamental in understanding their transport and fate in the environment [225], [229], as It can influence their cellular and environmental uptake and transportation. In addition, the stability of NPs dispersion can provide a base for a holistic ecotoxicological assessment of NPs in biological systems [233]. It is therefore essential that this evaluation is done in media that truly represent the likely environmental conditions for the ecotoxicity indicator species under investigation.

Taking a further step towards demonstrating the relevance of the studied nanohybrid as a model material in ecotoxicity research, the stability of GO and GO-Au was evaluated in three media: ultrapure water (control), natural borehole water (BHW) and a synthetic high hardness combo (HHC) medium (**Fig. 28-30**). While BHW is widely used in ecotoxicological studies for culturing many freshwater and marine organisms such as fish, daphnia, clams etc, HHC as an artificial medium has also been approved for use in culturing and testing model organisms in order to reduce variability in ecotoxicological testing results [234]. The use of both natural (BHW) and synthetic (HHC) media for toxicity testing is recommended by the US EPA, OECD and ISO [113], [114], [193].

The stability of GO and GO-Au nanohybrid in aquatic media is influenced by the presence (or absence) of aquatic environmental conditions such as natural

organic matter (NOM), pH and the concentrations of ions and cations [32]. NOM tends to bind with NPs through hydrogen bonds, steric repulsive forces and Lewis' acid-base interactions, thereby increasing the stability and subsequent bioavailability of suspended particles to aquatic organisms [235], [236].

In ultrapure water, both the GO and GO-Au nanohybrid demonstrated high stability for 48 hrs as shown by the absence of reduction in absorbance at 230nm (**Figure 30**). This could be explained by the elevated surface charge of the nanomaterials (ζ_{GO} = -56.4 ± 2.4 mV and $\zeta_{GO\text{-}Au}$ = -47.4 ± 2.5 mV) as the dispersion stability of colloidal particles depend mainly on the repulsive forces due to surface charge [237], [238].

However, in the borehole and HHC media, the absorbance of GO and GO-Au dispersion after 48hrs declined to less than 20% of the initial absorbance except the GO in the HHC media which decreased to more than 80% as shown in **Figure 29-30**. The surface charges also significantly dropped to ζ_{GO} = -23.6 ± 0.9 mV and $\zeta_{GO\text{-}Au}$ = -18.3 ± 0.6 mV for borehole, and ζ_{GO} = -34.2 ± 0.8 mV and $\zeta_{GO\text{-}Au}$ = -22.4 ± 1.4 mV for HHC. The decrease in the dispersion stability could be because of reduction in the ionic strength of the medium and the adsorption of protons to cationic salts (such as Mg^{2+}, Na^{+}) present in the medium [235]. This facilitates aggregation and flocculation of the nanoparticles into distinct phases that can be visually observed (**Figure 29-30**).

The colloidal stability of the nanomaterials in the presence of NOM was observed to be better than in its absence. After 24hrs in borehole media, the GO and GO-Au nanohybrid maintained approximately 50% and 80% of their initial absorbance

respectively. The values increased to 60 – 80% in the HHC media for the same duration. The concentration of the NOM at 20 mg/mL as recommended by OECD was sufficient to make the GO-Au nanohybrid stable in the test media. This emphasises the role of NOM in stabilising nanomaterials in different environmental media which was previously reported for other carbon-based nanomaterials [105], [239], [240]. It could therefore be suggested that the GO-Au nanohybrid can become bioavailable to aquatic organisms in any ecotoxicological study with the tested media.

Media play a crucial role in the fate, behaviour and toxicity testing of nanomaterials. As such, standard test media that contain NOM are preferred for toxicological assessments as they represent more realistic environmental conditions. The good stability performance of the GO and GO-Au nanohybrid in NOM-containing borehole and HHC underscores the active role of NOM in bio-nano interactions. These results further demonstrate that the proposed synthesis method can produce GO-Au nanohybrids that are stable in relevant media and may be bioavailable to model organisms in a natural environment. This is an important requirement for ecotoxicological research because biological responses are only triggered when exposure and/or uptake occurs between the GO-Au nanohybrid and the biological target.

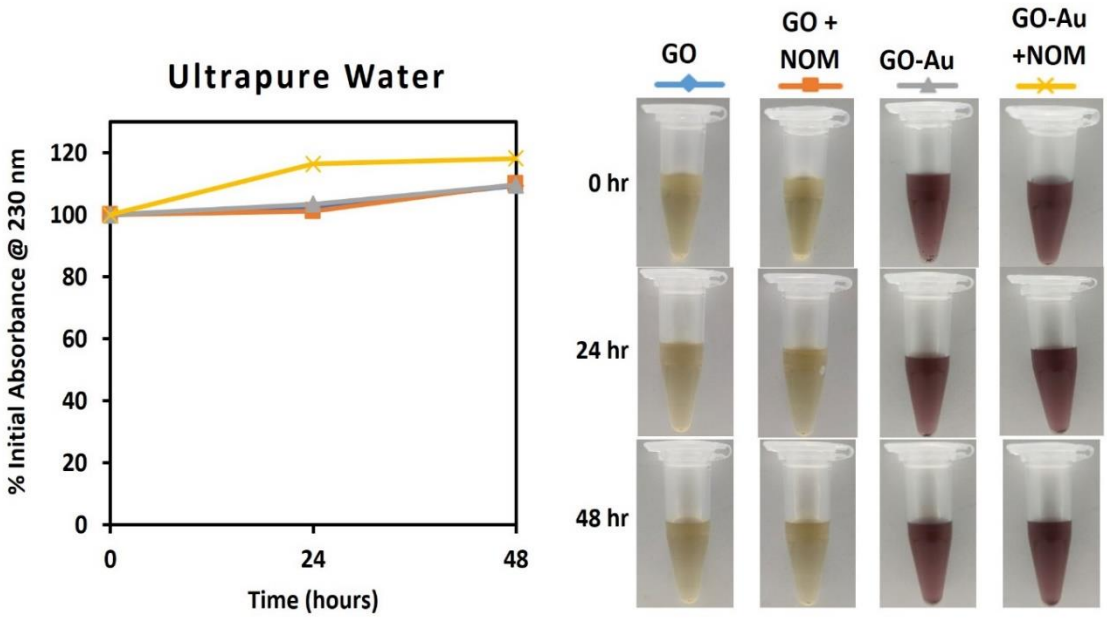

Figure 30: Monitoring of dispersion stability of GO and GO-Au in ultrapure water with and without NOM (20 mg/L). LEFT: Absorbance measured in UV-vis; RIGHT: images from visual observation

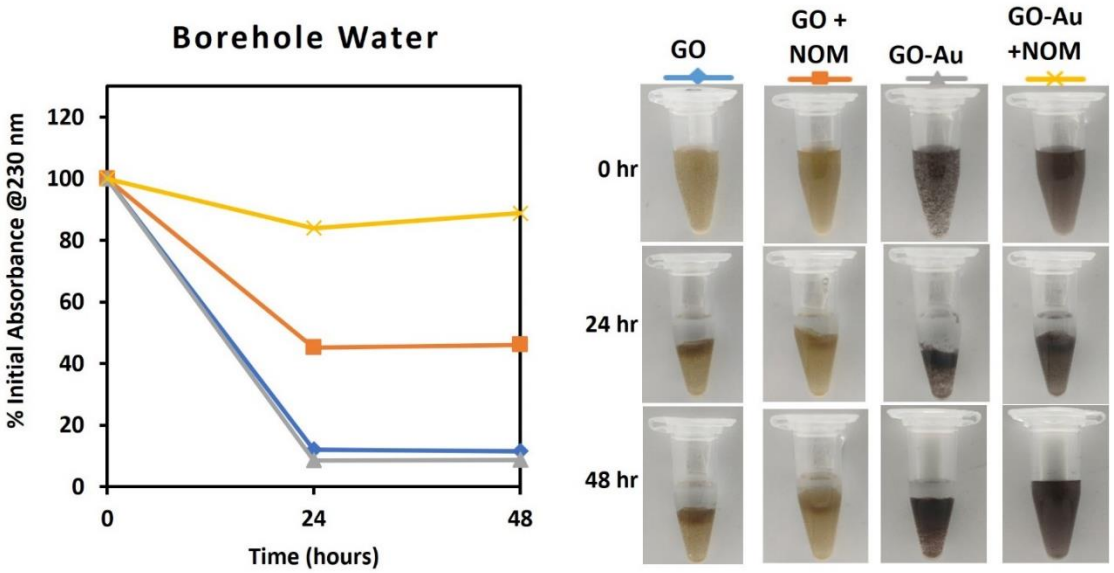

Figure 31: Monitoring of dispersion stability of GO and GO-Au in borehole water with and without NOM (20 mg/L). LEFT: Absorbance measured in UV-vis; RIGHT: images from visual observation

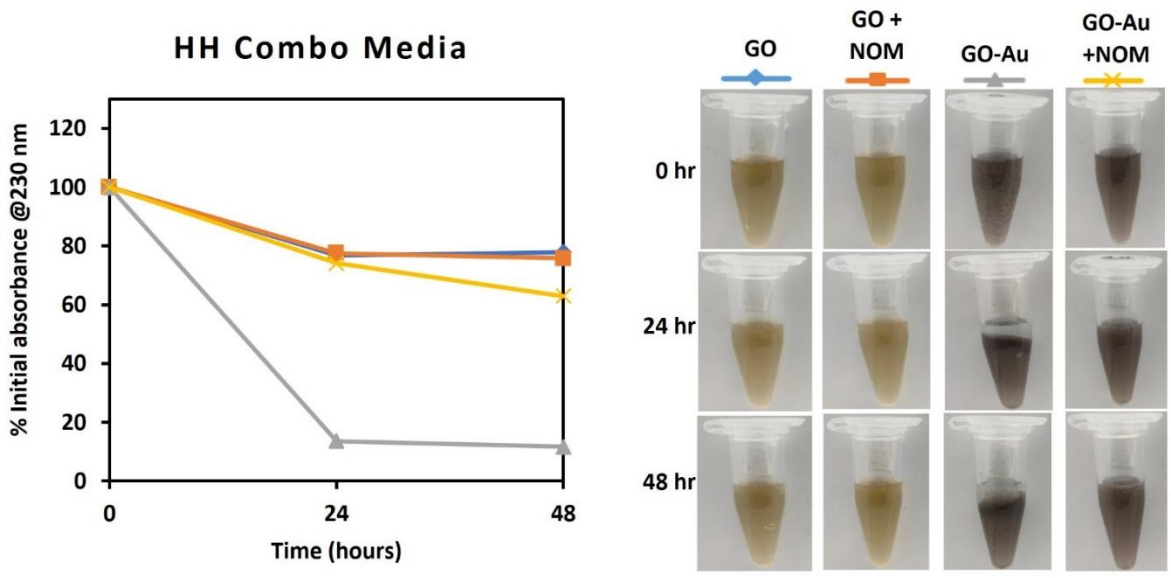

Figure 32: Monitoring of dispersion stability of GO and GO-Au in HH Combo media with and without NOM (20 mg/L). LEFT: Absorbance measured in UV-vis; RIGHT: images from visual observation

4.2.2. Acute Immoblization Test

To evaluate the short-term adverse effect of the nanohybrid on daphnia, an acute immobilization test was conducted on daphnia neonates (<24hrs old) for 48hrs. The result of the immobilisation tests for borehole media and HHC is presented in **table 4** as the percentage of neonates that survived after 48hrs. According to the test protocol, neonates that are unable to swim within 15 seconds of light agitation are considered immobile [112]. In the borehole media exposure for GO, all the organisms (including the control) survived after 48hrs except in the 1mg/L test vial where 93% survival was recorded. A similar result was recorded for the GO-Au nanohybrid: all the neonates in all test concentrations had 100% survival

except for 100 mg/L where 93% survival was recorded. In the HH combo media exposure for GO, the survival rate in all treatments was 100%. However, in the GO-Au exposure in HH combo media, all the treatments had 100% survival rate recorded except in the 100mg/L test vial where the rate was 80%.

The EC_{50} results indicate that the GO-Au nanohybrid did not induce any lethal ecotoxicological effect (mortality and immobilization) to *D. magna* neonates at the tested concentrations (1-100 mg/L) in both borehole and HH Combo media. According to the United Nations' global harmonised system of classification and labelling of chemicals [241], the GO-Au nanohybrid is not considered hazardous to the aquatic environment. This is similar to what Liu et al. (2017) reported for daphnia exposed to rGO-Au. In that study, there was no significant alteration to the growth and survival of the organisms after 48h. However, the chemical combination of GO and Au can inhibit toxicity to cells as Li et al. (2014) observed with GO-AuNPs nanocomposite causing reduced cytotoxicity of amyloid peptides.

The toxicity effects associated with daphnia exposure to nanomaterials are concentration dependent [87], [132]. Higher concentration of nanomaterials induces more effects compared to lower concentration. However, as observed in this work, high concentration of GO and GO-Au nanohybrid did not induce any deleterious effect on the exposed organisms. A combination of factors could possibly explain this reduced toxic effect. Daphnia are known to be able to remove harmful substances from their gut (depuration) within a short period [232], [243]. Degradation of the GO and GO-Au nanohybrid may have occurred in the

digestive tract of exposed daphnids, as has been observed in insects and microorganisms [107], [108].

In addition, the presence of NOM in the daphnia media could have mitigated toxic effects. Apart from stabilising nanomaterials in aqueous media, NOM can have an effect on the toxicity of nanoparticles to aquatic species. This is achieved by the physical and chemical interaction of the NOM with the nanoparticle surface, thereby altering the defects and surface functionalities. NOM was found to alleviate the toxicity of silver nanoparticle to the reproductive ability of daphnia by forming protective protein-rich coating around the nanoparticles [244]. Similarly, the acute and chronic toxicity of GO to *Daphnia magna* was mitigated by NOM by attenuating the induction of oxidative stress [245]. An understanding of the role played by NOM in nanomaterial toxicity will help to avoid an overestimation of nanomaterial risk.

Table 4: EC_{50} (48hr) result for daphnia neonates exposed to GO and GO-Au in borehole water and HH combo media

Percentage Survival after 48hr (%)				
Concentration (mg/L)	**Borehole**		**HH Combo media**	
	GO	**GO-Au**	**GO**	**GO-Au**
0	100	100	100	100
1	93	100	100	100
5	100	100	100	100
10	100	100	100	100
20	100	100	100	100
50	100	100	100	100
100	100	93	100	80

4.2.3. Light Microscope Imaging

Live images of daphnia neonates were taken for morphological observations after 48hr exposure to GO-Au nanohybrid. The results are presented in **table 5**. The images were taken following exposure for the following treatments: 0, 1, 50 and 100 mg/L GO-Au nanohybrid. Observing the test organisms under microscope enhances our understanding of their bioaccumulation/depuration activity and the transport of the nanohybrid within the organism.

As can be observed from the images below, GO-Au nanohybrid cannot be visibly seen in the digestive tracts of the daphnids in the control treatment. For the daphnia samples exposed to 1mg/L, some traces of GO-Au nanohybrid can be seen in the gut of the organisms (dark elongated structure). However, the nanohybrids in the gut of daphnids exposed to 50 and 100 mg/L are noticeably more concentrated than the those in the 1mg/L exposures. These visual observations agree with the result of ICP-MS quantification of GO-Au nanohybrid as described in section 4.2.4.

Exposure of daphnia to heavy metals and nanomaterials have been reported to have effect on embryonic development and induce tail loss and carapace shedding [131], [244], [246]. Daphnia are known to lose their antenna and spine in response to stress or toxicity. From the images taken, it is apparent that the daphnids in all the treatments have not lost any body parts. This also supports the acute toxicity test conclusion that the GO-Au nanohybrid did not cause any significant harm to daphnia at the tested concentration and within the time period studied.

Table 5: Daphnids exposed to GO-Au nanohybrid (1, 50 and 100 mg/L) (Scale = 1000 µm)

Test Concentrations	Daphnia Images after Exposure	
Control		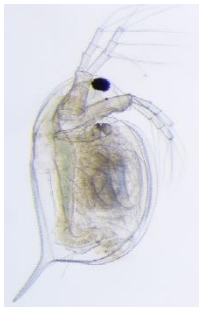
1 mg/L		
50 mg/L		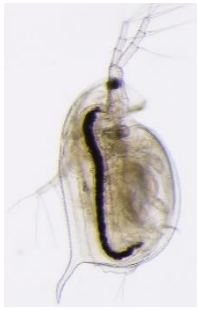
100 mg/L		

4.2.4. Bioaccumulation

The ability of *D. magna* neonates to bioaccumulate GO-Au nanohybrid was tested, and the result is presented in **Figure 33** below. Due to the difficulty in directly quantifying carbon nanomaterials in biological systems (abundant background carbon, absence of reliable quantification method etc) [247]–[249], the concentration of Au in the nanohybrid was used in this study as a chemical label for GO-Au. The concentration of GO-Au nanohybrid can then be estimated from the measured of Au concentration.

The bioaccumulation was carried out using 3 concentrations: 1, 50 and 100 mg/L. The mean concentration of Au measured in 100 μL of the digested daphnids exposed to 1mg/L was 67.05 ± 0.002 μg/L. For 50 and 100mg/L, the mean concentration of Au quantified were 210.31 ± 0.008 μg/L and 252.63 ± 0.006 μg/L respectively. The mass of Au in the daphnia samples was estimated from the concentration of Au and the quantity of the analysed homogenate sample (100 μL). The calculated mass of Au in the samples are 0.0067, 0.0210 and 0.0253 mg for the 3 test concentrations respectively (1, 50 and 100 mg/L).

The results confirmed that daphnia were indeed bioaccumulating the GO-Au nanohybrid, similar to what have been reported of their ability to bioaccumulate GO and other nanomaterials [124], [128], [232]. Likewise, daphnia are able to eliminate most of the bioaccumulated GO from their gut for a short-term exposure. The depuration ability has been linked to the organism's response to

acute toxicity [87]. This is corroborated by the acute toxicity experiment that found that daphnia were able to survive exposure to the nanohybrid within 48hrs.

It was also observed that the amount of GO-Au nanohybrid bioaccumulated increases as the concentration of the nanohybrid increases: daphnids exposed to the highest nanohybrid concentration (100mg/L) had the highest concentration of Au (252.63 µg/L) while those exposed to the lowest test concentration (1mg/L) produced the least amount of Au (67.05 µg/L).

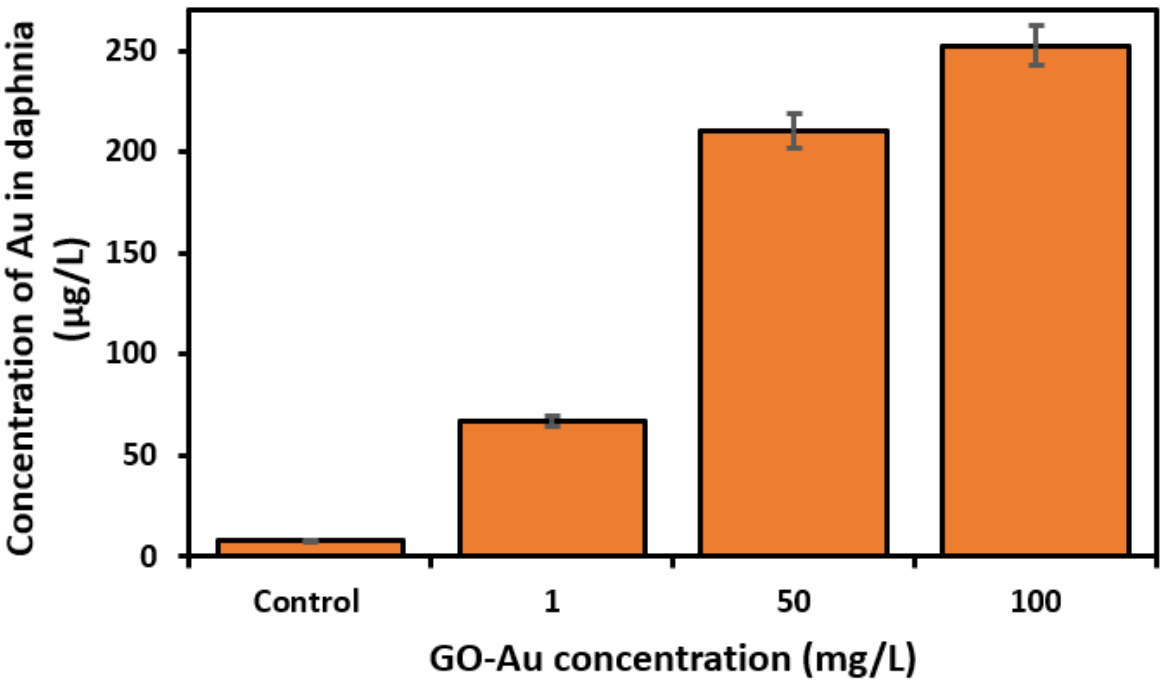

Figure 33: Quantification of Au in digested daphnia samples after exposure to GO-Au nanohybrid. Results represent the mean of three individual replicates and their standard deviation.

4.2.5. TEM Imaging

The TEM cross sectional images of the daphnids exposed to various GO-Au treatments for 48hrs are presented in **Figure 34**. The detailed images were taken to further evaluate toxicity of GO-Au nanohybrid and its impacts on the organism's gut and surrounding organelles. In the cross sections from the control group (**Figure 34A**), common structures found in the gut can be seen such as the nucleus (N), mitochondria (M), lysosome (L) and peritrophic membrane (PTM). As expected, there were no traces of the GO-Au nanohybrid (as AuNPs) in the gut in the control group. However, AuNPs can be seen in the cross sections of all the remaining treatment samples (**Figure 34, B – F**). An interaction of the GO-Au nanohybrid with the cell and formation of sizeable vacuole structures and lipid like cytoplasmic inclusions are observable.

AuNPs can be observed within the cellular matrix (**Figure 34E**), indicating that there may have been damages to the peritrophic membrane (PTM). Essentially, the function of the PTM is to provide protection for the gut's epithelial cells and to control the inward and outward movement of enzymes and nutrients [250]. Cellular absorption of some nanomaterials have been correlated to toxic effects such as mortality and morphological changes [244]. However, these effects were not observed in this study involving GO-Au nanohybrid. Internalization of the GO-Au nanohybrid may have led to the over-production of reactive oxygen species (ROS) that causes oxidative damage [251]. This sublethal effect could be responsible for the irregular shape and arrangement of organelles within the cells (**Figure 34C, D** and **F**). The AuNPs are generally well dispersed in the digestive

tracts of the examined images. However, some aggregated form of Au NPs can be seen in the gut located around the MV areas and in the lumen (**Figure 34D, E and F**) which may disrupt metabolism and transformation of chemical [250]. The distribution of AuNPs in daphnia gut is similar to what have been reported for Cu, ZnO and nanoplastics [133], [251], [252].

From the observation of the TEM images alone, it is diffcult to determine whether the AuNPs have dissociated from the GO or they are still attached to it. However, the GO could not be visibly seen in the gut probably due to biodegradation by enzymatic reactions in the daphnia [107]. In addition, TEM imaging of the GO could not be correctly done in tissue samples due to its single layer thickness which is obscurred by interference from background carbon in tissues.

The presence of the AuNPs in the gut confirms the ingestion of the GO-Au nanohybrid by the daphnia. This ingestion is crucial and significant for the bio-nano interaction process which preceeds the generation of biological responses. Therefore, it is highly possible that sublethal effects such as DNA damage and induction of biomarkers of stress (enzymes) could have occurred. In addition, the impact of these sublethal effects could be severe and become manifest in the offsprings of exposed daphnids when evaluated in a multi-generational study.

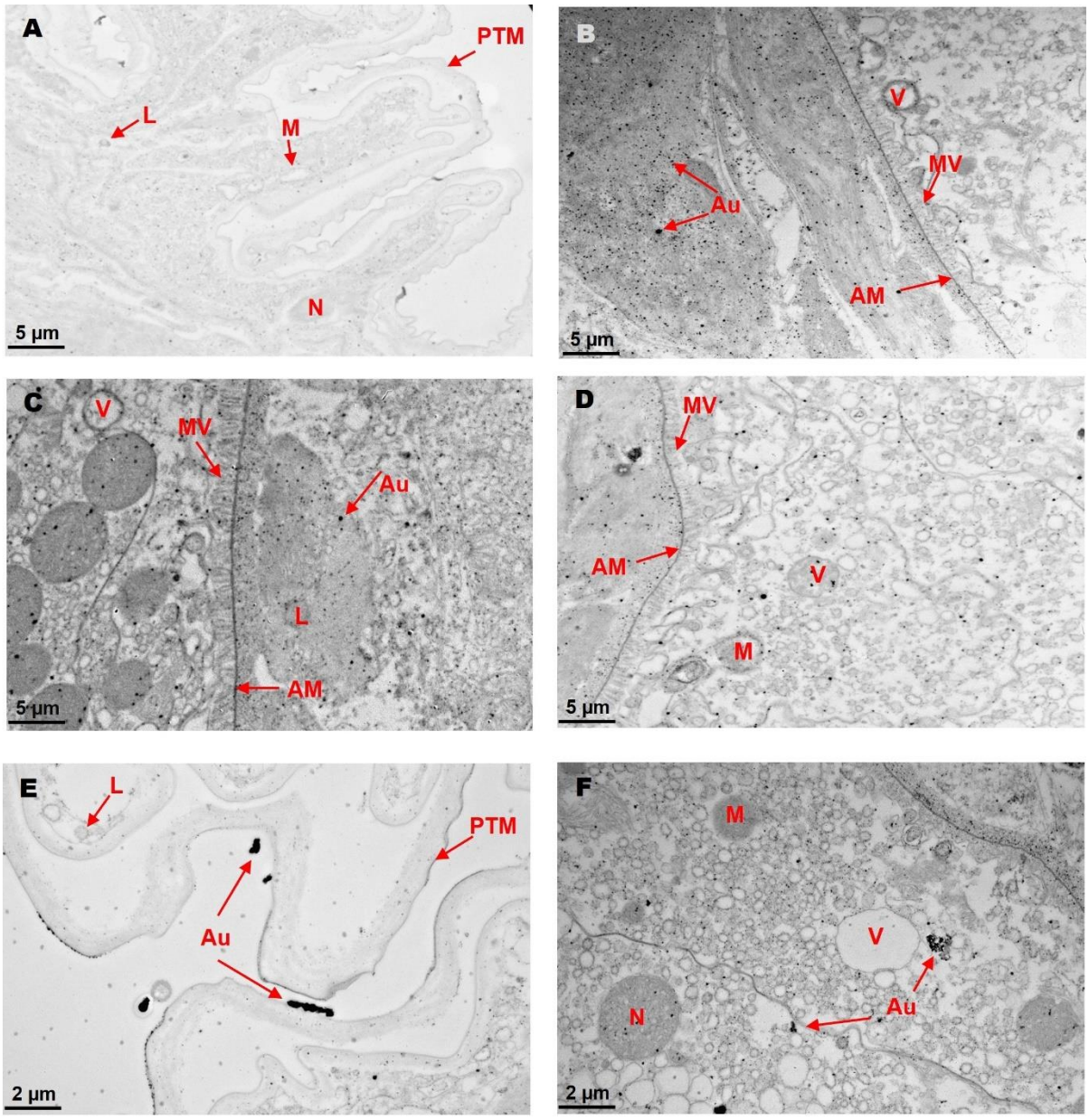

Figure 34: A representative images of TEM sections of daphnia neonates exposed to various concentrations of GO-Au nanohybrid. KEY: microvilli (MV), lysosome (L), mitochondria (M), nucleus (N), peritrophic membrane (PTM), vacuole (V), apical membrane (AM), AuNPs (Au).

4.3. Conclusions

An evaluation of the toxicity of GO-Au nanohybrid to neonates of *Daphnia magna* in borehole and HH Combo media was attempted in this work. The outcome of the EC_{50} toxicity test and bioaccumulation study showed that the nanohybrid does not cause any lethal ecotoxicological effect (mortality and immobilization) on daphnids. This is despite the moderate stability of the GO-Au nanohybrid in the tested media that ensured the bioavailability of the nanohybrid to the organism within the test period.

Morphological observations of the digestive tract of the exposed daphnids did not reveal any serious damage to internal structures, although disorganisation and irregular shape of some organelles may be attributed to oxidative stress. Also, an assessment of the fate and movement of the GO-Au nanohybrid gave an insight into the distribution of the AuNPs in the digestive tract of daphnia. While most of the AuNPs seen in the digestive tracts were well dispersed, few aggregates were observable that can affect metabolism.

This work represents a significant step in our understanding of the environmental risks associated with the use of GO-Au nanohybrid. With the expanding use of GO-Au nanohybrid in various applications, there is a need for continuous evaluation of the nanosafety of the nanomaterial to the ecosystem and human health. Future research should focus on the chronic toxicity and sublethal effects (growth, reproduction, hormonal changes) of the nanohybrid on daphnia neonates.

Chapter 5:

Cellular Toxicity Assessment of Graphene Oxide-Gold Nanohybrid

5.1. Introduction

The discovery and characterization of graphene stimulated significant research interest in the material and its derivatives such as graphene oxide (GO) and reduced graphene oxide (rGO) [1], [5], [6]. The high surface area of GO, an oxidised form of graphene, make it a suitable substrate for the development of nanohybrids – blending of nanomaterials with distinct features to produce a material with enhanced or new functionalities [253].

Graphene oxide-gold (GO-Au) nanohybrid, for example, has remarkable properties that make it useful for diverse applications such as biosensing and cancer therapy [18]–[20]. However, their widespread usage also makes them a subject of concern for toxicologists due to their potential environmental exposure. As this is a relative new material, their safety to the environmental has not been well studied [22], [23]. Hence they pose a potential threat that demands urgent critical assessment.

The use of cells (*in vitro*) for nanotoxicological assessments is a convenient alternative to animal testing due to cost, ethical concerns and high thoroughput [155]. Although total replacement of animal studies is still unachievable, *in vitro* assays enable nanotoxicological evaluation without sacrificing animals [254]. Common *in vitro* assays used for assessing cytotoxicity include MTT, comet assay, lactate dehydrogenase (LDH), DNA damage, Annexin-V-PI assays etc. The combination of these assays serve as weight of evidence that allows for extensive evaluation of cytotoxicological effects such as oxidative stress, cell viability, cell proliferation, changes to the cell membrane, damage to internal structures and cell death [155], [255], [256].

In this chapter, we present a series of cellular assays to assess the cytotoxicity of zebrafish embryo cell line (ZF4) and human lung adenocarcinoma cell line (A549). The use of zebrafish as well as its embryo for toxicity testing is well established and accepted by the Organisation for Economic Cooperation and Development (OECD) [257], [258]. *In vitro* assays based on fish cells have been considered a favourbale alternative to the use of whole fish in aquatic toxicological studies, in line with the principle of 3Rs (replacement, reduction and refinement) [153]. Since its initiation in 1973 [166], the A549 cell line has been well used as a model for *in vitro* cytotoxicity of numerous potential toxicants, including nanomaterials, due to its relative ease of culture and for serving as a representation of lung exposure [259], [260].

In addition, oxidative stress and mechanisms of cell death were assessed in ZF4 and A549 cells following exposure to a wide range of concentration of GO and GO-Au nanohybrid. The dispersion stability of GO and GO-Au nanohybrid were also evaluated in ultrapure water as well as in the cell culture media (CCM) for ZF4 and A549 cells prior to the cytotoxicity assays.

5.2. Results and Discussion

5.2.1. Dispersion Stability of GO and GO-Au Nanohybrids

It is well established that chemical and physical properties of nanomaterials have significant influence on biological responses [233]. As such, assessments on cellular toxicity would be incomplete without an evaluation of physical attributes such as dispersion stability of the nanomaterials in culture media. Cell culture media (CCM) are important sources of nutrient and energy required for cell growth and regulatory processes. They contain biomolecules such as proteins that have potential to interact with GO and GO-Au, thereby influencing their colloidal stability and internalisation by the cells [261]. This interaction can have crucial implication on cellular responses and nanotoxicity [262]–[264].

The dispersion stability of GO and GO-Au nanohybrid was assessed in ZF4 and A549 culture media, and the results are presented in **Figure 35** and **36** below. The measurement of absorbance by UV-vis at the characteristic GO peak at 230nm allows to indirectly characterise the stability of the GO and GO-Au nanohybrids over time. The composition of the CCM for ZF4 and A549 have been described in **section 2.4.2** in **Chapter Two**. In ZF4 media, both GO and GO-Au nanohybrid exhibited high stability with percentage absorbances of 97% and 102% after 48hrs respectively as shown in **Figure 35**. Both nanomaterials also demonstrated similar stability after 48hrs in A549 media with 109% and 92% percentage absorbances respectively (**Figure 36**).

Therefore, both GO and GO-Au show high stability in CCM media for ZF4 and A549 cells after 48hrs. This outcome is corroborated by the visual observation of

the dispersion vials (**Figure 35** and **36**). Some sedimentation of GO and GO-Au can however be seen after 24 and 48hrs monitoring period which is expected. This high stability is similar to what was reported by Duran et al (2015) in a study that assessed the stability of GO in thirteen different biological media including DMEM [260]**.** There is however no known study on the evaluation of dispersion stability of GO-Au nanohybrid in cell culture media.

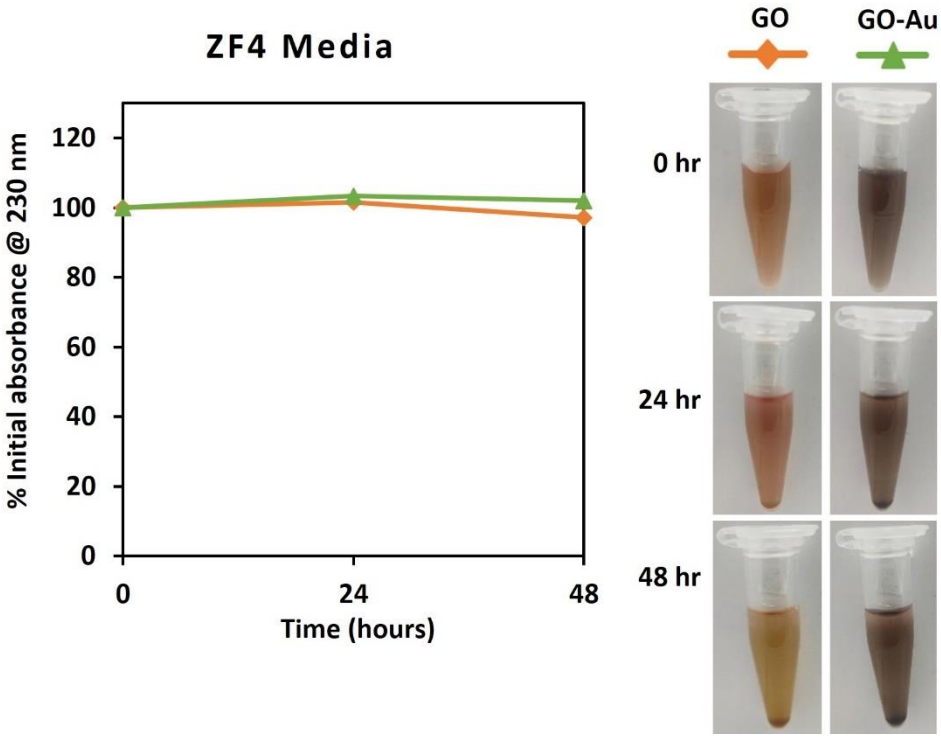

Figure 35: Monitoring of dispersion stability of GO and GO-Au in ZF4 media. LEFT: Absorbance measured at 230nm in ultraviolet-visible spectroscopy; RIGHT: Visual observation of GO and GO-Au dispersions.

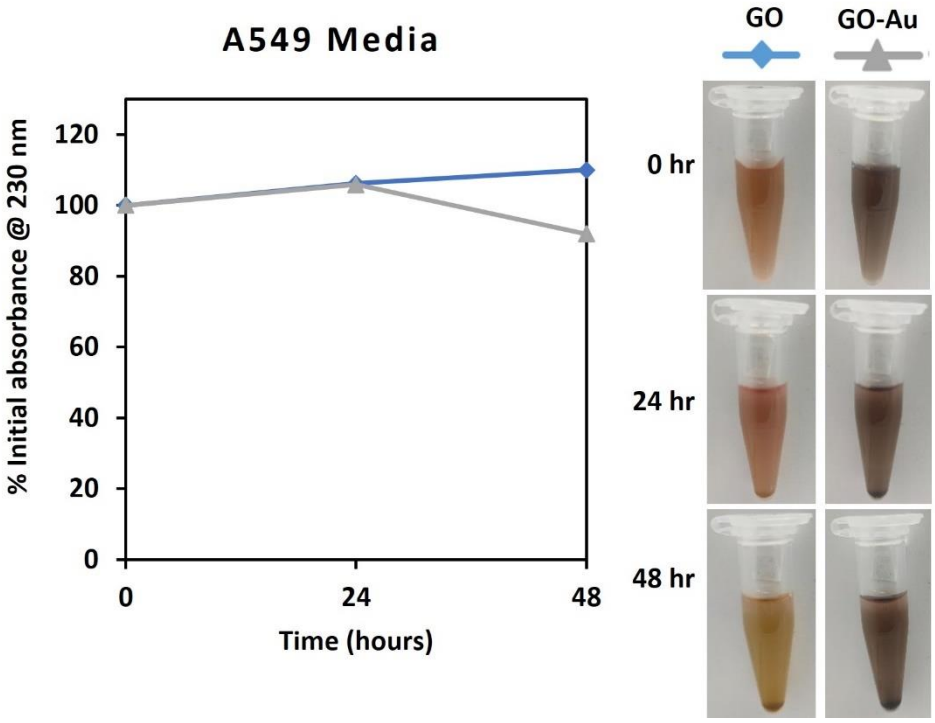

Figure 36: Monitoring of dispersion stability of GO and GO-Au in A549 media. LEFT: Absorbance measured at 230nm in ultraviolet-visible spectroscopy; RIGHT: Visual observation of GO and GO-Au dispersions.

5.2.2. Cytotoxicity Assessment (MTT and LDH)

The cytotoxicity of GO and GO-Au in ZF4 and A549 cells were assessed based on cell viability (as a function of LDH release) and metabolic activity using the modified LDH [265] and MTT [266] assays respectively. As shown in **Figure 37** and **38**, there is a clear relationship between the decrease in both the percentage of viable cells and metabolic activity on one hand, and the increase in GO and GO-Au concentrations (2.5 - 150 µg/mL) and period of incubation (24 – 72 hr) on the other hand.

After 24 hr of incubation, the cell viability of ZF4 cells exposed to GO was preserved up to 10 µg/mL but started decreasing from 20 µg/mL (**Fig. 37A)**. All

the treatments showed decrease in cell viability after 48 and 72 hr of incubation with 150 µg/mL having the most significant decrease in cell viability (41.7% and 39.5% respectively). Likewise, a dose and time dependent reduction in metabolic activity can be observed in ZF4 cells exposed to GO as shown in **Figure 37B.** The metabolic activity of the cells was maintained up to 10 µg/mL after 24 hr incubation but started decreasing from 20 µg/mL. After 48 and 72 hrs of incubation, all the treatments exhibited reduction in metabolic activities with the most significant decrease seen in 150 µg/mL treatment to GO (35.5% and 29.8% respectively).

ZF4 cells exposed to GO-Au nanohybrid exhibited similar time and dose dependent cytotoxicity to those exposed to GO. In **Figure 37C,** all the GO-Au treatments showed significant decrease in cell viability after 24 hr incubation except for 2.5 and 5 µg/mL. The cell viability decreased with the increase in concentration with 150 µg/mL exhibiting the most significant decrease. After 48 and 72 hrs incubation, the only ZF4 cells whose viability was not affected were those exposed to 2.5 µg/mL; the viability of the remaining treatments decreased with the most significant decrease seen in 150 µg/mL (54.5% and 45.8% respectively to time). The metabolic activity of the ZF4 cells treated with GO-Au also showed a dose- and time-dependent decrease starting at a concentration of 40 µg/mL after incubation for 24 hr and from a concentration of 5 µg/mL after 48 and 72 hr of incubation (**Fig. 37D**).

This result demonstrates that both GO and GO-Au nanohybrid induced dose dependent cytotoxic effects on ZF4 cells. This is confirmed by the decrease in both cell viability and metabolic activity of the treated cells at concentration of 5

μg/mL within 24 hr of exposure. To the best of our knowledge, this is the first study that investigated the cytotoxicity of GO or GO-Au nanohybrid in ZF4 cells. However, there have been reports of induction of cytotoxic effects on ZF4 cells by other nanomaterials. For instance, Quevedo et al. (2021a) found that silver nanoparticles induced cytotoxicity to ZF4 cells in a size-dependent manner. Likewise, a dose-dependent decrease in cell viability was observed when ZF4 cells were exposed to 3 stable lanthanides (neodymium, gadolinium and ytterbium) within concentration range of 50 – 400 μg/mL [162].

The bioavailability of the nanomaterials can have huge influence on their cellular uptake and cytotoxicity [233]. Due to the ability of GO to agglomerate and form sediments, Martinez et al. (2020) suggested that the dispersion stability of GO can affect their nanotoxicity. In addition, the stability of GO and GO-Au nanohybrid in CCM is crucial in gaining insights into their toxicity and evaluating their risk to the environment [225], [229]. The analyses of our GO and GO-Au nanohybrid dispersion stability in ZF4 media indicated that their stability may have contributed significantly to the cytotoxic effects induced in the treated cells.

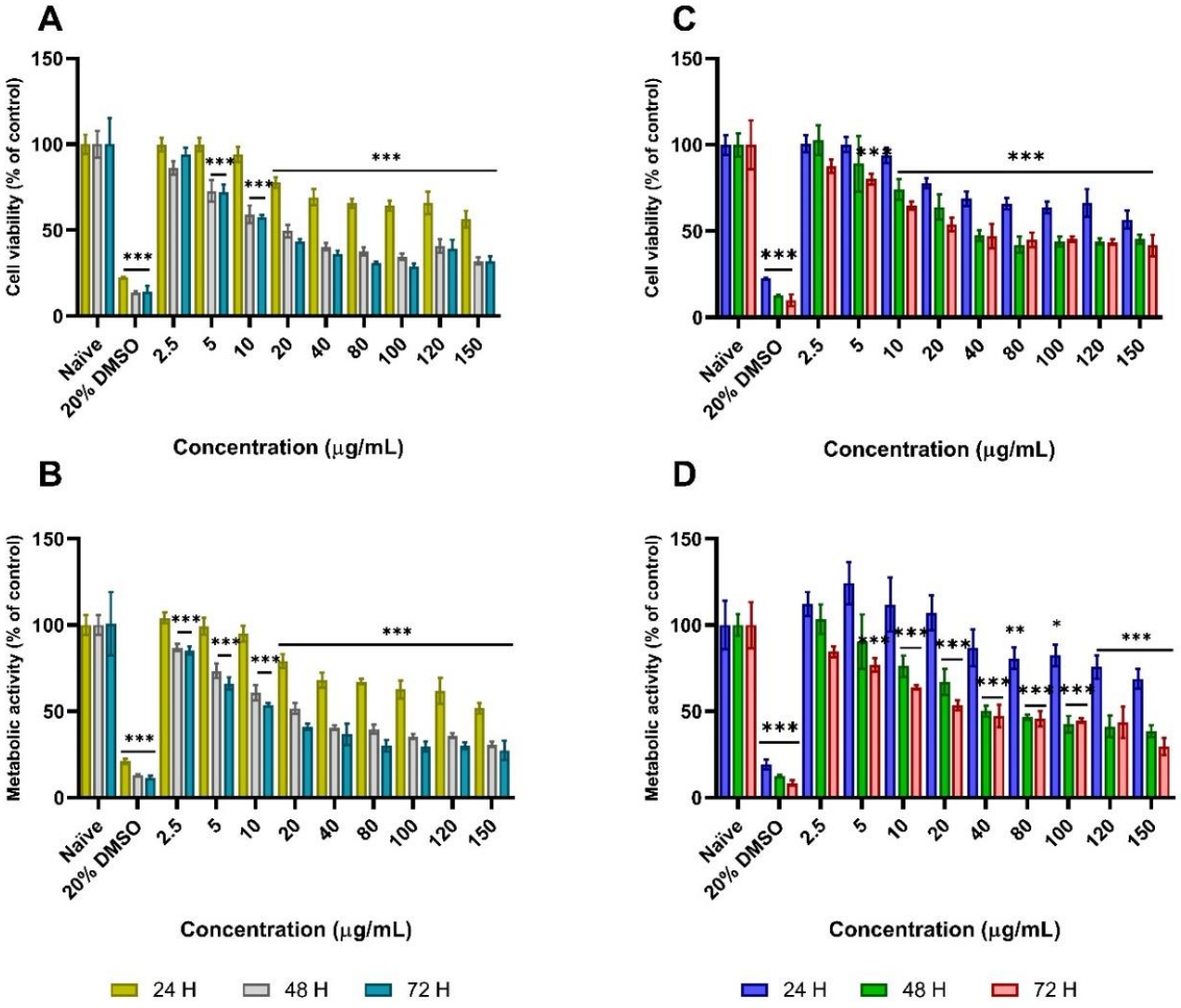

Figure 37: Percentage cytotoxicity of embryonic ZF4 cells treated with GO and GO-Au for 24, 48 and 72 hrs determined by mLDH and MTT assay with concentration range of 2.5-150 µg/ml. (**A**) Cell viability of ZF4 cells treated with GO measured by mLDH (**B**) Metabolic activity of ZF4 cells treated with GO measured by MTT (**C**) Cell viability of ZF4 cells treated with GO-Au measured by mLDH (**D**) Metabolic activity of ZF4 cells treated with GO-Au measured by MTT. A positive control of 20 % DMSO was used. Data with asterisks (*) indicate a statistically significant difference (∗p < 0.05, ∗∗p < 0.01, and ∗∗∗p < 0.001) compared with naive cells (untreated control).

Moreover, in order to understand the cytotoxic effect of GO and GO-Au nanohybrid in A549 cells, cell viability and metabolic activity were also assessed using modified LDH and MTT assays respectively. As shown in **Figure 38A,** a decrease in cell viability with GO can be observed from a concentration of 80 µg/mL within 24 hrs of incubation. All concentrations below that (2.5 – 40 µg/mL) did not show any significant difference compared to the naive (untreated control). However, a decrease in cell viability can be noticed after 48 (62.6%) and 72 hrs (53.7%) with the highest decrease seen at 150 µg/mL. Likewise, a dose dependent decrease in metabolic activity can be seen in A549 cells treated with GO as shown in **Figure 38B.** Apart from the treatment concentration at 2.5 µg/mL after 24 hr incubation, all the other treatments were significantly different ($p<0.001$) from the naïve.

In addition, A549 cells demonstrated a dose-dependent response to GO-Au exposure, similar to that of GO. In **Figure 38C,** the percentage cell viability of the A549 started decreasing in the first 24 hrs of incubation from concentration of 5 µg/mL. By the end of 48 and 72 hrs incubation period, all the treatments caused a decrease in cell viability and showed a significant difference from the naïve ($p < 0.001$). The 2.5 µg/mL had the lowest reduction in cell viability in 48 and 72 hrs (92.5 % and 87.9% respectively) while 150 µg/mL caused the highest reduction (62.6 % and 53.7% respectively).

In addition, a dose dependent decrease in metabolic activity of A549 cells treated with a wide range of GO-Au concentrations (2.5 – 150 µg/mL) was observed as shown in **Figure 38D**. The metabolic activity of the exposed cells decreased from concentration of 5 µg/mL after 24 hr of incubation, from 10 µg/mL after 48 hr of

incubation and from 2.5 µg/mL after 48 hr of incubation. The highest decrease in metabolic activity across the incubation periods (24 – 72 hr) was seen in 150 µg/mL.

Therefore, a significant dose-dependent cytotoxic effect on A549 cells exposed to both GO and GO-Au nanohybrid were observed. This can be linked to oxidative stress via the increase in ROS generation reported earlier. Although there are studies on the cytotoxic effect of GO on A549 cells, direct comparison must be cautiously made due to the different cytotoxicity assays and GO synthesis protocols used. The dose-dependent effect of GO observed in this research is similar to what was previously reported when the adverse effect of GO was assessed on A549 cells [207]. Also, Chang et al. (2011) reported a dose-dependent induction of oxidative stress on A549 cells exposed to GO.

It is noteworthy to mention that this is the first study on the cytotoxicity of GO-Au nanohybrid on A549 cells. Research on the cytotoxic effect of combined nanomaterials is scarce. Nevertheless, a study concluded that GO reduced the cytotoxicity of ZnO nanoparticles to A549 cells [268].

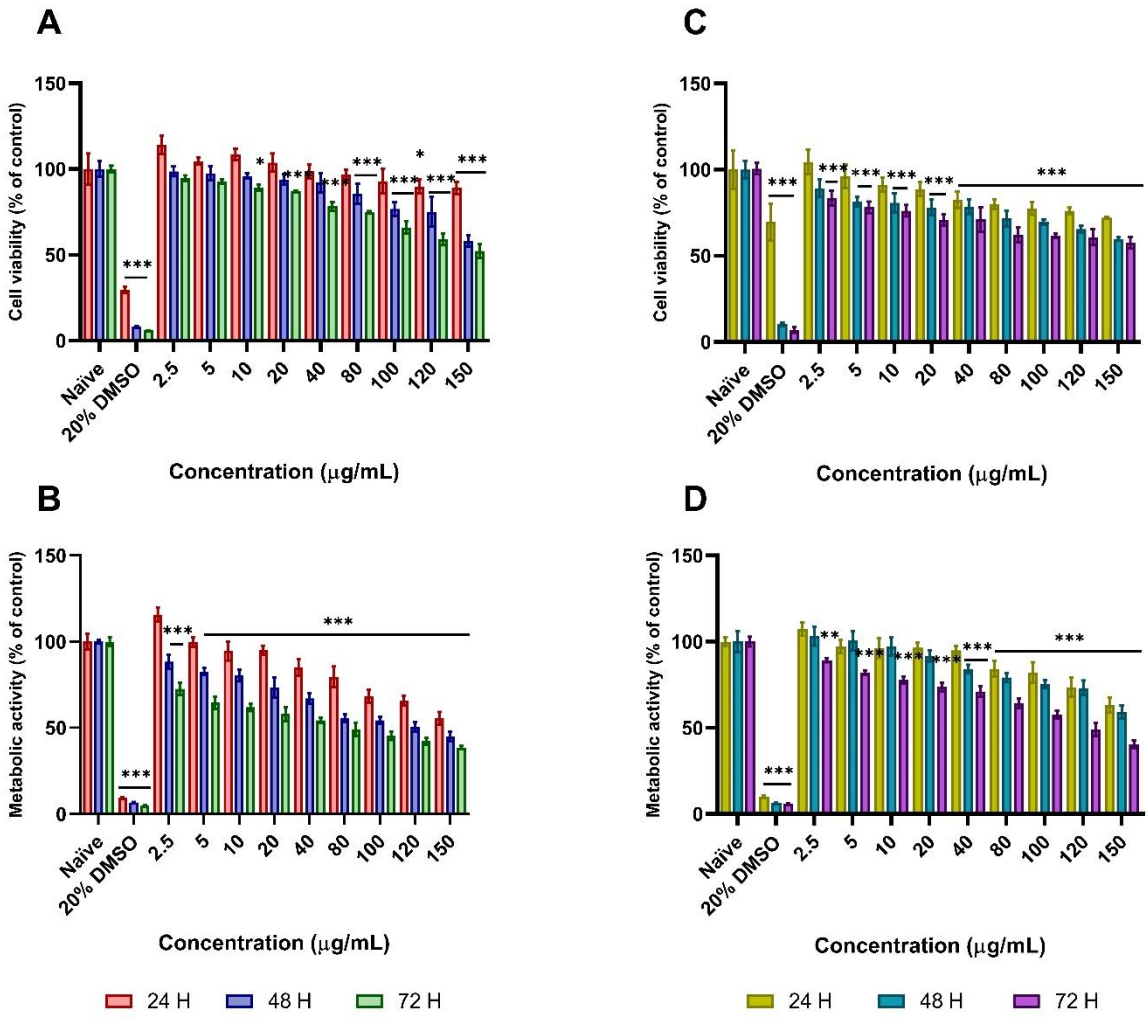

Figure 38: Percentage Cytotoxicity of A549 cells treated with GO and GO-Au for 24, 48 and 72 hrs determined by mLDH and MTT assay with concentration range of 2.5-150 µg/ml. (A) Cell viability of A549 cells treated with GO measured by mLDH (B) Metabolic activity of A549 cells treated with GO measured by MTT (C) Cell viability of A549 cells treated with GO-Au measured by mLDH (D) Metabolic activity of A549 cells treated with GO-Au measured by MTT. A positive control of 20 % DMSO was used. Data with asterisks (*) indicate a statistically significant difference of the Au NP treatments (∗p < 0.05, ∗∗p < 0.01, and ∗∗∗p < 0.001) compared with naive cells at each time point.

5.2.3. Oxidative Stress

Low generation of ROS are intrinsically present in normal cells and are linked to regular cell functioning [269]. However, overgeneration of ROS (precursor to oxidative stress) which occurs as a response to environmental stress and cellular disruption can cause diseases and harm to cell structures [267]. ROS generation was assessed in ZF4 and A549 cells treated with 1, 50 and 100 µg/mL of GO and GO-Au nanohybrid using CellRox deep red kit.

As shown in **Figure 39A-B,** all the GO and GO-Au nanohybrid treatments activated a dose-dependent increase in the production of ROS in ZF4 cells. However, the GO alone generated far more ROS than the cells exposed to GO-Au nanohybrid. A mild dose-dependent generation of ROS can also be observed in A549 cells exposed to GO and GO-Au nanohybrid (**Figure 40A-B**). Only the highest concentration (100 µg/mL) of GO and GO-Au generated a significantly higher ROS from the naïve.

A clear dose-dependent increase in the generation of ROS can be observed in all the treatments which is indicative of oxidative stress in the exposed cells. A correlation exists between the concentration, functionalisation and lateral size of GO and the activation of cytotoxic responses in cells have been described by others [270]. Mittal *et al*. (2016) reported a dose-dependent increase in ROS generation in A549 cells following exposure to GO. In addition, Zhang *et al*. (2012) also attributed elevated ROS generation to GO toxicity in a time- and dose-dependent manner.

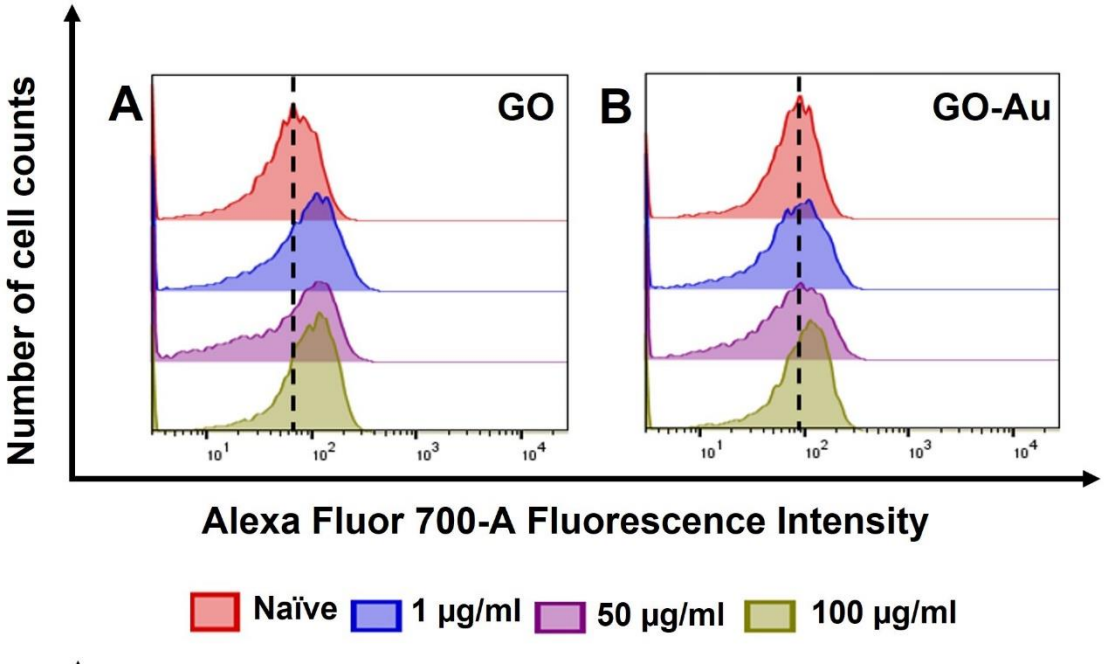

Figure 39: Histogram plots for the generation of ROS in ZF4 cells after exposure to 1, 50 and 100 µg/mL concentrations of (**A**) GO and (**B**) GO-Au nanohybrid measured by flow cytometry. The vertical black dashed line indicates the mean intensity of the control (naive), and it is used as a benchmark to understand the shift in peaks (as an indication of oxidative stress).

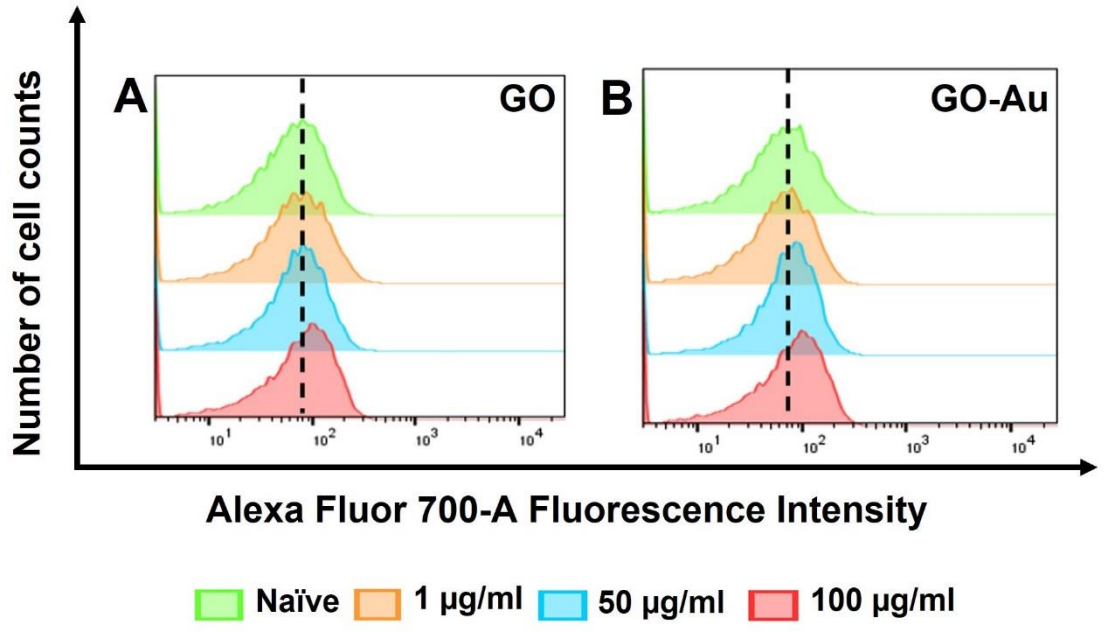

Figure 40: Histogram plots for the generation of ROS in A549 cells after exposure to 1, 50 and 100 µg/mL concentrations of (**A**) GO and (**B**) GO-Au nanohybrid measured by flow cytometry.

The vertical black dashed line indicates the mean intensity of the control (naive), and it is used as a benchmark to understand the shift in peaks (as an indication of oxidative stress).

5.2.4. Apoptosis/Necrosis

Cell death is an important mechanism in maintaining cellular homeostasis [273]. Both the regulated cell death (apoptosis) and pathological process (necrosis) were assessed in ZF4 and A549 cells exposed to GO and GO-Au nanohybrid. A dose-dependent increase in apoptosis and necrosis can be observed for both A549 and ZF4 cells as shown in **Figure 41-42.** Scatter dot plots made using FlowJo software are presented in the appendix (**Figure S5** and **S6)**.

The ability of GO and related materials to induce apoptosis and necrosis in cells have been well documented [274]–[277]. Physicochemical characteristics of GO (such as surface chemistry, functional groups, lateral dimension) have been suspected of triggering apoptosis through several signalling pathways [278]. Exposure to high concentration of GO has shown to activate the generation of ROS that causes oxidative stress and damage to the mitochondria, thereby expediting apoptosis [247].

As presented in **Figure 41A-B**, the induction of apoptosis and necrosis was slightly higher in ZF4 cells exposed to the treated concentrations (1, 50 and 100 µg/mL) of GO and GO-Au nanohybrids. GO appears to induce more apoptotic responses than GO-Au nanohybrid. While the highest test concentration (100 µg/mL) induced 14.6% necrosis in ZF4 cells exposed to GO-Au nanohybrid, necrosis induction was remarkably higher (53.1%) in the GO treatment. While there is scarce published work on the cell death mechanism of ZF4 cells exposed

to GO, there are reports of apoptotic effects to ZF4 cells from other nanomaterials such as AuNPs [161] and polystyrene nanoplastics [164].

Both GO and GO-Au induced nominal apoptosis and necrosis in A549 cells at the same concentrations (1, 50 and 100 µg/mL) as shown in **Figure 42A-B**. GO and GO-Au nanohybrid had more than 85% live cells. The highest concentration of GO and GO-Au (100 µg/mL) exhibited the lowest percentage of viable cells (87.3% and 86.9% respectively). Chang *et al*. (2011) also concluded that GO did not induce any significant cell death to A549 cells.

Interestingly, cyctotoxic effects have been reported to drastically reduce when GO is functionalised [279]–[281]. This is similar to what was found in this study where ZF4 cells treated with GO-Au nanohybrid exhibited far less apoptotic response than GO-treated cells. However, apoptosis results in A549 cells were comparable in both GO and GO-Au nanohybrid. Hence, funtionalisation could be considered as a win-win strategy for improving properties of nanomaterials as well as reducing their toxic effects.

The induction of significant necrosis in ZF4 cells indicates that cellular exposure to the GO-Au nanohybrid at high concentration could result in pathological conditions such as tissue damage and membrane integrity loss. The chronic effect in the natural environment could alter growth and reproduction in aquatic organisms that are vital in the food chain.

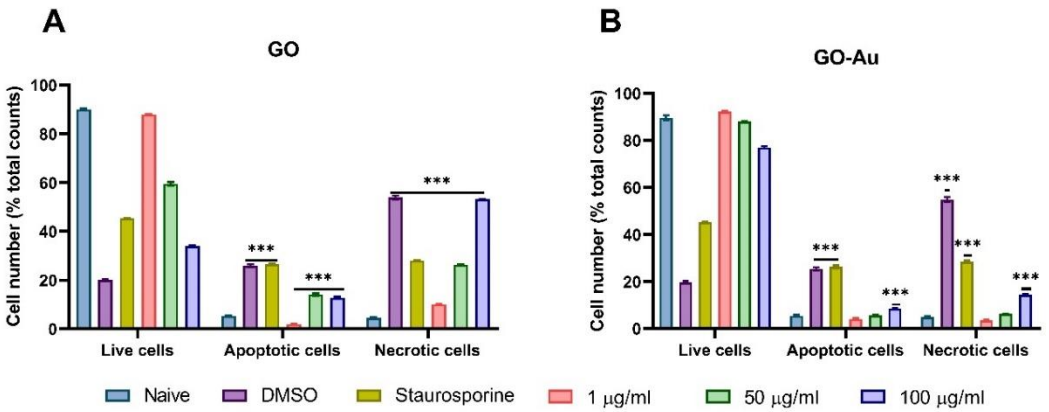

Figure 41: Apoptosis and necrosis of embryonic ZF4 cells measured by flow cytometry (A) Apoptosis and necrosis of embryonic ZF4 cells treated with GO at concentration of 1, 50 and 100 µg/mL (B) Apoptosis and necrosis of embryonic ZF4 cells treated with GO-Au at concentration of 1, 50 and 100 µg/mL. 10% DMSO and 1µm of Staurosporine was used as a positive control for necrosis and apoptosis. Data with asterisks (*) indicate a statistically significant difference (∗p < 0.05, ∗∗p < 0.01, and ∗∗∗p < 0.001) compared with naive cells (untreated control).

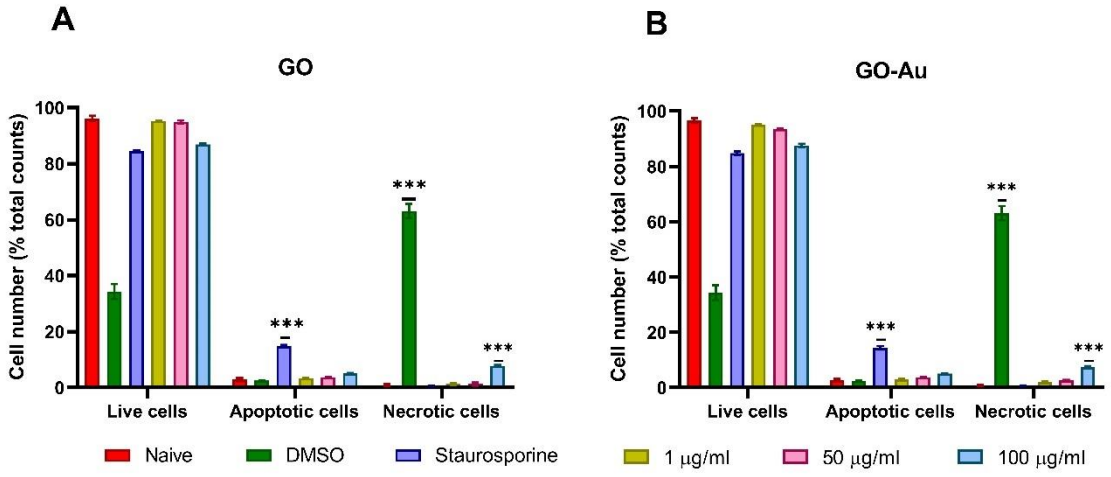

Figure 42: Apoptosis and necrosis of A549 cells measured by flow cytometry (A) Apoptosis and necrosis of A549 cells treated with GO at concentration of 1, 50 and 100 µg/mL (B) Apoptosis and necrosis of A549 cells treated with GO-Au at concentration of 1, 50 and 100 µg/Ml. 10% of DMSO and 1 µm of Staurosporine was used as a positive control for necrosis and apoptosis. Data with asterisks (*) indicate a statistically significant difference (∗p < 0.05, ∗∗p < 0.01, and ∗∗∗p < 0.001) compared with naive cells (untreated control).

5.3. Conclusions

The continuous use of nanomaterials such as GO and GO-Au nanohybrid pose health and safety risk to the environment due to their ability to penetrate biological barriers and cause harm. This study demonstrated the stability of GO and GO-Au nanohybrid in CCM and ultrapure water over 48 hrs. Both GO and GO-Au nanohybrid induced significant oxidative stress in ZF4 cells than in A549 cells as a result of an increase in ROS production. However, cells treated with GO generated far more ROS than cells treated with GO-Au nanohybrid.

In addition, a dose-dependent decrease in cell viability and metabolic activity was observed in ZF4 and A549 cells exposed to GO and GO-Au nanohybrid. Cell death effects were minimal in both ZF4 and A549 cells exposed to both GO and GO-Au nanohybrid but the apoptotic effects were more significant in GO than GO-Au and in ZF4 cells than in A549 cells. The cytotoxic effect of GO appears to be mitigated by the presence of AuNPs in both ZF4 and A549 cells which have masked the GO surface.

Interestingly, this study provides new insight into the potential use of ZF4 cells as reliable models for toxicity research instead of animals in line with the principles of 3Rs (replacement, reduction and refinement). This study now provides some baseline data on the dispersion stability and cytotoxicity of GO and GO-Au to ZF4 cells.

Chapter 6:

General Discussion, Conclusions and Future works

6.1 General Discussion

The successful synthesis of the graphene oxide (GO) and graphene oxide-gold nanohybrid (GO-Au) in this research is an important milestone in the assessment of their ecotoxicities and environmental risks. The need to develop well characterised standardised nanomaterials as a means towards improving reproducibility in nano(eco)toxicity studies is well established [282] and yet the availability of such standards is limited. Notwithstanding efforts from international standardisation committees, such as OECD and ISO, and a limited number of standard nanomaterials available by the US NIST (National Institute of Standards and Technology), Europe's JRC (Joint Research Centre) and a few other national standards institute, activity around standardised nanomaterials has remained limited despite early calls for their need [283].

Work towards standards development is often perceived as applied research that may not generate publishable outputs. Additionally, there is confusion about what constitutes a standard material, with terms such as "test nanomaterial", "reference nanomaterial" and "certified reference nanomaterial" all referring to increasing levels of scrutiny in their production and characterisation. As a result, nanomaterials standards are limited, and when available, they are expensive to acquire and usually available only in very small quantities. This is a concern for toxicology, but even more so for ecotoxicology, where experimental designs (often involving in vivo trials) require large quantities of material.

To our knowledge, there has been no previous attempt to initiate a standardisation process for anything but the simplest and most commonly used nanomaterials, and thus the nanohybrid presented here is a novel step in the standardisation direction. The data presented above establish the nanohybrid's reproducibility, provide a high level of characterisation information, notably in ecotoxicity relevant matrices, and demonstrate the potential to produce quantities suitable for large-scale experimentation. In addition, our results show that ageing up to 4 months does not affect the physicochemical properties of the hybrid. Previous work on aged nanomaterials has demonstrated clear differences in toxicological response, when ageing affects material properties [284] and thus, it is important that stability for a defined period of time has been established. Ecotoxicological studies, particularly when environmentally relevant concentrations of the test material are being assesses, may require longer term assessment and thus it is important to have confidence that the test material will not age during testing.

Despite the progress achieved here, further work would be required for the nanohybrid to go beyond a simple test material and to become a reference material. Future work should, for example, demonstrate that the nanohybrid is clear of endotoxin, particularly for toxicity experimentation, and that it can be synthesised in other labs following the protocol presented here and maintain the same physicochemical properties.

The pristine and aged GO-Au nanohybrid exhibited a high level of similarity in terms of physical attributes and chemical composition, highlighting its suitability for acute and chronic ecotoxicological studies. As a model test material, the GO-Au nanohybrid should behave well in relevant environmental media for internationalisation to take place. This behaviour (stability) influences the fate, toxicity and bio-nano interaction of the nanomaterials with biological systems as we have observed in this study. The natural organic matter (NOM) used in this work enhanced the dispersion stability of the nanohybrid in all the tested media and mitigated the toxic effects of the nanohybrid on daphnia, underscoring the critical role of NOM in toxicity testing of advanced nanomaterials.

The use of daphnia neonates and cells in this work was driven by the quest to understand the toxicity of the GO-Au nanohybrid at the different levels of the food chain i.e. cellular and organism level. Interestingly, the outcomes have been markedly distinct: toxic effects were more pronounced at the cellular level than organism level. We believe that the higher stability of the GO-Au nanohybrid in cell culture media contributed significantly to the elevated toxic effects observed at the cellular level than at organism level. Therefore, it is necessary to be cautious in estimating the risk associated with exposure to nanomaterials. In addition, our findings show that even at the cellular level, the biological responses can be different as the human carcinogenic cells (A549) showed more resistance to toxicity than zebrafish neonatal cells (ZF4).

With the expanding use of GO-Au nanohybrid in many applications, a broad understanding of the toxic nature of the nanohybrid becomes very crucial. Toxicity assessments of nanohybrids such as those carried out in this research add to baseline knowledge that will enable policymakers to set appropriate guidelines for their safe use. This research is important baseline information on the cytotoxicity and dispersion stability of GO and GO-Au nanohybrid to ZF4 and A549 cells. They will facilitate further research on the nanosafety of the materials and provide new insights on the relevance of ZF4 as a dependable alternative to animal use in toxicity studies.

6.2 Conclusions

This research work investigated the behaviour, fate and ecotoxicity of a GO-Au nanohybrid in the environment using *Daphnia magna* and cells (ZF4 and A549) as toxicity models. The study made the first known attempt to develop a reproducible standardised protocol for the synthesis of a GO-Au nanohybrid that is suitable as a test material for ecotoxicological testing. The stability of the nanohybrid in different media and the effect of ageing on the quality of the nanohybrid were also assessed. In addition, the study described how the GO-Au nanohybrid did not induce significant acute toxic effects to neonates of *Daphnia magna* but induced significant cytotoxicity, oxidative stress and apoptosis to ZF4 and A549 cells. Overall, the results documented in this thesis present the first evidence of the ecotoxicological assessment of a GO-Au nanohybrid. The outcome emphasises the need for continuous evaluation of the nanosafety of the nanohybrid to the ecosystem and human health.

6.3 Future Work

The development of a standardised protocol for the synthesis of GO-Au nanohybrid is a remarkable step in evaluating the safety of the nanomaterial in the environment. Further experimentation of the modified synthesis protocol may be necessary to investigate, for instance, the role of different GO drying methods on the quality of GO-Au nanohybrid. Likewise, ageing of the nanohybrid under various environmentally relevant conditions could be evaluated.

Although the ecotoxicological assessment of the GO-Au nanohybrid concludes that there is no significant lethal toxicity (mortality or immobilisation) to daphnia, the morphological observation of the internal organelles shows some abnormalities that require further evaluation. Future research should focus on chronic toxicity, assessment of sublethal effects (growth, reproduction, uptake/depuration) and biomarker responses of the GO-Au nanohybrid on daphnia.

Additionally, the cellular toxicity assessments covered cell viability, membrane activity and oxidative stress in ZF4 and A549 cell. The assessment could be extended to other types of cells such as MRC-5 cell line. The cell death mechanism as a result of exposed to GO and GO-Au nanohybrid was also investigated. However, the uptake mechanism and internalisation process of the nanomaterials could be examined to better understand the nano-biological interaction. Furthermore, enzymatic activities of the cells as a response to toxic exposure could be explored for a reliable cytotoxicity evaluation.

References

[1] A. K. Geim and K. S. Novoselov, “The rise of graphene,” *Nat. Mater.*, vol. 6, no. 3, pp. 183–191, 2007.

[2] A. Bianco *et al.*, “All in the graphene family - A recommended nomenclature for two-dimensional carbon materials,” *Carbon N. Y.*, vol. 65, pp. 1–6, 2013.

[3] P. R. Wallace, “The Band Theory of Graphite,” *Phys. Rev.*, vol. 71, no. 9, pp. 622–634, 1947.

[4] B. C. Brodie, “On the Atomic Weight of Graphite,” *R. Chem. Soc.*, vol. XIII, pp. 249–259, 1859.

[5] E. P. Randviir, D. A. C. Brownson, and C. E. Banks, “A decade of graphene research: Production, applications and outlook,” *Mater. Today*, vol. 17, no. 9, pp. 426–432, 2014.

[6] K. S. Novoselov *et al.*, “Electric Field Effect in Atomically Thin Carbon Films,” *Science (80-.).*, vol. 306, no. 5696, pp. 666–669, 2004.

[7] K. S. Novoselov, V. I. Fal’Ko, L. Colombo, P. R. Gellert, M. G. Schwab, and K. Kim, “A roadmap for graphene,” *Nature*, vol. 490, no. 7419, pp. 192–200, 2012.

[8] P. Wick *et al.*, “Classification framework for graphene-based materials,” *Angew. Chemie - Int. Ed.*, vol. 53, no. 30, pp. 7714–7718, 2014.

[9] W. Yu, L. Sisi, Y. Haiyan, and L. Jie, “Progress in the functional modification of graphene/graphene oxide: A review,” *RSC Adv.*, vol. 10,

no. 26, pp. 15328–15345, 2020.

[10] D. Wang *et al.*, “Next-generation multifunctional carbon-metal nanohybrids for energy and environmental applications,” *Environ. Sci. Technol.*, vol. 53, no. 13, pp. 7265–7287, 2019.

[11] N. Zhao *et al.*, “Versatile Types of Organic/Inorganic Nanohybrids: From Strategic Design to Biomedical Applications,” *Chem. Rev.*, vol. 119, no. 3, pp. 1666–1762, 2019.

[12] H. Fallatah, M. Elhaneid, H. Ali-boucetta, T. W. Overton, H. El Kadri, and K. Gkatzionis, “Antibacterial effect of graphene oxide (GO) nano-particles against Pseudomonas putida biofilm of variable age,” 2019.

[13] P. E. Buffet *et al.*, “A marine mesocosm study on the environmental fate of silver nanoparticles and toxicity effects on two endobenthic species: The ragworm Hediste diversicolor and the bivalve mollusc Scrobicularia plana,” *Sci. Total Environ.*, vol. 470–471, pp. 1151–1159, 2014.

[14] S. Jaworski *et al.*, “Graphene oxide-based nanocomposites decorated with silver nanoparticles as an antibacterial agent,” *Nanoscale Res. Lett.*, vol. 13, no. 1, 2018.

[15] K. Chandraker, R. Nagwanshi, S. K. Jadhav, K. K. Ghosh, and M. L. Satnami, “Antibacterial properties of amino acid functionalized silver nanoparticles decorated on graphene oxide sheets,” *Spectrochim. Acta - Part A Mol. Biomol. Spectrosc.*, vol. 181, pp. 47–54, 2017.

[16] M. N. I. Amir, A. Halilu, N. M. Julkapli, and A. Ma’amor, “Gold-graphene

oxide nanohybrids: A review on their chemical catalysis," *J. Ind. Eng. Chem.*, vol. 83, pp. 1–13, 2020.

[17] C. Santhosh, M. Saranya, R. Ramachandran, S. Felix, V. Velmurugan, and A. N. Grace, "Graphene/Gold Nanocomposites-Based Thin Films as an Enhanced Sensing Platform for Voltammetric Detection of Cr(VI) Ions," vol. 2014, 2014.

[18] G. Neri, E. Fazio, P. G. Mineo, A. Scala, and A. Piperno, "SERS sensing properties of new graphene/gold nanocomposite," *Nanomaterials*, vol. 9, no. 9, pp. 1–13, 2019.

[19] L. A. Al-Ani, M. A. AlSaadi, F. A. Kadir, N. M. Hashim, N. M. Julkapli, and W. A. Yehye, "Graphene– gold based nanocomposites applications in cancer diseases; Efficient detection and therapeutic tools," *Eur. J. Med. Chem.*, vol. 139, pp. 349–366, 2017.

[20] K. Turcheniuk, R. Boukherroub, and S. Szunerits, "Gold-graphene nanocomposites for sensing and biomedical applications," *J. Mater. Chem. B*, vol. 3, no. 21, pp. 4301–4324, 2015.

[21] P. C. Ray, H. Yu, and P. P. Fu, "Toxicity and Environmental Risks of Nanomaterials: Challenges and Future Needs," *Env. Sci Heal. C Env. Carcinog Ecotoxicol Rev*, vol. 27, no. 1, pp. 1–35, 2010.

[22] D. Bradley, "Is graphene safe?," *Mater. Today*, vol. 15, no. 6, p. 230, 2012.

[23] C. Bussy, H. Ali-Boucetta, and K. Kostarelos, "Safety considerations for

graphene: Lessons learnt from carbon nanotubes," *Acc. Chem. Res.*, vol. 46, no. 3, pp. 692–701, 2013.

[24] Y. Liu, W. Fan, Z. Xu, W. Peng, and S. Luo, "Transgenerational effects of reduced graphene oxide modified by Au, Ag, Pd, Fe3O4, Co3O4 and SnO2 on two generations of Daphnia magna," *Carbon N. Y.*, vol. 122, pp. 669–679, 2017.

[25] J. Yin *et al.*, "Toxicity of reduced graphene oxide modified by metals in microalgae: Effect of the surface properties of algal cells and nanomaterials," *Carbon N. Y.*, vol. 169, pp. 182–192, 2020.

[26] L. Stobinski *et al.*, "Graphene oxide and reduced graphene oxide studied by the XRD, TEM and electron spectroscopy methods," *J. Electron Spectros. Relat. Phenomena*, vol. 195, pp. 145–154, 2014.

[27] M. Wojtoniszak *et al.*, "Synthesis, dispersion, and cytocompatibility of graphene oxide and reduced graphene oxide," *Colloids Surfaces B Biointerfaces*, vol. 89, no. 1, pp. 79–85, 2012.

[28] O. C. Compton and S. T. Nguyen, "Graphene oxide, highly reduced graphene oxide, and graphene: Versatile building blocks for carbon-based materials," *Small*, vol. 6, no. 6, pp. 711–723, 2010.

[29] F. De Clippel, M. Dusselier, S. Van De Vyver, L. Peng, P. A. Jacobs, and B. F. Sels, "Tailoring nanohybrids and nanocomposites for catalytic applications," *Green Chem.*, vol. 15, no. 6, pp. 1398–1430, 2013.

[30] I. Khalil, N. M. Julkapli, W. A. Yehye, W. J. Basirun, and S. K. Bhargava,

Graphene-gold nanoparticles hybrid-synthesis, functionalization, and application in a electrochemical and surface-enhanced raman scattering biosensor, vol. 9, no. 6. 2016.

[31] H. A. Becerril, J. Mao, Z. Liu, R. M. Stoltenberg, Z. Bao, and Y. Chen, “Evaluation of solution-processed reduced graphene oxide films as transparent conductors,” *ACS Nano*, vol. 2, no. 3, pp. 463–470, 2008.

[32] J. Song *et al.*, “Synthesis of au/graphene oxide composites for selective and sensitive electrochemical detection of ascorbic acid,” *Sci. Rep.*, vol. 4, pp. 1–7, 2014.

[33] R. P. Feynman, “There’s plenty of room at the bottom,” in *Micromechanics and MEMS: Classic and Seminal Papers to 1990*, vol. 1, no. 1, 1992, pp. 60–66.

[34] N. Taniguchi, “On the basic concept of nanotechnology,” *ci.nii.ac.jp*, 1974.

[35] B. Gulson and H. Wong, “Stable isotopic tracing - A way forward for nanotechnology,” *Environ. Health Perspect.*, vol. 114, no. 10, pp. 1486–1488, 2006.

[36] K. A. D. Guzmán, M. R. Taylor, and J. F. Banfield, “Environmental risks of nanotechnology: National nanotechnology initiative funding, 2000-2004,” *Environ. Sci. Technol.*, vol. 40, no. 5, pp. 1401–1407, Mar. 2006.

[37] B. Zhang, H. Misak, P. S. Dhanasekaran, D. Kalla, and R. Asmatulu, “Environmental Impacts of Nanotechnology and Its Products,” *Am. Soc. Eng. Educ.*, vol. 1, no. December 2016, pp. 1–9, 2016.

[38] G. Lespes, S. Faucher, and V. I. Slaveykova, “Natural Nanoparticles, Anthropogenic Nanoparticles, Where Is the Frontier?,” *Front. Environ. Sci.*, vol. 8, p. 71, May 2020.

[39] M. F. Hochella *et al.*, “Natural, incidental, and engineered nanomaterials and their impacts on the Earth system,” *Science (80-.).*, vol. 363, no. 6434, Mar. 2019.

[40] A. Barhoum *et al.*, “Review on Natural, Incidental, Bioinspired, and Engineered Nanomaterials: History, Definitions, Classifications, Synthesis, Properties, Market, Toxicities, Risks, and Regulations,” *Nanomaterials*, vol. 12, no. 2, Jan. 2022.

[41] Wich Lab, “Multifunctional Biopolymers,” pp. 10–11, 2022.

[42] B. Samiey, C. H. Cheng, and J. Wu, “Organic-Inorganic Hybrid Polymers as Adsorbents for Removal of Heavy Metal Ions from Solutions: A Review,” *Mater. 2014, Vol. 7, Pages 673-726*, vol. 7, no. 2, pp. 673–726, Jan. 2014.

[43] M. Nanko, “Definitions and Categories of Hybrid Materials,” *AZojomo*, vol. 6. pp. 1–8, 2009.

[44] D. R. Dreyer, R. S. Ruoff, and C. W. Bielawski, “From conception to realization: An historial account of graphene and some perspectives for its future,” *Angew. Chemie - Int. Ed.*, vol. 49, no. 49, pp. 9336–9344, 2010.

[45] Y. Zhu *et al.*, “Graphene and graphene oxide: Synthesis, properties, and applications,” *Adv. Mater.*, vol. 22, no. 35, pp. 3906–3924, 2010.

[46] Royal Swedish Academy of Sciences, “Scientific Background on the Nobel Prize in Physics 2010 GRAPHENE,” vol. 50005, no. October, pp. 0–10, 2010.

[47] T. S. Sreeprasad and T. Pradeep, “Graphene for environmental and biological applications a review,” *Int. J. Mod. Phys. B*, vol. 26, no. 21, pp. 1–26, 2012.

[48] L. De Marchi, C. Pretti, B. Gabriel, P. A. A. P. Marques, R. Freitas, and V. Neto, “An overview of graphene materials: Properties, applications and toxicity on aquatic environments,” *Sci. Total Environ.*, vol. 631–632, pp. 1440–1456, 2018.

[49] G. Diankov, M. Neumann, and D. Goldhaber-Gordon, “Extreme monolayer-selectivity of hydrogen-plasma reactions with graphene,” *ACS Nano*, vol. 7, no. 2, pp. 1324–1332, 2013.

[50] A. A. Balandin *et al.*, “Superior Thermal Conductivity of Single-Layer Graphene,” *Nano Lett.*, vol. 8, no. 3, pp. 902–907, 2008.

[51] X. Xu *et al.*, “Length-dependent thermal conductivity in suspended single-layer graphene,” *Nat. Commun.*, vol. 5, pp. 1–6, 2014.

[52] J. U. Lee, D. Yoon, H. Kim, S. W. Lee, and H. Cheong, “Thermal conductivity of suspended pristine graphene measured by Raman spectroscopy,” *Phys. Rev. B - Condens. Matter Mater. Phys.*, vol. 83, no. 8, pp. 1–4, 2011.

[53] C. Lee, X. Wei, J. W. Kysar, and J. Hone, “Measurement of the Elastic

Properties and Intrinsic Strength of Monolayer Graphene," *Science*, vol. 321, no. July, pp. 385–388, 2008.

[54] S. C. Ray, "Application and Uses of Graphene Oxide and Reduced Graphene Oxide," *Appl. Graphene Graphene-Oxide Based Nanomater.*, pp. 39–55, Jan. 2015.

[55] M. Rogala *et al.*, "Graphene oxide overprints for flexible and transparent electronics," *Appl. Phys. Lett.*, vol. 106, no. 4, p. 041901, Jan. 2015.

[56] G. Eda *et al.*, "Graphene oxide gate dielectric for graphene-based monolithic field effect transistors," *Appl. Phys. Lett.*, vol. 102, no. 13, p. 133108, Apr. 2013.

[57] S. Jia *et al.*, "Graphene oxide/graphene vertical heterostructure electrodes for highly efficient and flexible organic light emitting diodes," *Nanoscale*, vol. 8, no. 20, pp. 10714–10723, May 2016.

[58] L. A. Dobrzański, M. Prokopiuk Vel Prokopowicz, A. Drygała, A. Wierzbicka, K. Lukaszkowicz, and M. Szindler, "Carbon Nanomaterials Application as a Counter Electrode for Dye-Sensitized Solar Cells," *Arch. Metall. Mater.*, vol. 62, no. 1, pp. 27–32, Mar. 2017.

[59] G. Kakavelakis *et al.*, "Efficient and Highly Air Stable Planar Inverted Perovskite Solar Cells with Reduced Graphene Oxide Doped PCBM Electron Transporting Layer," *Adv. Energy Mater.*, vol. 7, no. 7, p. 1602120, Apr. 2017.

[60] R. R. Nair, H. A. Wu, P. N. Jayaram, I. V. Grigorieva, and A. K. Geim,

“Unimpeded permeation of water through helium-leak-tight graphene-based membranes,” *Science (80-.).*, vol. 335, no. 6067, pp. 442–444, Jan. 2012.

[61] P. Sun *et al.*, “Selective ion penetration of graphene oxide membranes,” *ACS Nano*, vol. 7, no. 1, pp. 428–437, Jan. 2013.

[62] S. He *et al.*, “A Graphene Nanoprobe for Rapid, Sensitive, and Multicolor Fluorescent DNA Analysis,” *Adv. Funct. Mater.*, vol. 20, no. 3, pp. 453–459, Feb. 2010.

[63] L. Zhang, J. Xia, Q. Zhao, L. Liu, and Z. Zhang, “Functional Graphene Oxide as a Nanocarrier for Controlled Loading and Targeted Delivery of Mixed Anticancer Drugs,” *Small*, vol. 6, no. 4, pp. 537–544, Feb. 2010.

[64] C. Lu, H. Yang, C. Zhu, X. Chen, and G. Chen, “A Graphene Platform for Sensing Biomolecules,” *Angew. Chemie*, vol. 121, no. 26, pp. 4879–4881, Jun. 2009.

[65] A. Trapalis *et al.*, “TiO2/graphene composite photocatalysts for NOx removal: A comparison of surfactant-stabilized graphene and reduced graphene oxide,” *Appl. Catal. B Environ.*, vol. 180, pp. 637–647, Jan. 2016.

[66] D. J. Babu *et al.*, “Adsorption of pure SO2 on nanoscaled graphene oxide,” *RSC Adv.*, vol. 6, no. 43, pp. 36834–36839, Apr. 2016.

[67] M. Seredych and T. J. Bandosz, “Mechanism of ammonia retention on graphite oxides: Role of surface chemistry and structure,” *J. Phys. Chem.*

C, vol. 111, no. 43, pp. 15596–15604, Nov. 2007.

[68] H. C. Hsu *et al.*, “Graphene oxide as a promising photocatalyst for CO2 to methanol conversion,” *Nanoscale*, vol. 5, no. 1, pp. 262–268, Dec. 2012.

[69] Y. F. Xu *et al.*, “A CsPbBr3 Perovskite Quantum Dot/Graphene Oxide Composite for Photocatalytic CO2 Reduction,” *J. Am. Chem. Soc.*, vol. 139, no. 16, pp. 5660–5663, Apr. 2017.

[70] G. Zhao *et al.*, “Removal of Pb(II) ions from aqueous solutions on few-layered graphene oxide nanosheets,” *Dalt. Trans.*, vol. 40, no. 41, pp. 10945–10952, Oct. 2011.

[71] G. K. Ramesha, A. Vijaya Kumara, H. B. Muralidhara, and S. Sampath, “Graphene and graphene oxide as effective adsorbents toward anionic and cationic dyes,” *J. Colloid Interface Sci.*, vol. 361, no. 1, pp. 270–277, Sep. 2011.

[72] A. Molla, Y. Li, B. Mandal, S. G. Kang, S. H. Hur, and J. S. Chung, “Selective adsorption of organic dyes on graphene oxide: Theoretical and experimental analysis,” *Appl. Surf. Sci.*, vol. 464, pp. 170–177, Jan. 2019.

[73] W. S. Hummers and R. E. Offeman, “Preparation of Graphitic Oxide,” *J. Am. Chem. Soc.*, vol. 80, no. 6, p. 1339, 1958.

[74] A. Jiříčková, O. Jankovský, Z. Sofer, and D. Sedmidubský, “Synthesis and Applications of Graphene Oxide,” *Materials (Basel).*, vol. 15, no. 3, Feb. 2022.

[75] S. N. Alam, N. Sharma, and L. Kumar, “Synthesis of Graphene Oxide

(GO) by Modified Hummers Method and Its Thermal Reduction to Obtain Reduced Graphene Oxide (rGO)*," *Graphene*, vol. 06, no. 01, pp. 1–18, 2017.

[76] N. I. Zaaba, K. L. Foo, U. Hashim, S. J. Tan, W. W. Liu, and C. H. Voon, "Synthesis of Graphene Oxide using Modified Hummers Method: Solvent Influence," in *Procedia Engineering*, 2017, vol. 184, pp. 469–477.

[77] G. Santamaría-Juárez, E. Gómez-Barojas, E. Quiroga-González, E. Sánchez-Mora, M. Quintana-Ruiz, and J. Deisy Santamaría-Juárez, "Safer modified Hummers' method for the synthesis of graphene oxide with high quality and high yield," *iopscience.iop.org*, vol. 6, p. 125631, 2019.

[78] L. Shahriary and A. A. Athawale, "Graphene oxide synthesized by using modified hummers approach," *Int. J. Renew. Energy Env.*, vol. 02, no. 01, 2014.

[79] A. Pareek, J. Shanthi Sravan, and S. Venkata Mohan, "Graphene modified electrodes for bioelectricity generation in mediator-less microbial fuel cell," *J. Mater. Sci.*, vol. 54, no. 17, pp. 11604–11617, Sep. 2019.

[80] J. D. Lanphere, B. Rogers, C. Luth, C. H. Bolster, and S. L. Walker, "Stability and Transport of Graphene Oxide Nanoparticles in Groundwater and Surface Water," *Environ. Eng. Sci.*, vol. 31, no. 7, pp. 350–359, 2014.

[81] A. B. Seabra, A. J. Paula, R. De Lima, O. L. Alves, and N. Durán, "Nanotoxicity of graphene and graphene oxide," *Chem. Res. Toxicol.*, vol. 27, no. 2, pp. 159–168, 2014.

[82] O. Akhavan and E. Ghaderi, “Toxicity of graphene and graphene oxide nanowalls against bacteria,” *ACS Nano*, vol. 4, no. 10, pp. 5731–5736, Oct. 2010.

[83] C. Hu, Q. Wang, H. Zhao, L. Wang, S. Guo, and X. Li, “Ecotoxicological effects of graphene oxide on the protozoan Euglena gracilis,” *Chemosphere*, vol. 128, pp. 184–190, 2015.

[84] C.-J. Lu *et al.*, “Graphene oxide nanosheets induce DNA damage and activate the base excision repair (BER) signaling pathway both in vitro and in vivo,” *Chemosphere*, vol. 184, pp. 795–805, 2017.

[85] P. Zhang, H. Selck, S. R. Tangaa, C. Pang, and B. Zhao, “Bioaccumulation and effects of sediment-associated gold- and graphene oxide nanoparticles on Tubifex tubifex,” *J. Environ. Sci. (China)*, vol. 51, pp. 138–145, 2017.

[86] J. C. Soares, T. C. B. Pereira, K. M. Costa, T. Maraschin, N. R. Basso, and M. R. Bogo, “Developmental neurotoxic effects of graphene oxide exposure in zebrafish larvae (Danio rerio),” *Colloids Surfaces B Biointerfaces*, vol. 157, pp. 335–346, 2017.

[87] L. Xiaohui *et al.*, “A mechanism study on toxicity of graphene oxide to Daphnia magna: Direct link between bioaccumulation and oxidative stress,” *Environ. Pollut.*, vol. 234, pp. 953–959, 2018.

[88] I. Fekete-Kertész *et al.*, “Ecotoxicity assessment of graphene oxide by daphnia magna through a multimarker approach from the molecular to the physiological level including behavioral changes,” *Nanomaterials*, vol. 10,

no. 10, pp. 1–16, 2020.

[89] A. Tkaczyk, A. Bownik, J. Dudka, K. Kowal, and B. Ślaska, “Daphnia magna model in the toxicity assessment of pharmaceuticals: A review,” *Sci. Total Environ.*, vol. 763, 2021.

[90] L. Q. Chen, P. P. Hu, L. Zhang, S. Z. Huang, L. F. Luo, and C. Z. Huang, “Toxicity of graphene oxide and multi-walled carbon nanotubes against human cells and zebrafish,” *Sci. China Chem. 2012 5510*, vol. 55, no. 10, pp. 2209–2216, May 2012.

[91] N. A. El-Yamany, T. A. Salaheldin, W. N. Abd El-Mohsen, A. S. Amin, F. F. Mohamed, and A. A. Tohamy, “Graphene oxide nanosheets induced genotoxicity and pulmonary injury in mice,” *Exp. Toxicol. Pathol.*, vol. 69, no. 6, pp. 383–392, 2017.

[92] Z. Clemente, D. S. T. Martinez, L. S. Franqui, C. A. Silva, and V. L. S. S. Castro, “Nanotoxicity of graphene oxide: Assessing the influence of oxidation debris in the presence of humic acid,” *Environ. Pollut.*, vol. 225, pp. 118–128, 2017.

[93] J. Han, Y. Zhuo, Y. Q. Chai, L. Mao, Y. L. Yuan, and R. Yuan, “Highly conducting gold nanoparticles–graphene nanohybrid films for ultrasensitive detection of carcinoembryonic antigen,” *Talanta*, vol. 85, no. 1, pp. 130–135, Jul. 2011.

[94] C. C. Okpala, “Nanocomposites-An Overview,” *Int. J. Eng. Res.*, vol. 8, no. 11, pp. 17–23, 2013.

[95] G. Q. Tao and J. Wang, “Gold nanorod@nanoparticle seed-SERSnanotags/graphene oxide plasmonic superstructured nanocomposities as an ‘on-off’ SERS aptasensor,” *Carbon N. Y.*, vol. 133, pp. 209–217, Jul. 2018.

[96] A. Alshammari and V. Kalevaru, “Supported gold nanoparticles as promising catalysts,” *books.google.com*, 2016.

[97] B. Esteban-Fernández De Ávila *et al.*, “Single Cell Real-Time miRNAs Sensing Based on Nanomotors,” *ACS Nano*, vol. 9, no. 7, pp. 6756–6764, Jul. 2015.

[98] G. V. Lowry, K. B. Gregory, S. C. Apte, and J. R. Lead, “Transformations of nanomaterials in the environment,” *Environ. Sci. Technol.*, vol. 46, no. 13, pp. 6893–6899, 2012.

[99] S. M. Louie, R. Ma, and G. V. Lowry, *Transformations of Nanomaterials in the Environment*, 1st ed., vol. 7. Elsevier Ltd., 2014.

[100] J. Zhao, Z. Wang, J. C. White, and B. Xing, “Graphene in the aquatic environment: Adsorption, dispersion, toxicity and transformation,” *Environ. Sci. Technol.*, vol. 48, no. 17, pp. 9995–10009, Sep. 2014.

[101] G. Zhao, J. Li, X. Ren, C. Chen, and X. Wang, “Few-layered graphene oxide nanosheets as superior sorbents for heavy metal ion pollution management,” *Environ. Sci. Technol.*, vol. 45, no. 24, pp. 10454–10462, Dec. 2011.

[102] R. Arvidsson, S. F. Hansen, and A. Baun, “Influence of natural organic

matter on the aquatic ecotoxicity of engineered nanoparticles: Recommendations for environmental risk assessment," *NanoImpact*, vol. 20, no. June, p. 100263, 2020.

[103] V. L. Castro *et al.*, "Nanoecotoxicity assessment of graphene oxide and its relationship with humic acid," *Environ. Toxicol. Chem.*, vol. 37, no. 7, pp. 1998–2012, 2018.

[104] Y. Jiang, R. Raliya, P. Liao, P. Biswas, and J. D. Fortner, "Graphene oxides in water: Assessing stability as a function of material and natural organic matter properties," *Environ. Sci. Nano*, vol. 4, no. 7, pp. 1484–1493, 2017.

[105] I. Chowdhury, M. C. Duch, N. D. Mansukhani, M. C. Hersam, and D. Bouchard, "Colloidal properties and stability of graphene oxide nanomaterials in the aquatic environment"," *Environ. Sci. Technol.*, vol. 47, no. 2, p. 1359, 2013.

[106] L. J. Cote, J. Kim, V. C. Tung, J. Luo, F. Kim, and J. Huang, "Graphene oxide as surfactant sheets," *Pure Appl. Chem.*, vol. 83, no. 1, pp. 95–110, Dec. 2011.

[107] J. Fan, C. D. Grande, and D. F. Rodrigues, "Biodegradation of graphene oxide-polymer nanocomposite films in wastewater," *Environ. Sci. Nano*, vol. 4, no. 9, pp. 1808–1816, Sep. 2017.

[108] Z. Liu *et al.*, "Biodegradation of Graphene Oxide by Insects (Tenebrio molitor Larvae): Role of the Gut Microbiome and Enzymes," *Environ. Sci. Technol.*, Nov. 2022.

[109] R. Kurapati *et al.*, “Dispersibility-Dependent Biodegradation of Graphene Oxide by Myeloperoxidase,” *Small*, vol. 11, no. 32, pp. 3985–3994, Aug. 2015.

[110] N. M. Korovchinsky, “On the history of studies on cladoceran taxonomy and morphology, with emphasis on early work and causes of insufficient knowledge of the diversity of the group,” *Hydrobiologia*, vol. 360, pp. 1–11, Dec. 1997.

[111] OECD, “OECD Guideline for Testing of Chemicals (211): Daphnia magna Reproduction Test,” *Test*, no. September, pp. 1–21, 1998.

[112] OECD, “OECD Guideline for Testing of Chemicals (202): Daphnia specie Acute Immobilisation Test,” no. April, pp. 1–12, 2004.

[113] ISO 6341, “Water quality — Determination of the inhibition of the mobility of Daphnia magna Straus (Cladocera, Crustacea) — Acute toxicity test,” *Int. Stand.*, vol. 6341, p. 11, 2012.

[114] USEPA, “Methods for Measuring the Acute Toxicity of Effluents and Receiving Waters to Freshwater and Marine Organisms Fifth Edition October 2002,” *United States Environ. Prot. Agency Off. Water*, vol. Washington, no. October, pp. 1–275, 2002.

[115] USEPA, “Ecological Effects Test Guidelines Daphnid Chronic Toxicity Test,” no. April, pp. 1–10, 1996.

[116] J. Seda and A. Petrusek, “Daphnia as a model organism in limnology and aquatic biology: Introductory remarks,” *J. Limnol.*, vol. 70, no. 2, pp. 337–

344, 2011.

[117] J. R. Shaw *et al.*, “Daphnia as an emerging model for toxicological genomics,” *Adv. Exp. Biol.*, vol. 2, no. 08, pp. 5–7, 2008.

[118] E. D. and Bethesda (MD), “Introduction to Daphnia Biology - Ecology, Epidemiology, and Evolution of Parasitism in Daphnia - NCBI Bookshelf,” *National Center for Biotechnology Information (US)*, 2005. [Online]. Available: https://www.ncbi.nlm.nih.gov/books/NBK2042/. [Accessed: 16-Nov-2022].

[119] P. Lavens and P. Sorgeloos, “Manual on the production and use of live food for aquaculture,” *FAO Tech. Pap.*, no. 361, p. 295, 1996.

[120] W. M. De Coen and C. R. Janssen, “The use of biomarkers in Daphnia magna toxicity testing - I. The digestive physiology of daphnids exposed to toxic stress,” *Hydrobiologia*, vol. 367, no. 1–3, pp. 199–209, 1998.

[121] R. Klaper, J. Crago, J. Barr, D. Arndt, K. Setyowati, and J. Chen, “Toxicity biomarker expression in daphnids exposed to manufactured nanoparticles: Changes in toxicity with functionalization,” *Environ. Pollut.*, vol. 157, no. 4, pp. 1152–1156, 2009.

[122] D. S. T. Martinez, G. H. Da Silva, A. M. Z. de Medeiros, L. U. Khan, A. G. Papadiamantis, and I. Lynch, “Effect of the albumin corona on the toxicity of combined graphene oxide and cadmium to daphnia magna and integration of the datasets into the nanocommons knowledge base,” *Nanomaterials*, vol. 10, no. 10, pp. 1–20, 2020.

[123] I. Ahmed, B. Zhang, M. Muneeb-Ur-Rehman, and W. Fan, “Effect of different shapes of Nano-Cu2O and humic acid on two-generations of Daphnia Magna,” *Ecotoxicol. Environ. Saf.*, vol. 207, no. 37, p. 111274, 2021.

[124] X. Zhu, Y. Chang, and Y. Chen, “Toxicity and bioaccumulation of TiO2 nanoparticle aggregates in Daphnia magna,” *Chemosphere*, vol. 78, no. 3, pp. 209–215, 2010.

[125] S. W. Lee, S. M. Kim, and J. Choi, “Genotoxicity and ecotoxicity assays using the freshwater crustacean Daphnia magna and the larva of the aquatic midge Chironomus riparius to screen the ecological risks of nanoparticle exposure,” *Environ. Toxicol. Pharmacol.*, vol. 28, no. 1, pp. 86–91, 2009.

[126] W. Fan *et al.*, “Bioaccumulation and biomarker responses of cubic and octahedral Cu2O micro/nanocrystals in Daphnia magna,” *Water Res.*, vol. 46, no. 18, pp. 5981–5988, 2012.

[127] X. Lv *et al.*, “Mechanisms underlying the acute toxicity of fullerene to Daphnia magna: Energy acquisition restriction and oxidative stress,” *Water Res.*, vol. 123, pp. 696–703, 2017.

[128] M. Du, H. Zhang, J. Li, C. Yan, X. Zhang, and X. Chang, “Bioaccumulation, Depuration, and Transfer to Offspring of 13C-Labeled Fullerenols by Daphnia magna,” *Environ. Sci. Technol.*, vol. 50, no. 19, pp. 10421–10427, 2016.

[129] A. M. Cano, J. D. Maul, M. Saed, S. A. Shah, M. J. Green, and J. E.

Cañas-Carrell, “Bioaccumulation, stress, and swimming impairment in Daphnia magna exposed to multiwalled carbon nanotubes, graphene, and graphene oxide,” *Environ. Toxicol. Chem.*, vol. 36, no. 8, pp. 2199–2204, 2017.

[130] I. Martín-de-Lucía, F. Leganés, F. Fernández-Piñas, and R. Rosal, “Hyperbranched polymeric nanomaterials impair the freshwater crustacean Daphnia magna,” *Environ. Pollut.*, vol. 249, pp. 581–588, 2019.

[131] M. Djekoun, S. Bensoltane, A. Bourechrouche, M. Bourechrouche, and H. Berrebah, “In vitro toxicity of cadmium on the development of parthenogenetic eggs of a freshwater cladoceran: Daphnia magna,” *J. Mater. Environ. Sci.*, vol. 6, no. 4, pp. 957–962, 2015.

[132] A. Baun, S. N. Sørensen, R. F. Rasmussen, N. B. Hartmann, and C. B. Koch, “Toxicity and bioaccumulation of xenobiotic organic compounds in the presence of aqueous suspensions of aggregates of nano-C60,” *Aquat. Toxicol.*, vol. 86, no. 3, pp. 379–387, 2008.

[133] Y. Chae, D. Kim, S. W. Kim, and Y. J. An, “Trophic transfer and individual impact of nano-sized polystyrene in a four-species freshwater food chain,” *Sci. Rep.*, vol. 8, no. 1, pp. 1–12, 2018.

[134] K. Hund-Rinke and M. Simon, “Ecotoxic effect of photocatalytic active nanoparticles (TiO2) on algae and daphnids,” *Environ. Sci. Pollut. Res.*, vol. 13, no. 4, pp. 225–232, 2006.

[135] T. Malina, E. Maršálková, K. Holá, R. Zbořil, and B. Maršálek, “The

environmental fate of graphene oxide in aquatic environment—Complete mitigation of its acute toxicity to planktonic and benthic crustaceans by algae," *J. Hazard. Mater.*, vol. 399, no. January, p. 123027, 2020.

[136] Y. Liu, W. Fan, Z. Xu, W. Peng, and S. Luo, "Comparative effects of graphene and graphene oxide on copper toxicity to Daphnia magna: Role of surface oxygenic functional groups," *Environ. Pollut.*, vol. 236, pp. 962–970, 2018.

[137] C. Bussy and K. Kostarelos, "Carbon nanotubes in medicine and biology — Safety and toxicology," *Adv. Drug Deliv. Rev.*, vol. 65, no. 15, pp. 2061–2062, Dec. 2013.

[138] G. M. Vlăsceanu, H. Iovu, and M. Ioniţă, "Graphene inks for the 3D printing of cell culture scaffolds and related molecular arrays," *Compos. Part B Eng.*, vol. 162, pp. 712–723, Apr. 2019.

[139] K. Gold, B. Slay, M. Knackstedt, and A. K. Gaharwar, "Antimicrobial Activity of Metal and Metal-Oxide Based Nanoparticles," *Adv. Ther.*, vol. 1, no. 3, p. 1700033, Jul. 2018.

[140] R. Augustine, A. Hasan, R. Primavera, R. J. Wilson, A. S. Thakor, and B. D. Kevadiya, "Cellular uptake and retention of nanoparticles: Insights on particle properties and interaction with cellular components," *Mater. Today Commun.*, vol. 25, p. 101692, Dec. 2020.

[141] Y. Chang *et al.*, "In vitro toxicity evaluation of graphene oxide on A549 cells," *Toxicol. Lett.*, vol. 200, no. 3, pp. 201–210, 2011.

[142] R. Hu, G. Li, Q. Xu, and L. Chen, “Iron supplementation inhibits hypoxia-induced mitochondrial damage and protects zebrafish liver cells from death,” *Front. Physiol.*, vol. 13, no. August, pp. 1–15, 2022.

[143] Y. Tang *et al.*, “In vitro cytotoxicity of gold nanorods in A549 cells,” *Environ. Toxicol. Pharmacol.*, vol. 39, no. 2, pp. 871–878, 2015.

[144] P. Rees, J. W. Wills, M. R. Brown, C. M. Barnes, and H. D. Summers, “The origin of heterogeneous nanoparticle uptake by cells,” *Nat. Commun. 2019 101*, vol. 10, no. 1, pp. 1–8, May 2019.

[145] B. Rothen-Rutishauser, J. Bourquin, and A. Petri-Fink, “Nanoparticle-cell interactions: Overview of uptake, intracellular fate and induction of cell responses,” *Nanosci. Technol.*, pp. 153–170, 2019.

[146] E. C. Cho, L. Au, Q. Zhang, and Y. Xia, “The Effects of Size, Shape, and Surface Functional Group of Gold Nanostructures on Their Adsorption and Internalization by Cells,” *Small*, vol. 6, no. 4, pp. 517–522, Feb. 2010.

[147] J. Zhao and M. H. Stenzel, “Entry of nanoparticles into cells: the importance of nanoparticle properties,” *Polym. Chem.*, vol. 9, no. 3, pp. 259–272, Jan. 2018.

[148] P. Foroozandeh and A. A. Aziz, “Insight into Cellular Uptake and Intracellular Trafficking of Nanoparticles,” *Nanoscale Res. Lett. 2018 131*, vol. 13, no. 1, pp. 1–12, Oct. 2018.

[149] N. D. Donahue, H. Acar, and S. Wilhelm, “Concepts of nanoparticle cellular uptake, intracellular trafficking, and kinetics in nanomedicine,”

Adv. Drug Deliv. Rev., vol. 143, pp. 68–96, Mar. 2019.

[150] J. Mosquera, I. García, and L. M. Liz-Marzán, “Cellular Uptake of Nanoparticles versus Small Molecules: A Matter of Size,” *Acc. Chem. Res.*, vol. 51, no. 9, pp. 2305–2313, Sep. 2018.

[151] C. T. Ng, F. M. A. Tang, J. J. en Li, C. Ong, L. L. Y. Yung, and B. H. Bay, “Clathrin-mediated endocytosis of gold nanoparticles in vitro,” *Anat. Rec. (Hoboken).*, vol. 298, no. 2, pp. 418–427, Feb. 2015.

[152] J. Rejman, V. Oberle, I. S. Zuhorn, and D. Hoekstra, “Size-dependent internalization of particles via the pathways of clathrin- and caveolae-mediated endocytosis,” *Biochem. J.*, vol. 377, no. Pt 1, pp. 159–169, Jan. 2004.

[153] W. Russel and R. Burch, “The Principles of Humane Experimental Technique,” *Med. J. Aust.*, vol. 1, no. 13, pp. 500–500, Mar. 1960.

[154] NC3Rs, “The 3Rs,” 2022. [Online]. Available: https://nc3rs.org.uk/who-we-are/3rs. [Accessed: 13-Dec-2022].

[155] D. Zink, J. K. C. Chuah, and J. Y. Ying, “Assessing Toxicity with Human Cell-Based In Vitro Methods,” *Trends Mol. Med.*, vol. 26, no. 6, pp. 570–582, 2020.

[156] V. Kumar, N. Sharma, and S. S. Maitra, “In vitro and in vivo toxicity assessment of nanoparticles,” *Int. Nano Lett. 2017 74*, vol. 7, no. 4, pp. 243–256, Nov. 2017.

[157] S. Choorapoikayil, J. Overvoorde, and J. Den Hertog, “Deriving Cell Lines

from Zebrafish Embryos and Tumors," *Zebrafish*, vol. 10, no. 3, p. 316, Sep. 2013.

[158] W. Driever and Z. Rangini, "Characterization of a cell line derived from zebrafish (Brachydanio rerio) embryos," *In Vitro Cell. Dev. Biol. Anim.*, vol. 29A, no. 9, pp. 749–754, Sep. 1993.

[159] C. A. Ciarlo and L. I. Zon, "Embryonic cell culture in zebrafish," *Methods Cell Biol.*, vol. 133, p. 1, 2016.

[160] D. Vallone, C. Santoriello, S. B. Gondi, and N. S. Foulkes, "Basic Protocols for Zebrafish Cell Lines," pp. 429–441, 2007.

[161] A. C. Quevedo, I. Lynch, and E. Valsami-Jones, "Silver nanoparticle induced toxicity and cell death mechanisms in embryonic zebrafish cells," *Nanoscale*, vol. 13, no. 12, pp. 6142–6161, 2021.

[162] E. Fleurbaix, M. Parant, A. Maul, and C. Cossu-Leguille, "Toxicity of lanthanides on various fish cell lines," *Ecotoxicology*, vol. 31, no. 7, pp. 1147–1157, 2022.

[163] M. Rojas *et al.*, "How modular protein nanoparticles may expand the ability of subunit anti-viral vaccines: The spring viremia carp virus (SVCV) case," *Fish Shellfish Immunol.*, vol. 131, pp. 1051–1062, Dec. 2022.

[164] M. Yang and W. X. Wang, "Differential cascading cellular and subcellular toxicity induced by two sizes of nanoplastics," *Sci. Total Environ.*, vol. 829, p. 154593, Jul. 2022.

[165] ATCC, "ZF4 - CRL-2050," 2022. [Online]. Available:

https://www.atcc.org/products/crl-2050. [Accessed: 14-Dec-2022].

[166] D. Giard *et al.*, “In vitro cultivation of human tumors: establishment of cell lines derived from a series of solid tumors,” *J. Natl. Cancer Inst.*, vol. 51, no. 5, pp. 1417–1423, 1973.

[167] R. J. Swain, S. J. Kemp, P. Goldstraw, T. D. Tetley, and M. M. Stevens, “Assessment of Cell Line Models of Primary Human Cells by Raman Spectral Phenotyping,” *Biophys. J.*, vol. 98, no. 8, p. 1703, Apr. 2010.

[168] Z. H. Lu, X. J. Gu, K. Z. Shi, X. Li, D. D. Chen, and L. Chen, “Accessing anti-human lung tumor cell line (A549) potential of newer 3,5-disubstituted pyrazoline analogs,” *Arab. J. Chem.*, vol. 10, no. 5, pp. 624–630, Jul. 2017.

[169] L. Andrei *et al.*, “Advanced technological tools to study multidrug resistance in cancer,” *Drug Resist. Updat.*, vol. 48, p. 100658, Jan. 2020.

[170] A. Martin and A. Sarkar, “Overview on biological implications of metal oxide nanoparticle exposure to human alveolar A549 cell line,” *Nanotoxicology*, vol. 11, no. 6, pp. 713–724, 2017.

[171] ATCC, “A549 - CCL-185,” 2022. [Online]. Available: https://www.atcc.org/products/ccl-185. [Accessed: 14-Dec-2022].

[172] F. S. Rocha, A. J. Gomes, C. N. Lunardi, S. Kaliaguine, and G. S. Patience, “Experimental methods in chemical engineering: Ultraviolet visible spectroscopy—UV-Vis,” *Can. J. Chem. Eng.*, vol. 96, no. 12, pp. 2512–2517, 2018.

[173] British Standards Institution, “Nanotechnologies — Matrix of properties and measurement techniques for graphene and related two-dimensional (2D) materials,” no. March, 2019.

[174] S. Falke and C. Betzel, “Dynamic Light Scattering (DLS): Principles, Perspectives, Applications to Biological Samples,” *Radiat. Bioanal.*, vol. 8, p. 173, 2019.

[175] Anton Paar Wiki, “The principles of dynamic light scattering,” 2022. [Online]. Available: https://wiki.anton-paar.com/uk-en/the-principles-of-dynamic-light-scattering/. [Accessed: 24-Nov-2022].

[176] JASCO, “Principles of Raman spectroscopy (1) What is Raman spectroscopy?,” 2022. [Online]. Available: https://www.jasco-global.com/principle/1-what-is-raman-spectroscopy/. [Accessed: 24-Nov-2022].

[177] J. Bin Wu, M. L. Lin, X. Cong, H. N. Liu, and P. H. Tan, “Raman spectroscopy of graphene-based materials and its applications in related devices,” *Chem. Soc. Rev.*, vol. 47, no. 5, pp. 1822–1873, 2018.

[178] M. Lotya, P. J. King, U. Khan, S. De, and J. N. Coleman, “High-concentration, surfactant-stabilized graphene dispersions,” *ACS Nano*, vol. 4, no. 6, pp. 3155–3162, 2010.

[179] A. F. Rodrigues *et al.*, “A blueprint for the synthesis and characterisation of thin graphene oxide with controlled lateral dimensions for biomedicine,” *2D Mater.*, vol. 5, no. 3, 2018.

[180] Z. Zhang, H. C. Schniepp, and D. H. Adamson, “Characterization of graphene oxide: Variations in reported approaches,” *Carbon N. Y.*, vol. 154, pp. 510–521, 2019.

[181] L. E. Franken *et al.*, “A Technical Introduction to Transmission Electron Microscopy for Soft-Matter: Imaging, Possibilities, Choices, and Technical Developments,” *Small*, vol. 16, no. 14, p. 1906198, Apr. 2020.

[182] Technology Networks, “SEM vs TEM,” 2022. [Online]. Available: https://www.technologynetworks.com/analysis/articles/sem-vs-tem-331262. [Accessed: 24-Nov-2022].

[183] K. B. Ricardo and H. Liu, “Graphene-Encapsulated DNA Nanostructure: Preservation of Topographic Features at High Temperature and Site-Specific Oxidation of Graphene,” *Langmuir*, vol. 34, no. 49, pp. 15045–15054, 2018.

[184] A. Matković *et al.*, “Enhanced structural stability of DNA origami nanostructures by graphene encapsulation,” *New J. Phys.*, vol. 18, no. 2, 2016.

[185] D. Khalili, “Graphene oxide: A promising carbocatalyst for the regioselective thiocyanation of aromatic amines, phenols, anisols and enolizable ketones by hydrogen peroxide/KSCN in water,” *New J. Chem.*, vol. 40, no. 3, pp. 2547–2553, 2016.

[186] SCTCE, “The principle of TGA and its applications.” 2022.

[187] Z. Bacsik, J. Mink, and G. Keresztury, “FTIR Spectroscopy of the

Atmosphere. I. Principles and Methods," *https://doi.org/10.1081/ASR-200030192*, vol. 39, no. 3, pp. 295–363, Aug. 2007.

[188] R. S. Houk, V. A. Fassel, G. D. Flesch, H. J. Svec, A. L. Gray, and C. E. Taylor, "Inductively Coupled Argon Plasma as an Ion Source for Mass Spectrometric Determination of Trace Elements," *Anal. Chem*, vol. 52, pp. 2283–2289, 1980.

[189] S. C. Wilschefski and M. R. Baxter, "Inductively Coupled Plasma Mass Spectrometry: Introduction to Analytical Aspects," *Clin. Biochem. Rev.*, vol. 40, no. 3, p. 115, 2019.

[190] Hitachi, "Principle of ICP Mass Spectrometry (ICP-MS)," 2022. [Online]. Available: https://www.hitachi-hightech.com/global/products/science/tech/ana/icp/descriptions/icp-ms.html. [Accessed: 26-Nov-2022].

[191] T. Sandle, "Microbiology laboratory techniques," in *Pharmaceutical Microbiology*, Woodhead Publishing, 2016, pp. 63–80.

[192] F. Mokobi, "Light Microscope- Definition, Principle, Types, Parts, Labeled Diagram, Magnification," *Microbe Notes*, 2022. [Online]. Available: https://microbenotes.com/light-microscope/. [Accessed: 28-Nov-2022].

[193] OECD, "Guideline 202: Daphnia sp., Acute Immobilisation Test.," *OECD Guidel. Test. Chem.*, no. April, pp. 1–12, 2004.

[194] K. N. Baer and C. E. Goulden, "Evaluation of a High-Hardness COMBO Medium and Frozen Algae forDaphnia magna," *Ecotoxicol. Environ. Saf.*,

vol. 39, no. 3, pp. 201–206, Mar. 1998.

[195] S. S. Kilham, D. A. Kreeger, S. G. Lynn, C. E. Goulden, and L. Herrera, “COMBO: a defined freshwater culture medium for algae and zooplankton,” *Hydrobiol. 1998 3771*, vol. 377, no. 1, pp. 147–159, 1998.

[196] T. Mosmann, “Rapid colorimetric assay for cellular growth and survival: Application to proliferation and cytotoxicity assays,” *J. Immunol. Methods*, vol. 65, no. 1–2, pp. 55–63, Dec. 1983.

[197] F. Denizot and R. Lang, “Rapid colorimetric assay for cell growth and survival. Modifications to the tetrazolium dye procedure giving improved sensitivity and reliability,” *J. Immunol. Methods*, vol. 89, no. 2, pp. 271–277, May 1986.

[198] Sigma-Aldrich, “MTT Assay for Cell Viability and Proliferation,” *Merck KGaA*, pp. 5–7, 2021.

[199] M. M. Nachlas, S. I. Margulies, J. D. Goldberg, and A. M. Seligman, “The determination of lactic dehydrogenase with a tetrazolium salt,” *Anal. Biochem.*, vol. 1, no. 4–5, pp. 317–326, Dec. 1960.

[200] C. Batandier, E. Fontaine, C. Kériel, and X. M. Leverve, “Determination of mitochondrial reactive oxygen species: methodological aspects,” *J. Cell. Mol. Med.*, vol. 6, no. 2, pp. 175–187, 2002.

[201] OECD, “Dispersion Stability of Nanomaterials in Simulated Environmental Media,” *Oecd Guidel. Test. Chem.*, no. October, pp. 1–4, 2017.

[202] M. Sakuma, “Probit analysis of preference data,” *Appl. Entomol. Zool.*,

vol. 33, no. 3, pp. 339–347, 1998.

[203] C. Pretti *et al.*, “Ecotoxicity of pristine graphene to marine organisms,” *Ecotoxicol. Environ. Saf.*, vol. 101, no. 1, pp. 138–145, 2014.

[204] Z. Wang, F. Zhang, S. Wang, and W. J. G. M. Peijnenburg, “Assessment and prediction of joint algal toxicity of binary mixtures of graphene and ionic liquids,” *Chemosphere*, vol. 185, pp. 681–689, 2017.

[205] W. Zou, Q. Zhou, X. Zhang, L. Mu, and X. Hu, “Characterization of the effects of trace concentrations of graphene oxide on zebrafish larvae through proteomic and standard methods,” *Ecotoxicol. Environ. Saf.*, vol. 159, no. May, pp. 221–231, 2018.

[206] V. Kumar, A. Kumar, D. J. Lee, and S. S. Park, “Estimation of number of graphene layers using different methods: A focused review,” *Materials (Basel).*, vol. 14, no. 16, 2021.

[207] H. Ali-Boucetta, D. Bitounis, R. Raveendran-Nair, A. Servant, J. Van den Bossche, and K. Kostarelos, “Purified Graphene Oxide Dispersions Lack In Vitro Cytotoxicity and In Vivo Pathogenicity,” *Adv. Healthc. Mater.*, vol. 2, no. 3, pp. 433–441, 2013.

[208] A. Kumar and C. K. Dixit, “Methods for characterization of nanoparticles,” in *Advances in Nanomedicine for the Delivery of Therapeutic Nucleic Acids*, 2017, pp. 44–58.

[209] J. M. Berg, A. Romoser, N. Banerjee, R. Zebda, and C. M. Sayes, “The relationship between pH and zeta potential of ~ 30 nm metal oxide

nanoparticle suspensions relevant to in vitro toxicological evaluations," *Nanotoxicology*, vol. 3, no. 4, pp. 276–283, 2009.

[210] D. A. Jasim, N. Lozano, and K. Kostarelos, "Synthesis of few-layered, high-purity graphene oxide sheets from different graphite sources for biology," *2D Mater.*, vol. 3, no. 1, 2016.

[211] A. M. Z. de Medeiros *et al.*, "Graphene oxide-silver nanoparticle hybrid material: an integrated nanosafety study in zebrafish embryos," *Ecotoxicol. Environ. Saf.*, vol. 209, 2021.

[212] T. A. Pham, B. C. Choi, K. T. Lim, and Y. T. Jeong, "A simple approach for immobilization of gold nanoparticles on graphene oxide sheets by covalent bonding," *Appl. Surf. Sci.*, vol. 257, no. 8, pp. 3350–3357, 2011.

[213] M. Mokhtar, S. A. El Enein, M. Hassaan, M. Morsy, and M. Khalil, "Thermally Reduced Graphene Oxide: Synthesis, Structural and Electrical Properties," *Int. J. Nanoparticles Nanotechnol.*, vol. 3, no. 1, p. 8, 2017.

[214] M. Amouzadeh Tabrizi and J. N. Varkani, "Green synthesis of reduced graphene oxide decorated with gold nanoparticles and its glucose sensing application," *Sensors Actuators, B Chem.*, vol. 202, pp. 475–482, 2014.

[215] S. Chen, Y. Xiang, C. Peng, W. Xu, M. K. Banks, and R. Wu, "Synthesis of a novel graphene-based gold nanocomposite using PVEIM-: B -PNIPAM as a stabilizer and its thermosensitivity for the catalytic reduction of 4-nitrophenol," *Inorg. Chem. Front.*, vol. 6, no. 4, pp. 903–913, 2019.

[216] A. J. Caires, D. C. B. Alves, C. Fantini, A. S. Ferlauto, and L. O. Ladeira,

"One-pot in situ photochemical synthesis of graphene oxide/gold nanorod nanocomposites for surface-enhanced Raman spectroscopy," *RSC Adv.*, vol. 5, no. 58, pp. 46552–46557, 2015.

[217] S. Spoljaric, Y. Ju, and F. Caruso, "Protocols for Reproducible, Increased-Scale Synthesis of Engineered Particles - Bridging the 'upscaling Gap,'" *Chem. Mater.*, vol. 33, no. 4, pp. 1099–1115, Feb. 2021.

[218] J. P. Sitompul, H. W. Lee, Y. C. Kim, and M. W. Chang, "A scaling-up synthesis from laboratory scale to pilot scale and to near commercial scale for paste-glue production," *J. Eng. Technol. Sci.*, vol. 45 B, no. 1, pp. 9–24, 2013.

[219] M. S. Hull, A. J. Kennedy, J. A. Steevens, A. J. Bednar, C. A. Weiss, and P. J. Vikesland, "Release of metal impurities from carbon nanomaterials influences aquatic toxicity," *Environ. Sci. Technol.*, vol. 43, no. 11, pp. 4169–4174, Jun. 2009.

[220] H. Pan, S. Low, N. Weerasuriya, and Y. S. Shon, "Graphene oxide-promoted reshaping and coarsening of gold nanorods and nanoparticles," *ACS Appl. Mater. Interfaces*, vol. 7, no. 5, pp. 3406–3413, Feb. 2015.

[221] H. Pan, S. Low, N. Weerasuriya, B. Wang, and Y. S. Shon, "Morphological transformation of gold nanoparticles on graphene oxide: effects of capping ligands and surface interactions," *Nano Converg.*, vol. 6, no. 1, 2019.

[222] S. Zhou and A. Bongiorno, "Origin of the chemical and kinetic stability of graphene oxide," *Sci. Rep.*, vol. 3, pp. 1–7, 2013.

[223] Y. Shi, Y. Ji, F. Hui, H. H. Wu, and M. Lanza, “Ageing mechanisms and reliability of graphene-based electrodes,” *Nano Res.*, vol. 7, no. 12, pp. 1820–1831, 2014.

[224] S. Eigler, C. Dotzer, A. Hirsch, M. Enzelberger, and P. Müller, “Formation and decomposition of CO2 intercalated graphene oxide,” *Chem. Mater.*, vol. 24, no. 7, pp. 1276–1282, 2012.

[225] J. Jiang, G. Oberdörster, and P. Biswas, “Characterization of size, surface charge, and agglomeration state of nanoparticle dispersions for toxicological studies,” *J. Nanoparticle Res.*, vol. 11, no. 1, pp. 77–89, 2009.

[226] A. Gillespie, D. Jao, A. Andriola, T. Duda, C. F. Yang, and L. Yu, “Gold Nanoparticle Determination by Inductively Coupled Plasma-Mass Spectrometry, Anodic Stripping Voltammetry, and Flame Atomic Absorption Spectrophotometry,” *Anal. Lett.*, vol. 45, no. 10, pp. 1310–1320, 2012.

[227] A. Scheffer, C. Engelhard, M. Sperling, and W. Buscher, “ICP-MS as a new tool for the determination of gold nanoparticles in bioanalytical applications,” *Anal. Bioanal. Chem.*, vol. 390, no. 1, pp. 249–252, 2008.

[228] R. Allabashi, W. Stach, A. De La Escosura-Muñiz, L. Liste-Calleja, and A. Merkoçi, “ICP-MS: A powerful technique for quantitative determination of gold nanoparticles without previous dissolving,” *J. Nanoparticle Res.*, vol. 11, no. 8, pp. 2003–2011, 2009.

[229] G. Oberdörster *et al.*, “Principles for characterizing the potential human

health effects from exposure to nanomaterials: Elements of a screening strategy," *Part. Fibre Toxicol.*, vol. 2, pp. 1–35, 2005.

[230] A. Sani, C. Cao, and D. Cui, "Toxicity of gold nanoparticles (AuNPs): A review," *Biochem. Biophys. Reports*, vol. 26, p. 100991, 2021.

[231] R. A. Sperling, P. R. Gil, F. Zhang, M. Zanella, and W. J. Parak, "Biological applications of gold nanoparticles," *Chem. Soc. Rev.*, vol. 37, no. 9, pp. 1909–30, 2008.

[232] X. Guo, S. Dong, E. J. Petersen, S. Gao, Q. Huang, and L. Mao, "Biological uptake and depuration of radio-labeled graphene by Daphnia magna," *Environ. Sci. Technol.*, vol. 47, no. 21, pp. 12524–12531, 2013.

[233] A. E. Nel *et al.*, "Understanding biophysicochemical interactions at the nano-bio interface," *Nat. Mater.*, vol. 8, no. 7, pp. 543–557, 2009.

[234] K. N. Baer and C. E. Goulden, "Evaluation of a high-hardness COMBO medium and frozen algae for Daphnia magna," *Ecotoxicol. Environ. Saf.*, vol. 39, no. 3, pp. 201–206, 1998.

[235] K. He *et al.*, "Stability, transport and ecosystem effects of graphene in water and soil environments," *Nanoscale*, vol. 9, no. 17, pp. 5370–5388, 2017.

[236] A. Rodrigues, A. Brito, P. Janknecht, M. F. Proena, and R. Nogueira, "Quantification of humic acids in surface water: Effects of divalent cations, pH, and filtration]," *J. Environ. Monit.*, vol. 11, no. 2, pp. 377–382, 2009.

[237] A. Chouhan, H. P. Mungse, and O. P. Khatri, "Surface chemistry of

graphene and graphene oxide : A versatile route for their dispersion and tribological applications," *Adv. Colloid Interface Sci.*, vol. 283, p. 102215, 2020.

[238] D. Konios, M. M. Stylianakis, E. Stratakis, and E. Kymakis, "Dispersion behaviour of graphene oxide and reduced graphene oxide," *J. Colloid Interface Sci.*, vol. 430, pp. 108–112, 2014.

[239] N. B. Saleh, L. D. Pfefferle, and M. Elimelech, "Influence of biomacromolecules and humic acid on the aggregation kinetics of single-walled carbon nanotubes," *Environ. Sci. Technol.*, vol. 44, no. 7, pp. 2412–2418, 2010.

[240] K. L. Chen and M. Elimelech, "Influence of humic acid on the aggregation kinetics of fullerene (C60) nanoparticles in monovalent and divalent electrolyte solutions," *J. Colloid Interface Sci.*, vol. 309, no. 1, pp. 126–134, 2007.

[241] United Nations, *Globally harmonized system of Classification and Labelling of Chemicals (GHS)*, vol. 65, no. 1. 2011.

[242] J. Li *et al.*, "Reduced aggregation and cytotoxicity of amyloid peptides by graphene oxide/gold nanocomposites prepared by pulsed laser ablation in water," *Small*, vol. 10, no. 21, pp. 4386–4394, 2014.

[243] X. Lv *et al.*, "A mechanism study on toxicity of graphene oxide to Daphnia magna: Direct link between bioaccumulation and oxidative stress," *Environ. Pollut.*, vol. 234, pp. 953–959, 2018.

[244] L. J. A. Ellis *et al.*, “Multigenerational Exposures of Daphnia Magna to Pristine and Aged Silver Nanoparticles: Epigenetic Changes and Phenotypical Ageing Related Effects,” *Small*, vol. 16, no. 21, 2020.

[245] Y. Zhang *et al.*, “The effects of humic acid on the toxicity of graphene oxide to Scenedesmus obliquus and Daphnia magna,” *Sci. Total Environ.*, vol. 649, pp. 163–171, 2019.

[246] J. L. Giardini, N. D. Yan, and A. Heyland, “Consequences of calcium decline on the embryogenesis and life history of Daphnia magna,” *J. Exp. Biol.*, vol. 218, no. 13, pp. 2005–2014, 2015.

[247] K. Yang, Y. Li, X. Tan, R. Peng, and Z. Liu, “Behavior and toxicity of graphene and its functionalized derivatives in biological systems,” *Small*, vol. 9, no. 9–10, pp. 1492–1503, 2013.

[248] Y. Xin and B. Wan, “A label-free quantification method for measuring graphene oxide in biological samples,” *Anal. Chim. Acta*, vol. 1079, pp. 103–110, 2019.

[249] H. Wang, S. T. Yang, A. Cao, and Y. Liu, “Quantification of carbon nanomaterials in vivo,” *Acc. Chem. Res.*, vol. 46, no. 3, pp. 750–760, 2013.

[250] M. Heinlaan, A. Kahru, K. Kasemets, B. Arbeille, G. Prensier, and H. C. Dubourguier, “Changes in the Daphnia magna midgut upon ingestion of copper oxide nanoparticles: A transmission electron microscopy study,” *Water Res.*, vol. 45, no. 1, pp. 179–190, 2011.

[251] D. Kwon, H. W. Nho, and T. H. Yoon, “X-ray and electron microscopy studies on the biodistribution and biomodification of iron oxide nanoparticles in daphnia magna,” *Colloids Surfaces B Biointerfaces*, vol. 122, pp. 384–389, 2014.

[252] N. Santo *et al.*, “Toxic effects and ultrastructural damages to Daphnia magna of two differently sized ZnO nanoparticles: Does size matter?,” *Water Res.*, vol. 53, no. 0, pp. 339–350, 2014.

[253] L. A. V. Luna *et al.*, “Comparative in vitro toxicity of a graphene oxide-silver nanocomposite and the pristine counterparts toward macrophages,” *J. Nanobiotechnology*, vol. 14, no. 1, pp. 1–17, 2016.

[254] P. P. Adiseshaiah, J. B. Hall, and S. E. McNeil, “Nanomaterial standards for efficacy and toxicity assessment,” *Wiley Interdiscip. Rev. Nanomedicine Nanobiotechnology*, vol. 2, no. 1, pp. 99–112, 2010.

[255] M. Rocca, L. R. L. Morford, D. L. Blanset, W. G. Halpern, J. Cavagnaro, and C. J. Bowman, “Applying a weight of evidence approach to the evaluation of developmental toxicity of biopharmaceuticals,” *Regul. Toxicol. Pharmacol.*, vol. 98, pp. 69–79, Oct. 2018.

[256] P. O’Brien and J. R. Haskins, “In vitro cytotoxicity assessment.,” *Methods Mol. Biol.*, vol. 356, pp. 415–425, 2007.

[257] OECD, “Fish Toxicity Testing Framework,” *OECD Environ. Heal. Saf. Publ. Ser. Test. Assess.*, vol. 171, 2012.

[258] OECD, “Fish Embryo Acute Toxicity (FET) Test,” *OECD Guidel. Test.*

Chem., vol. 236, 2013.

[259] F. Xiaoli *et al.*, “Toxicology data of graphene-family nanomaterials: an update,” *Arch. Toxicol.*, vol. 94, no. 6, pp. 1915–1939, 2020.

[260] N. Durán *et al.*, “Interlab study on nanotoxicology of representative graphene oxide,” *J. Phys. Conf. Ser.*, vol. 617, no. 1, 2015.

[261] C. Bussy and K. Kostarelos, “Culture Media Critically Influence Graphene Oxide Effects on Plasma Membranes,” *Chem*, vol. 2, no. 3. Cell Press, pp. 322–323, 09-Mar-2017.

[262] G. Rischitor *et al.*, “Quantification of the cellular dose and characterization of nanoparticle transport during in vitro testing,” *Part. Fibre Toxicol.*, vol. 13, no. 1, pp. 1–16, 2016.

[263] G. Duan *et al.*, “Protein corona mitigates the cytotoxicity of graphene oxide by reducing its physical interaction with cell membrane,” *Nanoscale*, vol. 7, no. 37, pp. 15214–15224, Oct. 2015.

[264] L. S. Franqui *et al.*, “Interaction of graphene oxide with cell culture medium: Evaluating the fetal bovine serum protein corona formation towards in vitro nanotoxicity assessment and nanobiointeractions,” *Mater. Sci. Eng. C*, vol. 100, pp. 363–377, Jul. 2019.

[265] H. Ali-Boucetta *et al.*, “Cellular Uptake and Cytotoxic Impact of Chemically Functionalized and Polymer-Coated Carbon Nanotubes,” *Small*, vol. 7, no. 22, pp. 3230–3238, Nov. 2011.

[266] C. Beer, R. Foldbjerg, Y. Hayashi, D. S. Sutherland, and H. Autrup,

"Toxicity of silver nanoparticles—Nanoparticle or silver ion?," *Toxicol. Lett.*, vol. 208, no. 3, pp. 286–292, Feb. 2012.

[267] A. C. Quevedo, I. Lynch, and E. Valsami-Jones, "Cellular repair mechanisms triggered by exposure to silver nanoparticles and ionic silver in embryonic zebrafish cells," *Environ. Sci. Nano*, vol. 8, no. 9, pp. 2507–2522, 2021.

[268] B. Wu *et al.*, "Combined effects of graphene oxide and zinc oxide nanoparticle on human A549 cells: bioavailability, toxicity and mechanisms," *Environ. Sci. Nano*, vol. 6, no. 2, pp. 635–645, 2019.

[269] M. Herb, A. Gluschko, and M. Schramm, "Reactive Oxygen Species: Not Omnipresent but Important in Many Locations," *Front. Cell Dev. Biol.*, vol. 9, Sep. 2021.

[270] Y. Volkov, J. McIntyre, and A. Prina-Mello, "Graphene toxicity as a double-edged sword of risks and exploitable opportunities: A critical analysis of the most recent trends and developments," *2D Mater.*, vol. 4, no. 2, 2017.

[271] S. Mittal, V. Kumar, N. Dhiman, L. K. S. Chauhan, R. Pasricha, and A. K. Pandey, "Physico-chemical properties based differential toxicity of graphene oxide/reduced graphene oxide in human lung cells mediated through oxidative stress," *Sci. Rep.*, vol. 6, no. November, 2016.

[272] X. Zhang, W. Hu, J. Li, L. Tao, and Y. Wei, "A comparative study of cellular uptake and cytotoxicity of multi-walled carbon nanotubes, graphene oxide, and nanodiamond," *Toxicol. Res. (Camb).*, vol. 1, no. 1,

pp. 62–68, Jul. 2012.

[273] L. Galluzzi *et al.*, “Molecular mechanisms of cell death: Recommendations of the Nomenclature Committee on Cell Death 2018,” *Cell Death Differ.*, vol. 25, no. 3, pp. 486–541, 2018.

[274] M. J. Hajipour *et al.*, “Personalized disease-specific protein corona influences the therapeutic impact of graphene oxide,” *Nanoscale*, vol. 7, no. 19, pp. 8978–8994, May 2015.

[275] S. Jaworski *et al.*, “In vitro and in vivo effects of graphene oxide and reduced graphene oxide on glioblastoma,” *Int. J. Nanomedicine*, vol. 10, p. 1585, 2015.

[276] M. H. Lim *et al.*, “Graphene oxide induces apoptotic cell death in endothelial cells by activating autophagy via calcium-dependent phosphorylation of c-Jun N-terminal kinases,” *Acta Biomater.*, vol. 46, pp. 191–203, Dec. 2016.

[277] J. P. Souza, J. F. Baretta, F. Santos, I. M. M. Paino, and V. Zucolotto, “Toxicological effects of graphene oxide on adult zebrafish (Danio rerio),” *Aquat. Toxicol.*, vol. 186, pp. 11–18, May 2017.

[278] L. Ou, S. Lin, B. Song, J. Liu, R. Lai, and L. Shao, “The mechanisms of graphene-based materials- induced programmed cell death: a review of apoptosis, autophagy, and programmed necrosis,” *Int. J. Nanomedicine*, pp. 6633–6646, 2017.

[279] A. Magrez *et al.*, “Cellular toxicity of carbon-based nanomaterials,” *Nano*

Lett., vol. 6, no. 6, pp. 1121–1125, Jun. 2006.

[280] X. Ma *et al.*, “A functionalized graphene oxide-iron oxide nanocomposite for magnetically targeted drug delivery, photothermal therapy, and magnetic resonance imaging,” *Nano Res. 2012 53*, vol. 5, no. 3, pp. 199–212, Feb. 2012.

[281] W. Hu *et al.*, “Protein corona-mediated mitigation of cytotoxicity of graphene oxide,” *ACS Nano*, vol. 5, no. 5, pp. 3693–3700, May 2011.

[282] J. Beltran-Huarac, Z. Zhang, G. Pyrgiotakis, G. DeLoid, N. Vaze, and P. Demokritou, “Development of reference metal and metal oxide engineered nanomaterials for nanotoxicology research using high throughput and precision flame spray synthesis approaches,” *NanoImpact*, vol. 10, p. 26, Apr. 2018.

[283] G. Orts-Gil, K. Natte, and W. Österle, “Multi-parametric reference nanomaterials for toxicology: state of the art, future challenges and potential candidates,” *RSC Adv.*, vol. 3, no. 40, pp. 18202–18215, Sep. 2013.

[284] L. J. A. Ellis, E. Valsami-Jones, and I. Lynch, “Exposure medium and particle ageing moderate the toxicological effects of nanomaterials to Daphnia magna over multiple generations: a case for standard test review?,” *Environ. Sci. Nano*, vol. 7, no. 4, pp. 1136–1149, Apr. 2020.

Appendix 1: Characterisation Results

Figures **S1**, **S2**, **S3** and **S4** are characterisation results of GO and GO-Au nanohybrids that were described in Chapter 3, sub-section 3.2.

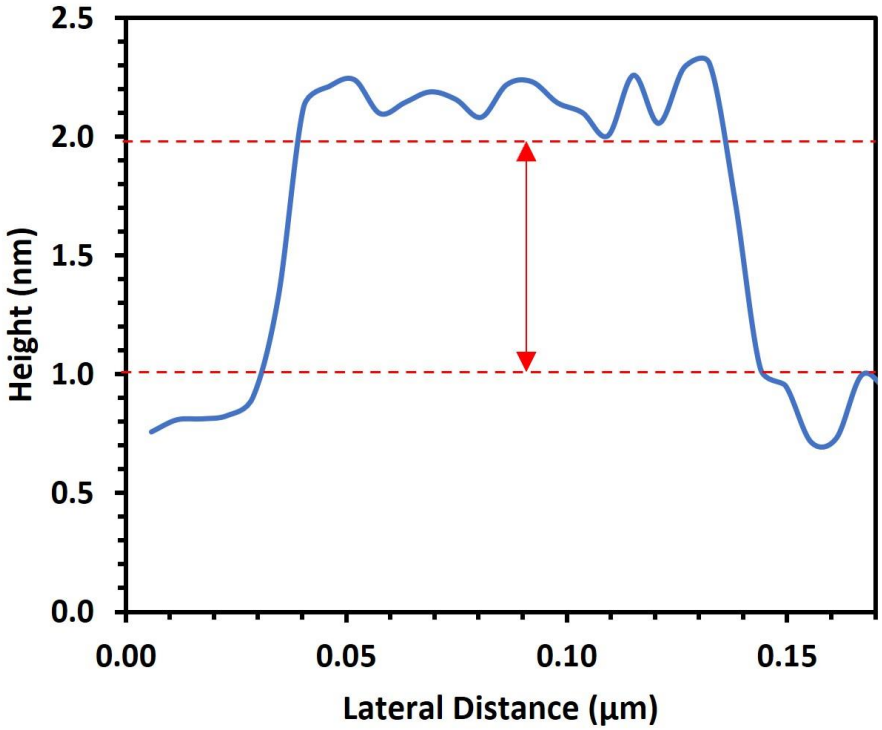

Figure S1: Line profile of graphene oxide (GO) height obtained from AFM measurements. The red arrow indicates the thickness of the GO which is 1nm

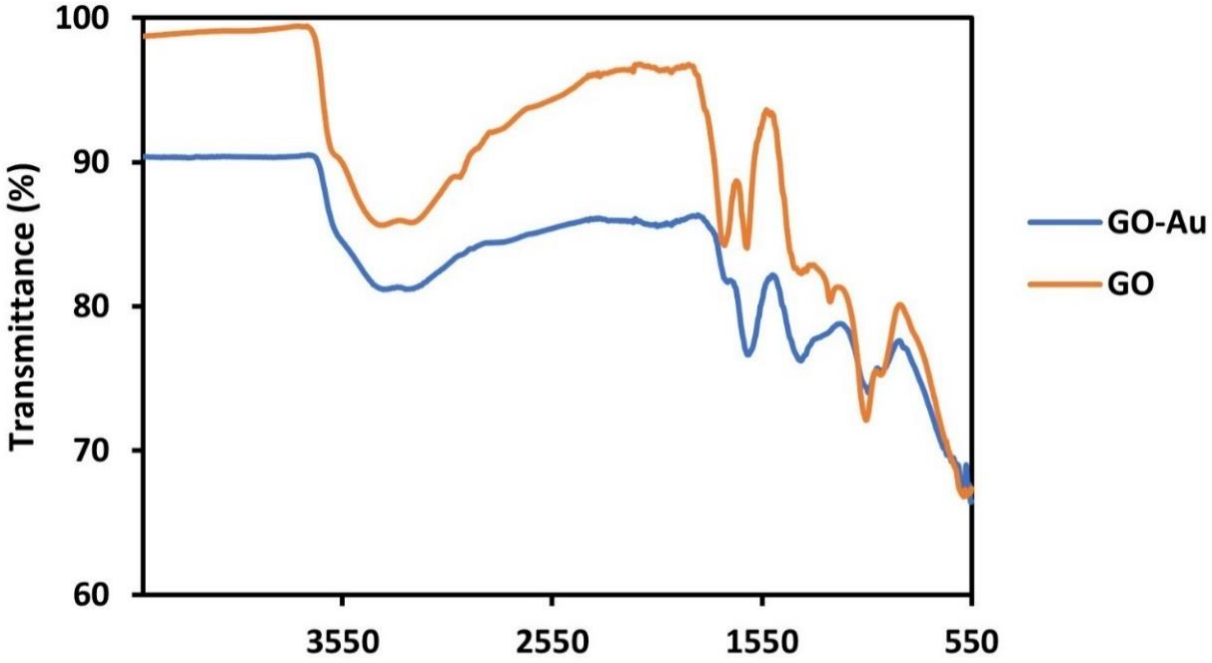

Figure S2: FTIR Spectra of GO and GO-Au nanohybrid

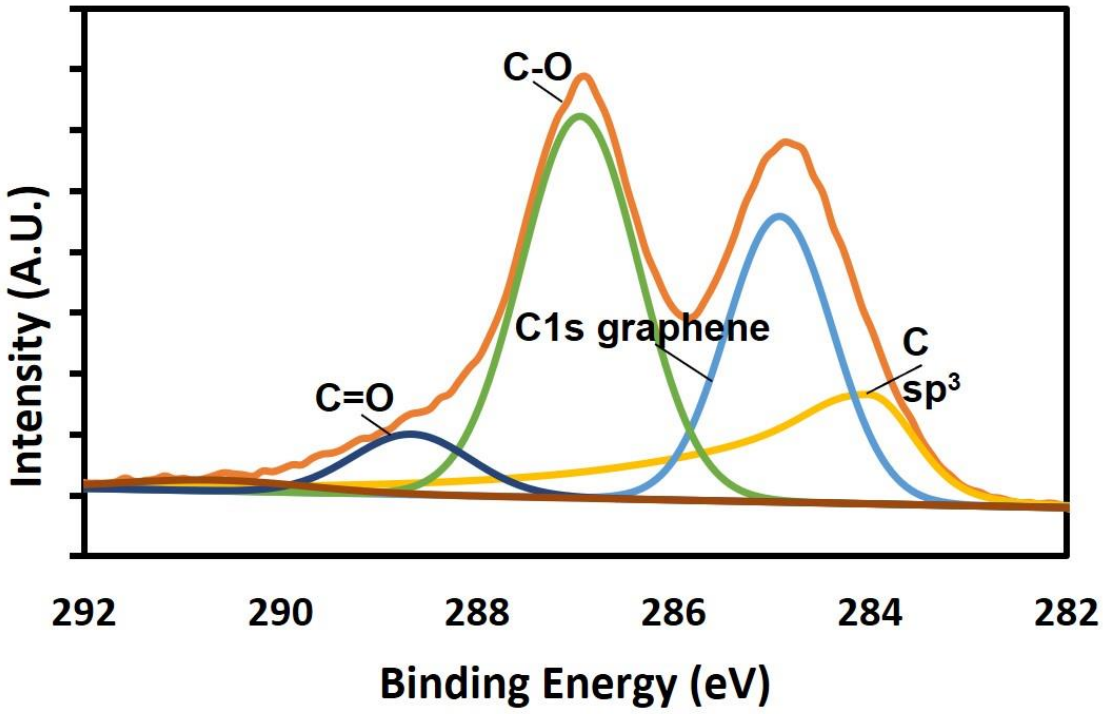

Figure S3: XPS C1s scan for GO-Au nanohybrid

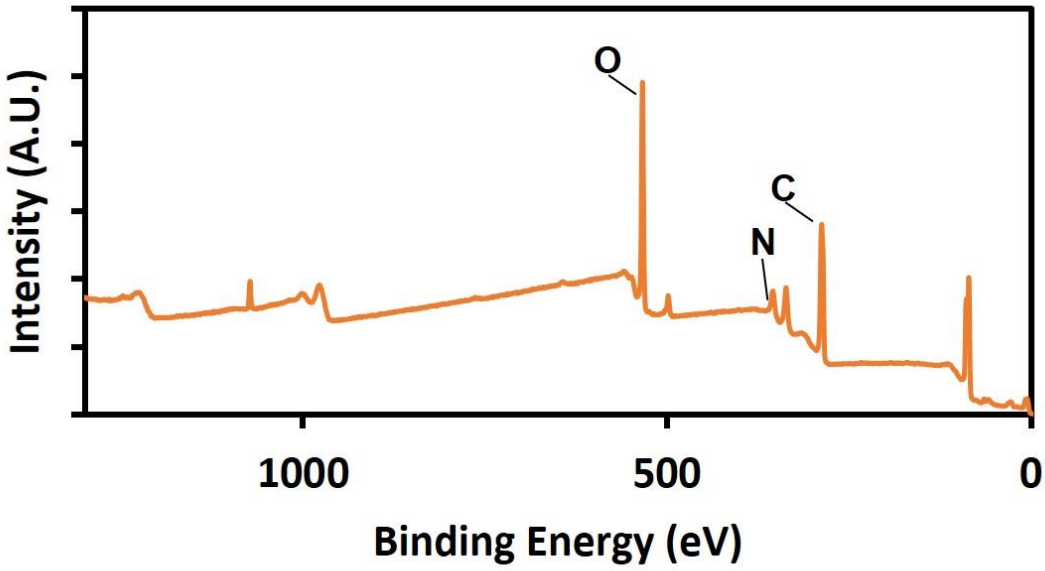

Figure S4: XPS Survey spectrum for GO-Au nanohybrid

Table S1: ICP-MS Operation and Measurement Parameters

Parameter	**Setting**
RF power	1600W
Plasma gas flow	18L/min
Auxiliary gas flow	1.2L/min
Nebuliser gas flow	0.9L/min
Pump flow rate	0.3mL/min
Measurements	15 sweeps 1 reading 20 replicates
Limit of detection of Au	0.1 µg/L

Appendix 2: Cell Dot Plots Analysis

Figures **S5** and **S6** are FlowJo dot plots analysis of ZF4 and A549 cells respectively. The plots have been discussed in Chapter 5, sub-section 5.2.4.

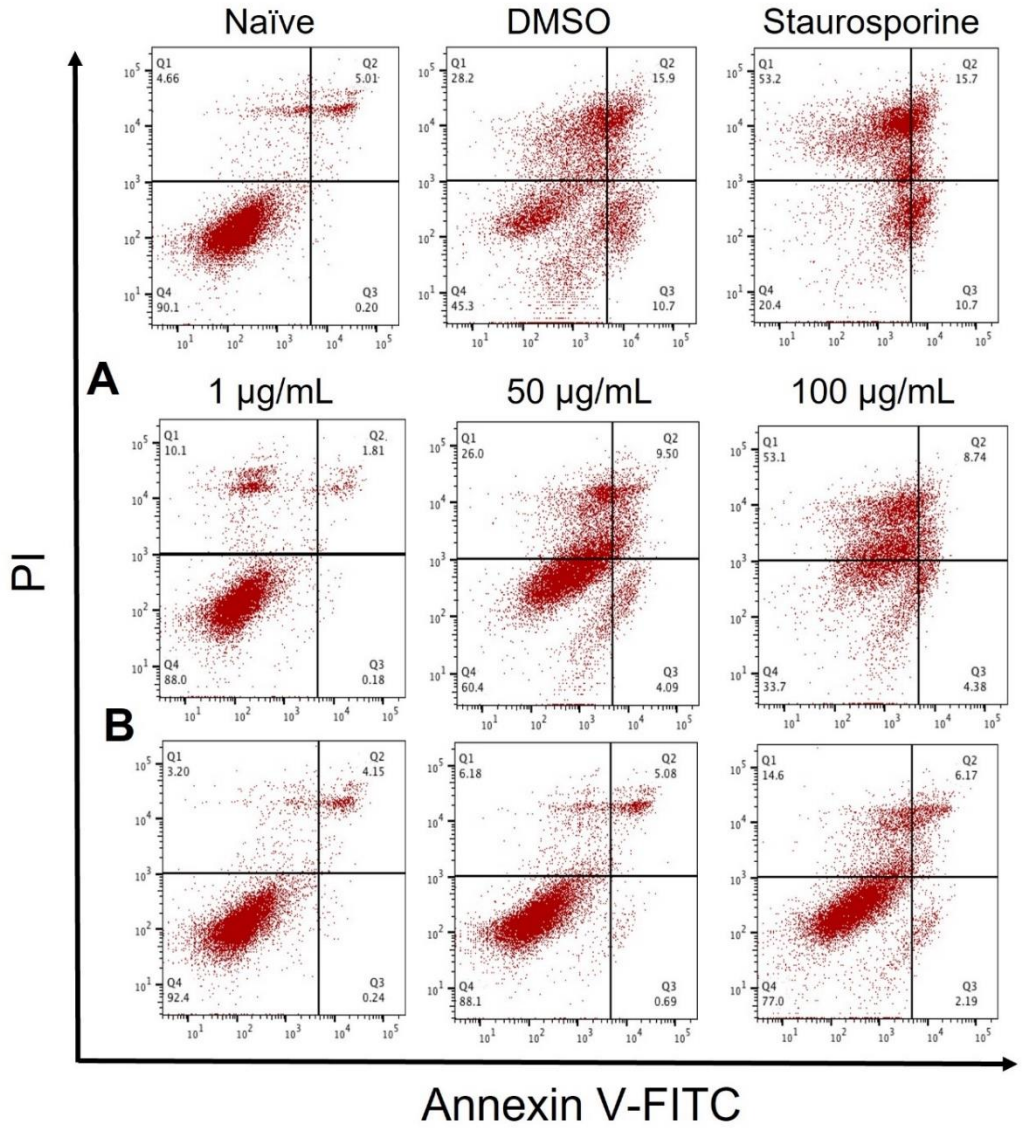

Figure S5: Dot plots of analysis of apoptosis and necrosis of embryonic ZF4 cells measured by flow cytometry (A) Apoptosis and necrosis of embryonic ZF4 cells treated with GO at concentration of 1, 50 and 100 µg/mL (B) Apoptosis and necrosis of embryonic ZF4 cells treated with GO-Au at concentration of 1, 50 and 100 µg/mL. Q1 = Necrosis, Q2 = Late Apoptosis, Q3 = Early Apoptosis, Q4 = Live cells. 10% DMSO and 1µm of Staurosporine was used as a positive control for necrosis and apoptosis.

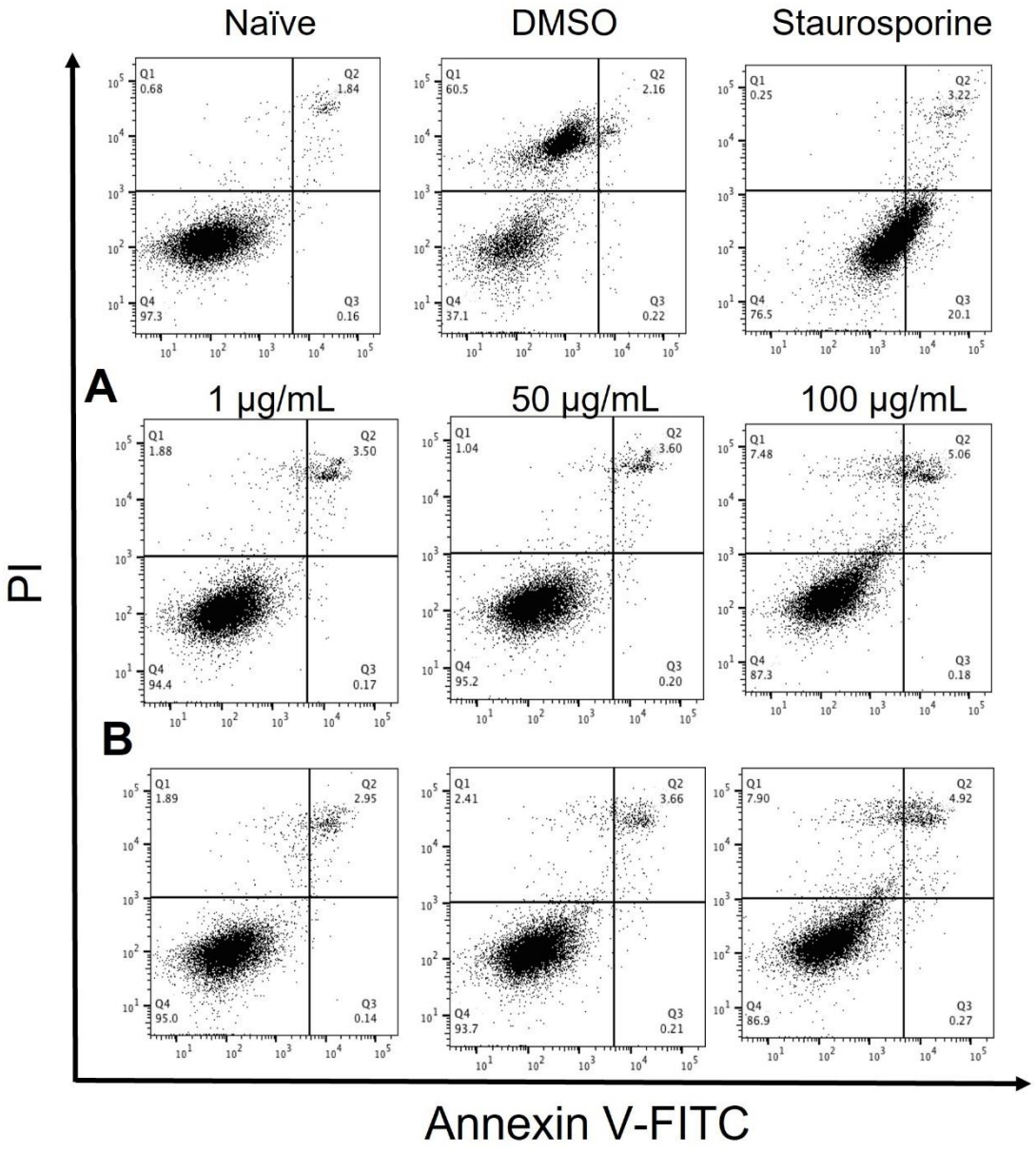

Figure S6: Dot plots of analysis of apoptosis and necrosis of A549 cells measured by flow cytometry (A) Apoptosis and necrosis of A549 treated with GO at concentration of 1, 50 and 100 µg/mL (B) Apoptosis and necrosis of A549 treated with GO-Au at concentration of 1, 50 and 100 µg/Ml. Q1 = Necrosis, Q2 = Late Apoptosis, Q3 = Early Apoptosis, Q4 = Live cells. 10% of DMSO and 1 µm of Staurosporine was used as a positive control for necrosis and apoptosis

Appendix 3: Quantification of Au

Table S2: Result of the quantification of Au in 100 µL of GO-Au Nanohybrid. X, Y and Z are the different batches of GO-Au nanohybrid produced.

	Au Concentration (mg/L)		
Replicates	**X**	**Y**	**Z**
1	0.1319	0.1461	0.1320
2	0.1265	0.1395	0.1236
3	0.1216	0.1447	0.1171
4	0.1276	0.1468	0.1250
5	0.1349	0.145	0.1444
Average	**0.128**	**0.144**	**0.128**
SD	**0.005**	**0.003**	**0.010**
x Dilution factor (10,000)	**1,285**	**1,444**	**1,284**

Table S3: Comparison of the stock concentration and the quantity of Au (concentration and mass) in each of the 3 batches of GO-Au nanohybrid.

GO-Au	Stock Conc (mg/L)	Conc of Au in 100uL (mg/l)	Mass of Au in 100uL (mg)
X	2,200	1,285	**0.13**
Y	4,700	1,444	**0.14**
Z	3,400	1,284	**0.13**

Appendix 4: Borehole Quality Parameters

Tables S3 and S4 contain the results of the water quality parameters of the borehole media used in this research as detailed in Chapter 4, sub-section 4.2.1-4.2.2.

Table S4: Water quality parameters of borehole water media used for dispersion stability and toxicity experiments. Cond = conductivity, DO = dissolved oxygen, Temp = temperature, TOC = total organic carbon, TN = total nitrogen

Sample ID	pH	Cond (µS/cm)	DO (% Sat)	Temp (°C)	TOC (mg/L)	TN (mg/L)
A	8.03	455.30	108.57	18.43	0.6873	5.9600
B	8.05	449.83	106.50	17.90	0.9493	1.9472
C	8.07	449.93	107.77	18.17	0.8883	6.2777
D	8.06	451.23	105.67	17.57	0.8903	6.0687
E	8.07	451.50	106.33	17.80	0.9884	6.0090

Table S5: Elemental composition of the borehole media as measured by ICP-OES

Sample ID	Ti 48 (ppb)	Mn 55 (ppb)	Fe 57 (ppb)	Ni 60 (ppb)	Cu 63 (ppb)	Zn 66 (ppb)	Cd 111 (ppb)	Hg 202 (ppb)	Pb 208 (ppb)	P 31 (ppb)	Mg 24 (ppm)	K 39 (ppm)	Ca 43 (ppm)
A1	0.6265	0.0343	120.1771	1.5177	0.4768	0.7891	0.0033	3.6525	0.0185	16.8295	17.0929	1.5649	50.6127
A2	-0.2254	0.0198	127.9203	1.1520	0.3512	0.8224	0.0024	1.5368	0.0117	15.8895	18.1787	1.6154	50.3031
A3	2.3615	0.0166	132.9965	1.0800	0.3259	1.0502	0.0009	1.0710	0.0084	15.6777	18.8887	1.6195	49.2164
B1	2.3319	0.0141	140.4039	1.1228	0.3903	1.1968	0.0030	0.8444	0.0083	16.0679	19.6463	1.6338	47.5879
B2	6.3047	0.0141	146.7040	1.1391	0.3446	0.7726	0.0016	0.6727	0.0076	16.1586	20.0361	1.6129	47.4033
B3	5.0909	0.0130	149.6215	1.1844	0.3355	0.9541	0.0024	0.5876	0.0072	16.1498	20.5246	1.6253	48.0946
C1	7.6017	0.0178	149.6959	1.1586	0.3593	1.1833	0.0025	0.5141	0.0068	16.0065	20.6367	1.6158	47.8937
C2	7.4065	0.0184	149.6578	1.1741	0.3550	1.1739	0.0023	0.4675	0.0046	15.7838	20.2727	1.5940	47.1101
C3	8.9336	0.0232	152.2085	1.1732	0.3775	1.2105	0.0016	0.4342	0.0049	15.5422	20.7715	1.6102	47.1611
D1	9.2285	0.0133	155.9447	1.1276	0.3380	0.9162	0.0015	0.3986	0.0045	15.5924	21.1208	1.6349	49.0243
D2	11.9227	0.0152	155.7003	1.1733	0.3169	0.8211	0.0012	0.3682	0.0037	15.7637	21.1289	1.6093	46.7691
D3	11.8417	0.0157	163.4611	1.1991	0.3393	0.8875	0.0008	0.3214	0.0039	15.2921	21.5937	1.6483	47.9672
E1	11.3920	0.0186	149.6093	1.1298	0.4307	1.5395	-0.0006	0.3248	0.0040	14.7385	19.9554	1.5234	44.2731
E2	11.4469	0.0174	154.4847	1.1423	0.3778	1.0758	-0.0008	0.2768	0.0019	14.8148	20.5902	1.5679	45.6040
E3	11.0080	0.0203	157.0267	1.1429	0.3279	0.7723	-0.0002	0.2648	0.0065	15.5459	21.3297	1.6080	47.9792

Appendix 5: Dispersion Stability

Table **S5** shows the raw results of absorbance measured using UV-vis of dispersion stability of GO and GO-Au nanohybrid in 3 environmental media, as discussed in Chapter 4, sub-section 4.2.1.

Table S6: UV-vis measurement of absorbance at 230nm of dispersion stability of GO and GO-Au in ultrapure water, borehole water and high hardness combo media.

		Ultrapure water (UPW)							
		GO		GO + NOM		GO-Au		GO-Au + NOM	
		Average	SD	Average	SD	Average	SD	Average	SD
230nm	0hr	1.5461	0.0120	1.6918	0.0062	1.6603	0.0171	1.8504	0.0087
	24hr	1.5807	0.0165	1.7119	0.0407	1.7179	0.1222	1.8401	0.0205
	48hr	1.6922	0.0212	1.8590	0.0292	1.8195	0.0286	2.0010	0.0232

		Borehole Water (BHW)							
		GO		GO + NOM		GO-Au		GO-Au + NOM	
		Average	SD	Average	SD	Average	SD	Average	SD
230nm	0hr	1.2920	0.0086	1.4377	0.0332	1.6856	0.0167	1.5584	0.0204
	24hr	0.1559	0.0166	0.6500	0.1876	0.1444	0.0092	1.3091	0.1779
	48hr	0.1490	0.0106	0.2622	0.0062	0.1474	0.0143	1.3837	0.0948

		High Hardness Combo (HHC)							
		GO		GO + NOM		GO-Au		GO-Au + NOM	
		Average	SD	Average	SD	Average	SD	Average	SD
230nm	0hr	1.4479	0.0120	1.6279	0.0559	1.1048	0.0100	1.3771	0.1507
	24hr	1.1102	0.0253	1.2619	0.0593	0.1506	0.0216	1.0210	0.0463
	48hr	1.1278	0.0935	1.2339	0.0461	0.1295	0.0012	0.8664	0.0825

Appendix 6: Daphnia Toxicity Protocol

Tables **S6** and **S7** show the preparation procedure of the range of concentrations of the test solutions (GO and GO-Au nanohybrid) used for the toxicity tests, as mentioned in Chapter 2, sub-section 2.3.2.

Table S7: Preparation of GO for acute immobilisation test

Conc (mg/L)	GO (mL)	BHW (mL)	NOM (mL)
1	0.05	48.95	1.0
5	0.25	48.75	1.0
10	0.50	48.50	1.0
20	1.00	48.00	1.0
50	2.50	46.50	1.0
100	5.00	44.00	1.0

Table S8: Preparation of GO-Au for acute immobilisation test

Conc (mg/L)	GO-Au (mL)	BHW (mL)	NOM (mL)
1	0.016	48.984	1.0
5	0.083	48.917	1.0
10	0.160	48.840	1.0
20	0.333	48.670	1.0
50	0.830	48.170	1.0
100	1.666	47.334	1.0

The final concentration of NOM (20mg/L) was prepared from a stock (1,000 mg/L). In the calculation shown in the tables above, the volume of GO and GO-Au prepared were 50mL.